

Safety in Mines Research Advisory Committee

Final Project Report

**Current practice and guidelines for
the safe design of water barrier
pillars**

**T Rangasamy
A R Leach
JJ van Vuuren
A P Cook
R Brummer**

**Research agency : Itasca Africa (Pty) Ltd.
Project number : COL 702
Date : August 2001**

Executive summary

The primary output of the project was the design of an easy to use guidebook that will enable the end user to simply and quickly estimate the optimum hydraulic barrier pillar width using water management criteria applicable to the mine.

Naturally occurring and stored underground water poses a threat to the safety of underground employees on coalmines. Often current workings are sited close to an underground reservoir, in particular old abandoned workings, which have been flooded. Rather than drain these reservoirs, it is normal practice to leave a barrier pillar between the new mining operations and the reservoir. At present, the barrier pillars that bound flooded underground compartments are designed primarily to ensure mechanical stability although their 'life of mine' function is to additionally prevent the inrush of water into current workings. No adequate local or international design addresses the hydraulic function of barrier pillars.

Underground instrumentation of roadways adjacent to barrier pillars was conducted to ascertain the relationship between compartment water head, barrier pillar width and flow rates for combinations of roof bound, coal bound and floor bound flow. The results obtained from the instrumentation sites were used to calibrate numerical models (UDEEC) used to determine the full inter-relationship between pillar size, pillar loading, rock mass geological condition, permeability, water pressure (head) and hence the degree of leakage through barrier pillars. A survey of South African Collieries revealed that water leakage associated with barrier pillars can be classed into seven predominant geotechnical flow categories.

Through extensive numerical modelling and case history matching, barrier pillar design charts (hydraulic) for the seven geotechnical flow regimes have been established. These charts will enable an engineering estimate to be made of either the barrier pillar width, tolerable water compartment head or roadway pumping rate required to manage water ingress into workings.

Acknowledgements

The authors wish to express their sincerest appreciation to the collieries that responded to the questionnaire and especially the collieries that accommodated and provided the team with their experiences, advice, information, equipment, labour and assistance during the test phases.

Contents

	Page
Executive summary.....	2
Acknowledgements	i
Contents	ii
Tables	viii
Terminology and abbreviations	ix
1 Introduction	1
2 Literature review.....	3
2.1 International literature review	3
2.1.1 Design practice and use of barrier pillars	3
2.1.1.1 Design approach.....	3
2.1.1.2 North America.....	4
2.1.1.2.1 <i>Legislation</i>	4
2.1.1.2.2 <i>Early barrier pillar design methods</i>	5
2.1.1.2.3 <i>Pennsylvania Mine Inspector’s Equation</i>	5
2.1.1.2.4 <i>Ash and Eaton’s Impoundment Equation</i>	6
2.1.1.2.5 <i>The North American Method</i>	7
2.1.1.2.6 <i>Outcrop Water Barrier Pillars</i>	8
2.1.1.3 Europe	8
2.1.1.3.1 <i>Old English Barrier Pillar Law</i>	9
2.1.1.3.2 <i>Pressure Arch Method</i>	9
2.1.1.3.3 <i>British Coal Rule of Thumb</i>	11
2.1.1.3.4 <i>Holland Convergence Method</i>	11
2.1.1.4 India.....	12
2.1.1.4.1 <i>Legislation</i>	12
2.1.1.4.2 <i>Water barrier pillar failures</i>	12
2.1.2 Design information and case studies.....	14
2.1.2.1 In-situ large-scale tests.....	14
2.1.2.1.1 <i>Case Studies</i>	14
2.1.2.2 Numerical methods and monitoring	18
2.1.3 Design parameters for water barrier pillars	20
2.1.3.1 Pillar size.....	20
2.1.3.2 Permeability and porosity of coal formations as a function of depth/stress.....	20
2.1.3.3 Pillar rock mass properties and distribution of major geological structures within the pillar ...	26
2.1.4 Summary and conclusions.....	26
2.2 National literature review.....	29
2.2.1 Coal barrier pillar design	29
2.2.2 Metalliferous barrier pillar design	30
2.2.3 Current Practices	30
3 Mechanical design of coal pillars	31

3.1	Square pillars.....	31
3.1.1	Applications and limitations:.....	32
3.2	Rectangular pillars.....	32
3.3	Continuous miner cut pillars.....	33
3.4	Squat pillar strength formula.....	33
3.5	Mining method influence on pillar fracturing.....	34
3.6	Ageing of pillars.....	34
4	Water flow in rock.....	35
4.1	Flow equations	35
4.2	Ground water in South African Coalfields.....	36
4.2.1	Groundwater associated with dolerite dykes	36
4.2.2	Groundwater associated with dolerite sills	36
4.2.3	Groundwater associated with sandstones.....	36
4.2.4	Groundwater associated with shales	36
4.2.5	Groundwater associated with underlying Karoo sediments	36
4.2.6	Water storage in South African Collieries	37
4.2.6.1	Compartment.....	37
4.2.6.2	Dams	38
4.2.6.3	Ponds.....	38
5	Data gathering for numerical models.....	40
5.1	National industry questionnaire.....	40
5.2	In situ monitoring.....	42
5.3	Geotechnical Survey	42
5.4	Geotechnical classification of flow regimes	44
5.5	Conclusions.....	48
6	Ground penetrating radar scan	49
7	Effect of water quality on coal strength.....	49
8	Numerical modelling.....	50
8.1	Suite of Numerical Models	50
8.1.1	Model hydraulic behaviour of rock fractures.....	50
8.2	Establishing modelling parameters.....	51

8.2.1	Hydraulic modelling parameters	51
8.2.1.1	Hydraulic aperture.....	51
8.2.1.2	Joint permeability factor.....	54
8.2.1.3	Explicit flow fractures.....	54
8.2.1.4	Incorporation of reservoir water pressure	55
8.2.2	Mechanical modelling parameters.....	55
8.2.2.1	Rock properties.....	55
8.2.2.2	Fracture properties	55
8.2.3	Constitutive behaviour of models.....	57
8.3	Representing Geotechnical flow regimes	57
8.4	Modelling methodology	58
8.4.1	Model size	58
8.4.2	Boundary conditions.....	59
8.4.3	Modelling strategy	60
8.5	Modelling Results	61
8.5.1	Response of Hydraulic Aperture to Loading.....	61
8.5.2	Flow paths	63
8.5.3	Formulating expressions for modelled flow	65
8.5.3.1	Modelled flow rates	66
8.5.3.2	Geotechnically classified fluid flow expressions	66
9	Design charts	70
9.1	Correction factors for depth below surface.....	70
9.2	Rate of water leakage	71
9.3	Correction factor for length of barrier pillar	73
9.4	Design chart operating ranges	73
9.5	Classification of flow regimes	73
9.6	Requirements and use of the design charts.....	76
9.6.1	Basic information required	76
9.7	Operation of Design Charts	77
9.7.1	Determining the Minimum Hydraulic Barrier Width – NEW BARRIERS.....	77
9.7.2	Determining the Maximum Tolerable Water Head – EXISTING BARRIERS	79
10	Recommendations for further research.....	81
11	Conclusions	82
12	References	84
	Appendix I: Summarized response to the national industry questionnaire	87

APPENDIX II Detailed analysis	88
Appendix III Uncombined flow charts for roof, coal and floor strata.....	104
APPENDIX IV DESIGN CHARTS.....	109
APPENDIX VI GPR scan.....	118

Figures

Figure 1: - Large range of pillar width calculated by various pillar strength equation (Peng, 1992)....	4
Figure 2: - Graphical representation of Pennsylvania mine inspector's equation for various seam thicknesses (Koehler et al. 1995).....	6
Figure 3: - Ash & Eaton impoundment equation for mining cover depths of 2000 ft (Koehler et al., 1995).....	7
Figure 4: -Graphical representation of North American Method (Koehler et al., 1995).....	8
Figure 5: -Graphical representation of Old English barrier pillar law (Koehler et al., 1995).....	9
Figure 6: -Conceptual illustration of maximum pressure arch (Koehler et al., 1995).....	10
Figure 7: -a) Location of Wattis seam instrumentation site, b) Location of underlying Third seam instrumentation site (Koehler et al., 1989).....	16
Figure 8: -Vertical BPC pressure profiles across study area for selected longwall face positions-looking inbye (Koehler et al. 1989).....	17
Figure 9: - Vertical BPC pressure change at maximum pillar load versus depth into Wattis barrier pillar from active mining side.....	18
Figure 10: -Variation of permeability as a function of stress-constant pore compressibility (McKee et al., 1988).....	22
Figure 11: -Laboratory-measured density versus depth data and theoretical match for shale core samples from northern Oklahoma (McKee et al., 1988).....	23
Figure 12: - Semilog plot of field-test-derived and estimated permeabilities with equivalent lithostatic depth (and effective stress) and match with theoretical curve for coal seams in the Piceance, San Juan, and Black Warrior basins (McKee et al., 1988).....	23
Figure 13: - Log-log plot of field-test-derived and estimated permeabilities with equivalent lithostatic depth (and effective stress) and match with theoretical curve for combined data from coal seams in the Piceance, San Juan, and Black Warrior basins (McKee et al., 1988).....	24
Figure 14: -Variations in geologic log-derived permeability with depth and match with theoretical curve for Miocene mudstone, Nagaoka plain, Japan (McKee et al., 1988).....	25
Figure 15: -Correlation of South African colliery barrier widths with internationally applied formulae.....	28
Figure 16: -Groundwater dewatering in total extraction area (after Hodgson).....	37
Figure 17: Retaining walls forming a dam.....	38
Figure 18: Water accumulating against barrier due to dip of seam.....	38
Figure 19: - volumetric vs. pressure increase.....	39
Figure 20: Mining depth range for South African collieries based on questionnaire data.....	40
Figure 21: Seam height range for South African collieries based on questionnaire data.....	41
Figure 22: Barrier pillar width range for South African collieries based on questionnaire data.....	41
Figure 23: Compartment water head range for South African collieries based on questionnaire data.....	42
Figure 24: Extent of laminations/bedding into the roof ascertained from geological logs.....	43
Figure 25: Extent of laminations/bedding into the floor ascertained from geological logs.....	44
Figure 26: Geotechnical classification of flow regimes according to condition of roof and floor strata i.e. massive, few vertical joints in competent strata, shear damaged zones in incompetent strata.....	46
Figure 27: Classification of 33 South African collieries by geotechnical character of the roof and floor strata.....	47
Figure 28: Geometry of calibration model used to obtain correct barrier pillar loading and required residual aperture to produce measured time dependent degradation in water pressure across the barrier pillar.....	52
Figure 29: Vertical stress state across 20m wide barrier pillar with 10m wide roadways (Roadway width chosen to obtain an average pillar stress of 7MPa).....	52

Figure 30: Worst measured water pressure degradation correlated against modelled distribution of water pressure along horizontal model joint for a residual aperture of 0.15mm.....	53
Figure 31: Modelled flow rate for in situ tested mine as a function of residual aperture and single horizontal fracture length.....	53
Figure 32: The three classes of fractures that form flow paths as represented in the UDEC models	54
Figure 33: Assigned deformable zone edge lengths and position of category of fractures.....	56
Figure 34: Representation of geotechnical flow regimes in UDEC were vertical fractures are indicative of the condition (competent or incompetent) of the roof and floor strata.....	58
Figure 35: Size of UDEC model for the simulation of a 35m wide barrier pillar.....	59
Figure 36: Hydraulic model boundary conditions	60
Figure 37: Response of hydraulic aperture to variations in depth (stress).....	62
Figure 38: High degree of pillar edge displacement (area of shear damage) results in reduced closure of discontinuity apertures at the edge of the pillar.....	62
Figure 39: Distribution of hydraulic aperture in a roof bound bedding plane as a function of barrier pillar width.....	63
Figure 40: UDEC fluid flow velocity lines showing the tapping effect of a discrete vertical roof and floor joint.....	64
Figure 41: UDEC fluid flow velocity lines showing the tapping effect of multiple vertical joints that represent shear damaged areas of incompetent roof and floor strata.....	64
Figure 42: Flow chart showing the methodology adopted to establish governing equations for flow using modelled flow rates and Darcy's equation.....	65
Figure 43: Cumulative hydraulic aperture as a function of barrier pillar width for geotechnical conditions of the roof, coal and floor.....	67
Figure 44: Best fit exponential functions for cumulative aperture as a function of barrier width using modelled flow rates for roof and floor geotechnical conditions	67
Figure 45: Best fit polynomial for cumulative aperture as a function of barrier width using modelled flow rates for coal bound flow only.....	68
Figure 46: Correction factor for rates of leakage (flow rate) for depth below surface	70
Figure 47: Dimensions used to calculate rate of leakage resulting in knee depth ponding (1m).....	71
Figure 48: Five categories for rate of leakage and time taken for knee depth ponding	72
Figure 49: Geotechnical classification of flow regions.....	75
Figure 50: Flow chart illustrating the information required to determine the minimum hydraulic barrier width for new water reservoirs and the maximum tolerable head for existing barrier pillar bound water reservoirs.....	76
Figure 51: Determining the minimum hydraulic width of barrier pillars for the design of new compartments (p.t.o).....	77
Figure 52: Determining the maximum tolerable compartment water head for existing barrier pillar bound reservoirs (p.t.o).....	79

Tables

Table 1: -Summary of strength equation from large-scale in-situ tests (Bieniawski, 1987).	15
Table 2 Hydraulic condition of rock mass derived from characteristics of the roof, coal and floor strata.....	47
Table 3 Rock type and properties used in UDEC models (after van der Merwe, 1998).....	55
Table 4 Properties assigned to categories of fractures.....	56
Table 5 Primary outputs derived from UDEC models	58
Table 6 Rate of water leakage on the dry side of the barrier pillar for variations in pillar width at a depth of 200m below surface.....	66
Table 7 Replacement of aperture in Darcy's equation for conditions of roof and floor strata	68
Table 8: Combinations of strata conditions listed in Table 4 to produce flow for seven geotechnical flow regimes	69
Table 9: Relating leakage rates for knee depth ponding to categories of leakage.....	71
Table 10: Operating ranges for geotechnically classified hydraulic design charts	73

Terminology and abbreviations

The following measurement unit abbreviations are used in this report.

Psi	: pounds per square inch
kPa	: kilo Pascal's
m	: metres
"	: inches
'	: feet
kg	: kilogram
w	: width of pillar
h	: height of roadway
b	: bordwidth
H	: depth below surface

As many units quoted are imperial, these can be approximately converted to SI units with the following table.

Conversion table

Imperial	SI (Approximate)
1 psi	6.893 kPa
20 psi	137 kPa
50 psi	345 kPa
1"	0,0254 m
6"	0,15 m
20"	0,50 m
1'	0,3 m
10'	3,0 m
15'	4,5 m
20'	6,0 m
200'	60 m

1 Introduction

Coal barrier pillars are intact blocks of coal left unmined to provide hydraulic barriers for water management as well as to provide roof support. Coal barrier pillars can be classified as peripheral barriers (intact coal at the edge of the deep mine works) or internal barriers (intact coal located in the interior of the mine works). ("A Handbook of Technologies for Avoidance and Re-mediation of Acid Mine Drainage." – Skousen, J. et. al, 2000.)

One of the most common problems concerning underground coal mining in South Africa is the post-mining management of water. There are essentially two sources for this water entering the underground workings:

- First, and by far the largest contributor, is the natural groundwater. The groundwater enters the underground workings percolating through the intact overburden, seeping through broken strata or being carried by geological structures such as dykes, faults and fissures. Groundwater will continue to flow into areas in which total extraction mining was practised long after mining has ceased. The influx will continue until the original hydraulic balance between the water table in these areas and surrounding areas has been reached.
- The second source is service water that is used primarily for dust suppression and cleaning.

As soon as this water is exposed to the coal bearing strata and the coal itself, it is contaminated with various minerals in suspension and solution. Due to environmental responsibility and current legislation, precluding the discharge of contaminated water into surface streams, rivers or dams, this water must be stored underground for an indefinite time. Various methods are employed to store this water, making use of dams, contour ponds and constructed compartments.

Two types of continuous barriers are found in South African Collieries:

Barriers are found on the boundary between neighbouring mines as required by legislation. The old workings can be flooded on one or either side of the barrier, particularly if one or both of the workings are abandoned mines. In most instances, the water pressure acting on such barriers and the volume stored is a function of the depth of mining and the seam floor contours.

The second category of barriers is found in-between panels and/or areas on a mine. Their primary function is:

- Create panels with independent pillar design parameters
- Prevent and contain regional pillar collapse through isolation from workings
- Minimise the effect of high abutment stresses on roadways and influence ground control in adjacent panels
- Control strata and surface subsidence
- Create independent ventilation districts
- Isolate development panels so they can easily be sealed off
- Act as ventilation and water barriers

With abandoned mines, there is an uncontrolled build-up of the water and the barrier on the mine boundary contains, depending on the contouring of the coal seam floor, this water.

On operating collieries, except for making use of contour ponds, the most common practice is to use areas surrounded by continuous barriers with the minimum construction needed to contain or seal in the water. Water build-up in other parts of the mine is controlled through pumping the water into these compartments or dams.

In general, the build-up of water against the boundary barrier or the water compartments was not included or planned in the initial planning and layout of the mines or the design of the

barriers. Panels or areas were laid out according to mine boundaries, legislative constraints, quality of coal, geological and rock-engineering constraints, life of mine strategy and the production and ventilation needs. They were not necessarily planned as water bearing structures or water compartments.

Whenever water storage capacity was required, the most suitable panel was found, seals built and water pumped in. The barrier pillars surrounding these panels or areas, were designed according to rock engineering principles and not for the storage of water.

The design procedures and practices for water compartments underground are in a process of change but still there are millions of litres of water stored in compartments not designed to handle water pressure, although most of them seem to cope rather well with the water.

The role of the water barrier is seen as to contain water up to a certain designed capacity without failing and causing a sudden inrush of water.

The work that has been done in South Africa on water barrier pillars mostly covers the design of barriers in between neighbouring mines. More work has been done on such barriers in metalliferous mines than on coal mines. The fact that this might be a water-bearing barrier has been taken into consideration but no in-depth study has been done on the long-term effects that the water might have on the barriers or the ageing and subsequent deterioration of the barrier.

This report looks at the current practices regarding the safe design of water barrier pillars in South African Collieries and compares them to what is being done internationally. It reports on typical in-situ parameters regarding flow through and around these barriers. It concludes by giving guidelines and procedures for the future safe design of water barrier pillars in South African Collieries.

2 Literature review

A literature review was conducted on a national and international level.

2.1 International literature review

2.1.1 Design practice and use of barrier pillars

Barrier pillars are pillars left to support main entries or to separate unmined or mined-out panels. For example, barrier pillars separate the rectangular mining panels in a room and pillar mining environment. To date, there are no specific design guidelines for barrier pillars, but where the roof is not caved or where pillars are left in place, design of barrier pillars assumes greater importance. According to the SME Handbook (1992), pillar stress is not necessarily evenly distributed, and where the floor and roof rocks are stiffer than the pillar rocks, stress will be transferred to an abutment. There is also the probability that deterioration or overmining of highly stressed pillars may lead to a reduction in load capacity of individual pillars and transfer of load to other pillars that may lead to progressive failure. This is one of the most common causes of extensive pillar collapse, and barrier pillars can control this.

2.1.1.1 Design approach

There are two methods for pillar design. The traditional method involves determining the pillar strength in the laboratory using small-sized coal samples and comparing it with the expected loading. The second method calls for numerical analysis of the mine, taking into account the interactions between roof, pillar, floor, and mining sequence.

In the traditional method it is recognised that coal pillar strength varies with size and shape of the specimen. The following equation (Peng, 1992) can be used for the size effects:

$$S_1 = K_1 \sqrt{d} \quad (1)$$

where: S_1 is the uniaxial compressive strength of the cubical pillar,
 d is the side length of the cubical specimen,
and K_1 is a constant.

Equation 1 is normally used to determine the value of the constant K and not the uniaxial compressive strength of the specimen, which is then used as input into coal pillar strength formulae.

For shape effects there are five applicable equations (Obert & Duvall, 1967; Holland, 1964; Holland & Gaddy, 1956; Salamon & Munro, 1967; Bieniawski, 1983). These equations can be seen from Bieniawski (1983). As an illustration, a comparison of pillar width calculated from these equations as a function of overburden depth is given in Figure 1. The pillar loading is usually determined by using the tributary area loading concept. This assumes that a pillar supports uniformly the weight of the rock overlaying the pillar as well as half of the width of rooms or entries on each side of the pillar. By employing any of the above referenced equations, for a given seam height, entry width, seam depth, and average known unit weight of rock, the pillar width can be determined by trial and error.

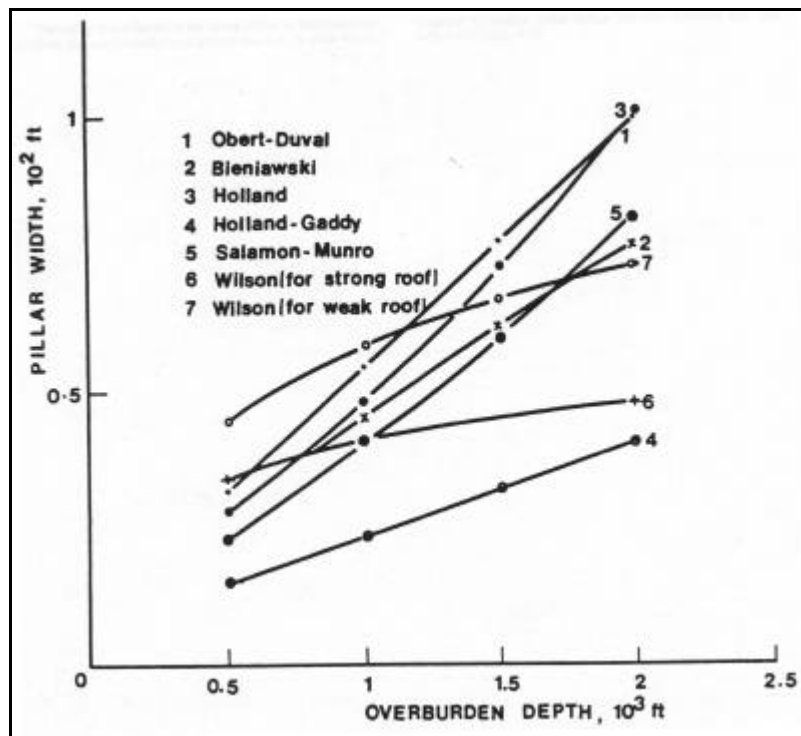


Figure 1: - Large range of pillar width calculated by various pillar strength equation (Peng, 1992).

In the second approach (i.e. the method involving numerical analysis) the stress distribution within the mine is determined using various numerical methods (e.g. finite element, finite difference, etc.). This method is more accurate because it takes into account the effects of variations in material properties in the roof and floor areas, which significantly affects the stress distribution within the pillar. Additionally, more complex material constitutive laws and failure criteria can be incorporated for the pillar and surrounding regions as well as pillar-roof/floor interfaces.

In the following sections various empirical techniques, which have been employed around the globe, are presented and discussed.

2.1.1.2 North America

2.1.1.2.1 Legislation

The Federal Coal Mine Safety Act of 1952 provided for annual inspections in certain underground coal mines, and gave the Bureau of Mines power to issue violation notices and imminent danger withdrawal orders. The 1952 Act also authorised the assessment of civil penalties against certain mine operators, and in 1966, Congress extended coverage of the 1952 Coal Act to all underground coal mines. The Federal Coal Mine Health and Safety Act of 1969, (the "Coal Act") was more comprehensive and more stringent than any previous Federal legislation governing the mining industry. The Coal Act included surface as well as underground coal mines within its scope and required annual inspections of all mines.

In 1973, the Secretary of the Interior, created the Mining Enforcement and Safety Administration (MESA) as a new departmental agency separate from the Bureau of Mines. MESA assumed the safety and health enforcement functions formerly carried out by the Bureau. This avoided any actual or perceived conflict of interest between the enforcement of mine safety and health standards and the Bureau's responsibilities for mineral resource development.

In 1977, the US Congress passed the Federal Mine Safety and Health Act of 1977 (Mine Act), the legislation that currently governs Mine Safety and Health Administration (MSHA) activities. The Mine Act amended the 1969 Coal Act in a number of significant ways, and consolidated all federal health and safety regulations of the mining industry under a single statutory scheme. The Mine Act also transferred responsibility for carrying out its mandates from the Department

of the Interior to the Department of Labour, and named the new agency the Mine Safety and Health Administration (MSHA). The various forms of legislation give MSHA power to require mines to design their underground workings (including water barrier pillars) according to accepted engineering standards under the supervision of competent individuals.

2.1.1.2.2 Early barrier pillar design methods

Dunn proposed the earliest known barrier pillar design method in 1846. This rule states that the width of a barrier pillar should be at least 15 feet at 180 ft of depth, to be increased by 3 feet for each additional 60 ft of depth. Dunn's rule can be described by the following equation:

$$W = \frac{(D - 180)}{20} + 15 \quad (2)$$

where W = barrier pillar width (ft)
and D = depth of mining cover (ft).

Recent observations and research shows that Dunn's rule gives significantly undersized barrier pillar dimensions for a given mining depth. This drawback would be more pronounced in cases of competent pillar roofs, which transfer higher load to the pillar, and also when water pressure on pillars is a concern. It does not account for the effects of seam thickness and side loads applied by water. Hence it is today considered to be an invalid equation for the design of barrier pillars.

2.1.1.2.3 Pennsylvania Mine Inspector's Equation

This equation states that the minimum barrier pillar should not be less than 20 ft, plus four times the thickness of the coal bed, plus 10 feet for each 100 ft or fraction thereof of cover at the boundary in question. The Pennsylvania Mine Inspector's Equation can be mathematically expressed by the following equation:

$$W = 20 + 4T + 0.1D \quad (3)$$

where D = depth of mining cover, or height of hydrostatic head if greater than thickness of overburden, rounded up to the nearest 100 ft.

Figure 2 gives a graphical representation of the above equation for coal seam thicknesses ranging from 4 ft to 12 ft and mining cover depths (or hydrostatic head) of up to 2000 ft. The advantage of this equation is that it considers the effects of seam thickness as well as mining depth. Additionally, it allows incorporating the water pressure, thereby making it a potential candidate equation for the design of water barrier pillars.

Pillar width (w)

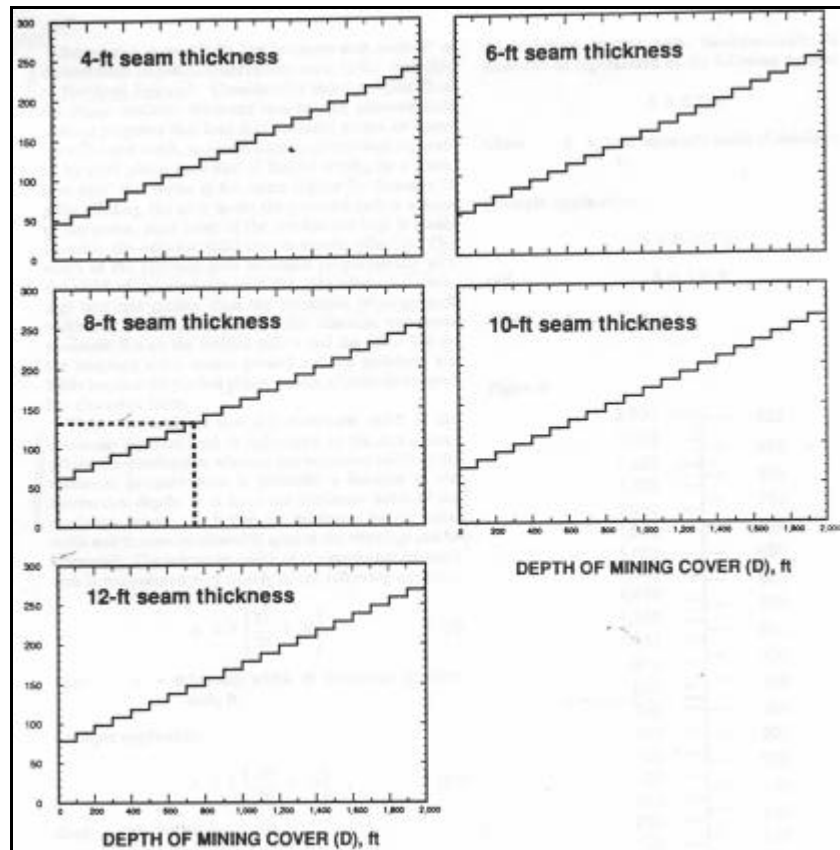


Figure 2: - Graphical representation of Pennsylvania mine inspector's equation for various seam thicknesses (Koehler at al. 1995).

2.1.1.2.4 Ash and Eaton's Impoundment Equation

In 1948, Ash and Eaton proposed a design equation that considered a barrier pillar as a water impoundment dam. The Ash & Eaton equation was intended for use in a coal bed with a slight dip of 3 degrees. The Ash & Eaton equation has the following form:

$$W = 50 + 0.426D \quad (4)$$

The graphical representation of the above equation (for mining depths of up to 2000 ft) is illustrated in Figure 3. Although this equation was developed for the design of water retention dams in the underground environment, there is no provision in the equation for variations in hydrostatic pressure. The impoundment equation gives extremely conservative barrier pillar sizes for a given depth of mining. This implies that the effect of side loading from retained water is indirectly accounted for in the oversize barrier pillar design width predicted by this equation. Additionally, this equation does not consider the effects of coal seam thickness and strength.

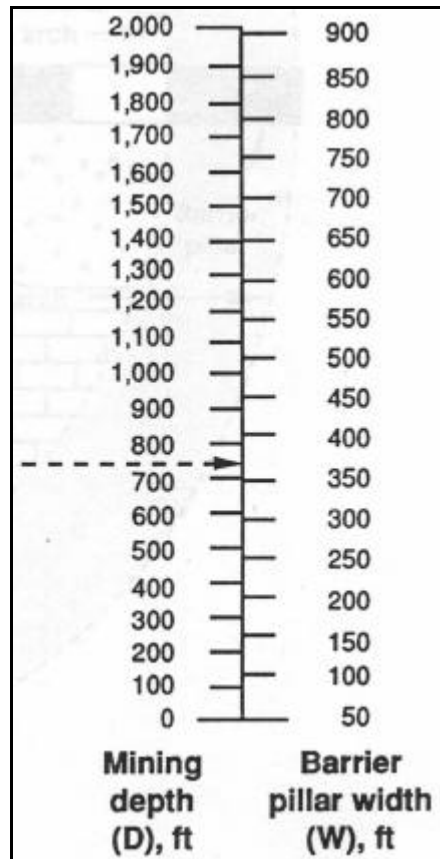


Figure 3: -: Ash & Eaton impoundment equation for mining cover depths of 2000 ft (Koehler et al., 1995).

2.1.1.2.5 The North American Method

The “North American Method” is an empirical barrier pillar design equation developed from observations made in the coal mines of the United State and Canada. The North American Method is expressed mathematically in the following form:

$$W = \frac{(D \times P)}{7000 - D} \quad (5)$$

where P = width of adjacent panel (ft), and D = depth (ft).

Figure 4 illustrates the North American Method, for mining cover depths ranging from 300 to 2,000 ft and adjacent panel widths ranging from 500 to 1,000 ft.

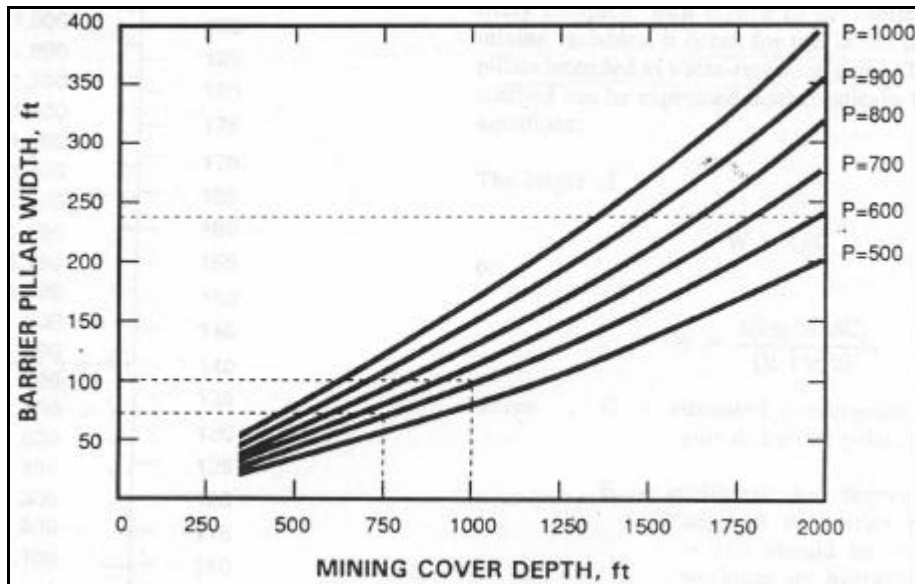


Figure 4: -Graphical representation of North American Method (Koehler et al., 1995).

This method is similar to the pressure arch method employed in Europe and it includes the effect of variations in adjacent panel width. The drawback of this method is that if the adjacent pillar width remains constant, the calculated barrier pillar width increases nonlinearly with depth of mining cover, resulting in over designed pillars at great depth. In the North American Method there is no provision for variations in coal seam thickness and also the effects of coal strength and water pressure are ignored.

2.1.1.2.6 Outcrop Water Barrier Pillars

Of some interest is the design method for outcrop water barrier pillars recently written into the coal mining regulations in Kentucky, USA. This was done in response to several mine "blowouts" in eastern Kentucky in early 1994. These occurred when water pressure built up inside mines and acted on the outcrop barrier pillar of unmined coal. Failure of the pillars allowed the rapid discharge of large volumes of impounded water onto the surface.

The "blowouts" resulted from leaving outcrop barrier pillars that were too narrow and weak to resist the eventual build up of water pressure or too weak to support the overburden. Outcrop barrier pillars are obviously relatively unstressed in comparison to barrier pillars at depth.

The Kentucky Dept subsequently required mines to use a width of at least 50 feet plus the maximum hydrostatic head that can build up on the outcrop barrier, i.e.:

$$W = 50 + H \tag{6}$$

For example, if water could be impounded in the mine to an elevation that is 25 feet above the base of the outcrop barrier, the barrier should be at least $(50 + 25) = 75$ feet wide. If water could be impounded in the mine to an elevation 150 feet above the base of the outcrop barrier, the barrier should be at least $(50 + 150) = 200$ feet wide. This equation is not considered to be appropriate for the design of water barrier pillars at depth, since it ignores the beneficial effects of stress on the pillar, and would require extremely wide pillars, with widths equal to the water head (plus 50ft). It does suggest however that 50 ft would be a minimum pillar width under low stress (and pressure) conditions.

2.1.1.3 Europe

2.1.1.3.1 Old English Barrier Pillar Law

This barrier pillar law is an empirical equation that addresses barrier design in anthracite coal seams. The original mathematical expression for the Old English law is presented as below:

$$W = \frac{H \times T}{100} + 5T \quad (7)$$

where H = hydrostatic head or depth below drainage level (ft), and T = coal seam thickness (ft). Figure 5 demonstrates the use of Old English barrier pillar law in a graphical manner.

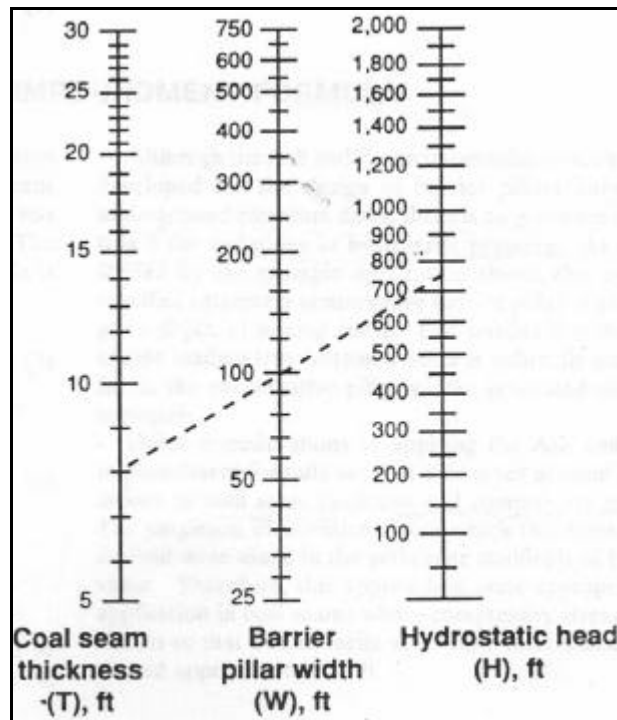


Figure 5: -Graphical representation of Old English barrier pillar law (Koehler et al., 1995).

This equation is based on studies of barrier pillars utilised as water impoundment dams. The use of this equation should be avoided for the design of barrier pillars whose intended function is other than that of an impoundment dam. The reason is that, if no water pressure exists (0 ft hydrostatic head), the equation determines the same barrier pillar width (five times the seam thickness) for all mining depths. The Old English rule also ignores the effect of coal strength. Lastly, this rule was developed from experiences in anthracite coal seams, suggesting additional caution when applying this rule to coal seams in excess of 15 ft in thickness.

2.1.1.3.2 Pressure Arch Method

The pressure arch method is derived from empirical observations made in the coalfields of Northern England, and was introduced in the 1950's. The pressure arch concept proposes that the load is transferred across an opening of limited width, or across a series of openings separated by yield pillars, by a pressure arch that forms in the overlaying strata. Figure 6 describes the pressure arch conceptually. Because of pillar yielding, the area under the pressure arch is a zone of low stress, since most of the overburden load is transferred to the adjacent solid coal or barrier pillar(s).

Field data indicate that (Koehler et al., 1995) the maximum width of the maximum pressure arch is influenced by the strata comprising the overburden, whereas the minimum width of the maximum pressure arch is primarily a function of the overburden depth. It is from the minimum

width of the maximum pressure arch that the minimum barrier pillar width and maximum allowable span of the workings can be calculated.

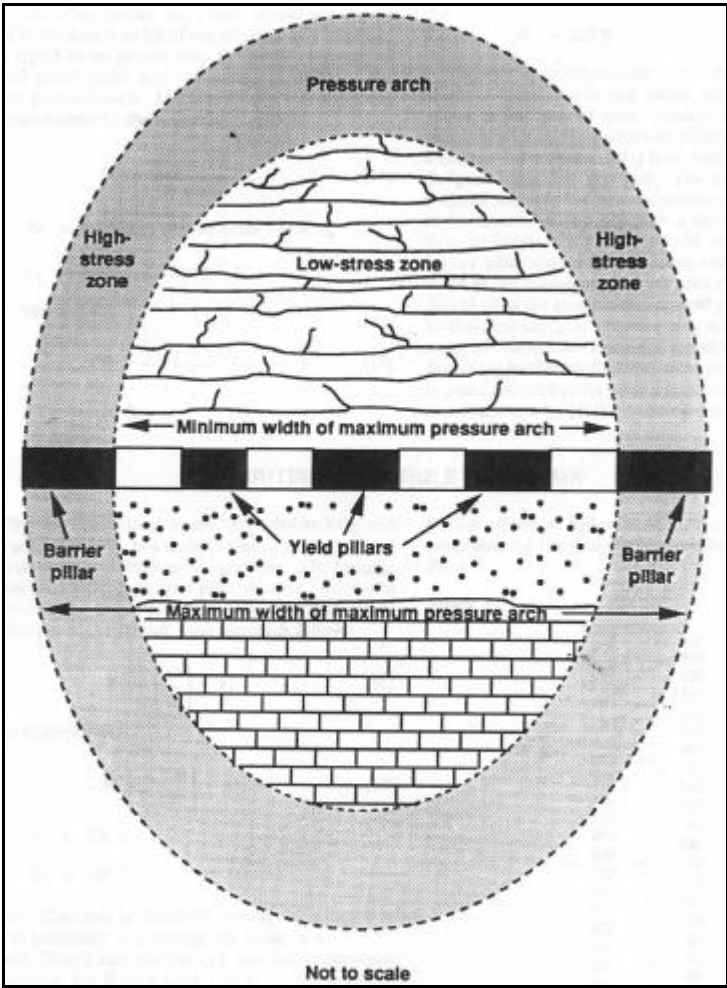


Figure 6: -Conceptual illustration of maximum pressure arch (Koehler at al., 1995).

The minimum width of the maximum pressure arch is represented very closely by the following equation:

$$A = 3 \left(\frac{D}{20} + 20 \right) \quad (8)$$

where A = minimum width of maximum pressure arch (ft).

This equation is not appropriate for overburden depths of less than 400 ft or greater than 2800 ft. Once the minimum width of the pressure arch is known, the proper panel and barrier pillar width may be calculated. The total width of the developed panel should not be wider than 75% of the minimum width of the maximum pressure arch. Then, the minimum width of adjacent pillars must be equal or greater than the mean (average) of the actual panel width and the minimum width of the maximum pressure arch.

2.1.1.3.3 British Coal Rule of Thumb

The “British Coal rule of thumb,” reported by King & Whittaker (1971), is a design equation developed and used successfully by British mine operators. The equation states that the width of a barrier pillar should be one-tenth of the overburden height plus 45ft. In mathematical form:

$$W = \left(\frac{D}{10} \right) + 45 \quad (9)$$

The British Coal rule of thumb does not account for variations in coal seam thickness and strength.

2.1.1.3.4 Holland Convergence Method

Introduced in 1973, the “Holland convergence method” is based on room closure studies conducted in several Polish mines by Borecki & Belinski (1964). The convergence method utilises the estimated entry closure on the high stress side of the barrier pillar to determine appropriate pillar size. Entry convergence is estimated using a best fit graph of field data collected in numerous coal seams having similar physical properties. Adjustments for variations in seam thickness and unconfined compressive strength of the coal are made to the estimated convergence value to be used in the following equations. Although the convergence method is relatively complete with regard to accounting for the basic mining parameters, it is not for use in the design of barrier pillars intended as water-retention dams. The convergence method has the following mathematical form:

The width (W) should be the larger of:

$$W = 15T \quad (10)$$

or

$$W = \frac{5(\log 50.8C)}{E \log e} \quad (11)$$

Where:

C = estimated convergence on high-stress side of barrier pillar (in),

E = coefficient for degree of extraction adjacent to barrier pillar; value $E = 0.07$ should be used if adjacent workings are hydraulically backfilled, value $E = 0.08$ should be used if strip packwalls are built next to the barrier pillar, value $E = 0.085$ should be used if partial extraction is practised, and value $E = 0.09$ should be used if complete caving will occur in adjacent panel, and

e = base of the natural system of logarithm

T = seam thickness

Appropriate engineering judgement is required when applying the Holland convergence rule, which is based on field data from a specific coal mining region of Europe.

2.1.1.4 India

India is important to this subject because there have been several accidents related to the failure of water barrier pillars in Indian coal mines.

2.1.1.4.1 Legislation

Under the constitution of India, Safety, Welfare and Health of workers employed in mines are the concern of the Central Government (Entry 55 – Union List – Article 246). Safety is regulated by the Mines Act, and is administered by the Directorate – General Mines Safety (DGMS) under the Union Ministry of Labour.

The first Mines Act to regulate Safety, Welfare and Health of person employed in mines was enacted in the year 1901. This was amended several times and the final one is called the Mines Act, 1952. This was also amended in 1959 and recently in 1983. The Coal Mines Regulation Act of 1957 mandates that abandoned mines are to be “filled with sand, in order to prevent fire or water percolating to adjoining mines”. (It would be surprising if this was in fact carried out). In India, it seems that water barrier pillar widths of 200 ft are considered “optimum”, but are often allowed to be less than this – 80 ft being a common width. Practical experience suggests that widths less than this 80 ft can result in failure.

The Coal Mines Regulation Act of 1957 mandates that mine maps should be updated every quarter. Section 127(3) of the Act prohibits mining in the vicinity of abandoned or adjoining mines. It seems that underground maps can be years out of date, and this may lead to accidental breaching of barrier pillars.

2.1.1.4.2 Water barrier pillar failures

India has suffered several recent mine disasters due to the failure of water barrier pillars. Of 15 major recent mine tragedies, seven have occurred in the Jharia region, and all have been the result of water inundation. Over 800 miners died in various mine accidents in the last two decades following flooding. These have in many cases resulted in multiple fatalities, for example:

- 29 miners died in February 2001 in the 240 m deep Bagdigi colliery. The mine flooded when water from the adjacent Jayrampur mine breached a barrier pillar.

Records and underground plans of the Bagdigi mine showed that the thickness of the barrier between Bagdigi and adjacent Jayrampur mine was reduced to 60 ft from 80 ft (though some reports suggest that it may have been only 30 ft wide at failure). It appears that reduced thickness of the barrier resulted in it failing under water pressure from the adjacent flooded mine.

Other major water inrush related disasters on coal mines which are not necessarily directly related to barrier pillar failures include:

- 64 miners died in an incident in the Gaslitand underground colliery of the Bharat Coking Coal Ltd. (BCCL) on September 26, 1995. The miners were trapped when water from the nearby Katra Jore canal gushed in following incessant rain.
- 70 miners were trapped in 1992 in the Mahabir coal mine near Ranigunje due to flooding of the pit,
- 375 miners died in the Chasnala mine tragedy in December 1975. This may be the worst ever mine disaster due to flooding (although details of similar mine accidents in China are difficult to come by). It appears that a large volume of water (135,000 cubic meters) rushed into the seam of the mine from a waterlogged incline that had been abandoned in 1949 following a blast for construction of a new drive.
- 3 miners died in the South Govindapur colliery, when the mine was flooded as a concrete roof caved in.

After the Chasnala mine disaster in 1975, an expert committee suggested steps to strengthen local expertise for mine safety and design.

2.1.2 Design information and case studies

2.1.2.1 In-situ large-scale tests

In order to assess the stability of large pillars, compression tests are most relevant. In-situ large-scale tests are conducted because they represent the rock mass condition better than laboratory specimens. According to Bieniawski (1987), numerous large-scale in-situ tests were conducted since 1937 mainly in connection with such projects as pillar design in coal and iron ore mines. The aim of these tests was to determine the strength behaviour of pillars, establish the deformation characteristics of the rock mass, and to obtain the post failure load-displacement data for coal pillars. A more detail review of some of these tests, which their results are applicable to actual engineering problems, is given in Bieniawski (1987).

Wang, Wolgamott & Skelly of Colorado School of Mines conducted the largest in-situ test in USA. This was a test performed in the Pocahontas No. 3 coal seam in southern West Virginia in which a square pillar of 80 ft wide (24 m) by 7 ft (2.3 m) high was systematically cut until it was reduced to a width of 24 ft (7.9 m). Analysis of the total stress changes and the estimated pre-mining stress lead to an original pillar strength being between 2900 psi and 3100 psi which could be represented by the equation given in Table 1. The applicable factor of safety ranged from 1.5 to 2.0.

In-situ large-scale tests on coal have shown that pillar failure was usually associated with gradual opening of vertical cleats and spalling from the corners of the specimens (Bieniawski, 1987, Bieniawski & Van Heerden, 1975). The pillars tested, failed in a controllable non-violent manner leading to gradual specimen disintegration and resulting in a symmetrical double pyramid at the conclusion of the test. At this stage the specimen was completely crushed and small pieces could be removed forcibly even from its core. The total axial deformation was of the order of 20 mm and there was a residual strength of the order of 1 MPa.

2.1.2.1.1 Case Studies

Traditional barrier pillar design methods do not adequately account for overburden caving characteristics, the timing and magnitude of associated load transfers, the occurrence of unusual geologic features, or the effects of multiple-panel mining (Koehler et al., 1989). Barrier pillar placement and performance is most important in multiple-seam mine settings where seam interaction is likely. It is estimated that 5 to 15% of recoverable reserves are lost to over-sized barrier pillars in modern coal mines. On the other hand, under-sized barrier pillars can result in significant reserve losses due to excessive load transfer to adjacent openings. The following presents a case study of a narrow barrier pillar at the Star Point No. 2 Mine, a multiple-seam narrow barrier pillar operation located in central Utah. This section gives a detail of investigation with respect to barrier pillar behaviour and demonstrates the use of the collected pressure data in projecting an improved barrier design.

Three mineable coal seams, dipping 2 to 3 degrees, exist within the Star Point No. 2 mine property and are in descending order, the Wattis, the Third, and the Hiawatha. Coal thickness ranges from 8 to 12 ft in the Wattis and Third seams and interburden between the seams varies from 15 to 55 ft. The immediate roof of the Wattis seam is composed of mudstone and siltstones. In January 1988, two superimposed instrumentation sites were established in the Wattis and Third seams as illustrated in Figure 7. This area was noted for high overburden depth and the occurrence of thick (> 30 ft) sandstone channels in the roof, floor, and interburden. Moreover, concentrated mining-induced loads were expected in this area as previous studies conducted had demonstrated a relationship between channel features and localised stress concentrations. The barrier pillar was 80 ft wide at the study site and overburden depth was approximately 1150 ft. Site instrumentation included USBM hydraulic borehole pressure cells (BPCs) discussed by Demarco et al. (1988), and roof-to-floor closure stations. Vertical-horizontal BPC combinations were installed to determine absolute ground pressures in the coal directly beneath the Wattis gateroads and barrier.

Year and country	Investigators	Coal seam	Specimen Cross-Section	Width h (m)	Height (m)	Width/Height Ratio	No. of Tests	Formula	Units	Remarks
1933-1939 USA	H.P. Greenwald H.C. Howarth I. Hartman	Pittsburgh	Square	0.81 - 1.61	0.78- - 1.61	0.50- - 1.03	5	$s_R = 700 \sqrt{w/h}$	(psi)	
1939-1941 USA	H.P. Greenwald H.C. Howarth I. Hartman	Pittsburgh	Square	0.30 - 1.07	0.74- - 0.77	0.41- - 1.68	7	$s_R = 2800 \left(\sqrt{w} / \sqrt{h^5} \right)$	(psi)	
1965-1966 South Africa	Z.T. Bieniawski	Witbank	Square	0.61 - 1.22	0.61- - 1.22	0.50- - 2.00	19	$s_R = 7.6 w^{0.16} / h^{0.55}$	(MPa) with w and h (m)	Valid for w/h <1 and w < 1.5m
1967-1968 South Africa	Z.T. Bieniawski	Witbank	Square	1.50 - 2.00	0.60- - 2.00	1.00- - 3.10	16	$s_R / s_1 = 0.64 + 0.36(w/h)$		Valid for w/h <1 and w > 1.5 m
1970-1972 South Africa	N.G.W Cook H. Wagner	Usutu	Square And rectangular	0.60 - 2.00	0.86- - 2.00	0.60 - 2.20	12	$s_R = \sqrt{w/h}$	(MPa)	$s_R = 7 + 4w/h$ (MPa) also Fits the data
1973 South Africa	W.L. van Heerden	New Largo	Square	1.40	0.41- - 1.24	1.14- - 3.39	10	$s_R = 10 + 4.2w/h$	(MPa)	
1977 USA	F. Wang J. Wolgamott W.A. Skelly	Pocahontas # 3	Square	7.90 - 24.0 0	1.76	4.48- - 13.60	1	$s_R / s_1 = 0.78 + 0.22w/h$		

Table 1: -Summary of strength equation from large-scale in-situ tests (Bieniawski, 1987).

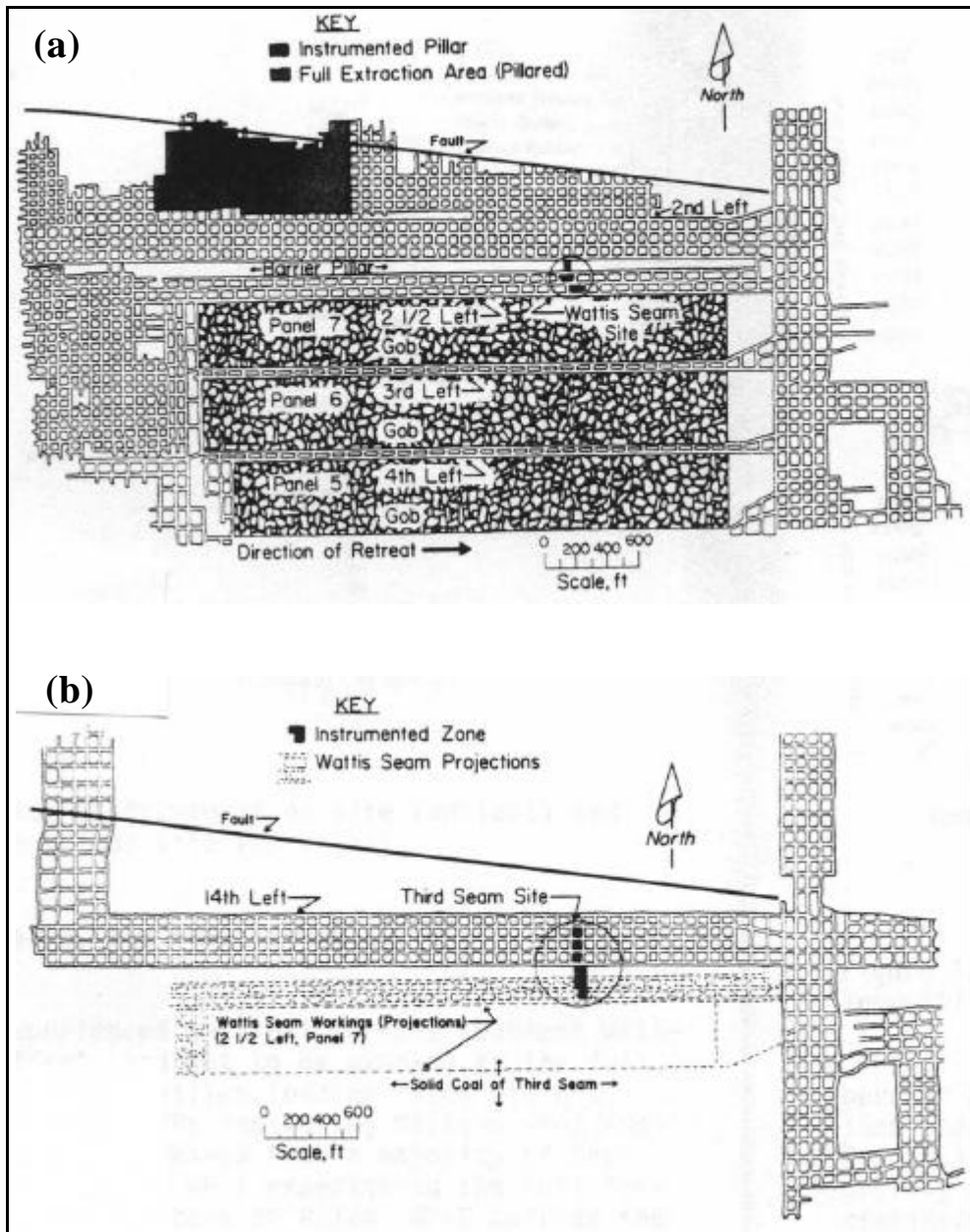


Figure 7: -a) Location of Wattis seam instrumentation site, b) Location of underlying Third seam instrumentation site (Koehler et al., 1989).

Figure 8 shows vertical BPC pressures across the study area for six phases of ground response to mining. Longwall face position (FP) relative to Wattis barrier pillar cells define pressure profile sequence and stage of mining (Note: - indicates inbye FP, + indicates outbye FP). Substantial forward abutment effects were seen at approximately -198 ft FP when accelerated loading of pillars wp-1 and wp-2 was noted. At -11 ft FP, pillar wp-2 experienced the full forward abutment while wp-1 pillar, because of the offset, had yet to be exposed to the full abutment load. Barrier and 14th left pillar loading rates did not accelerate between -189 ft and

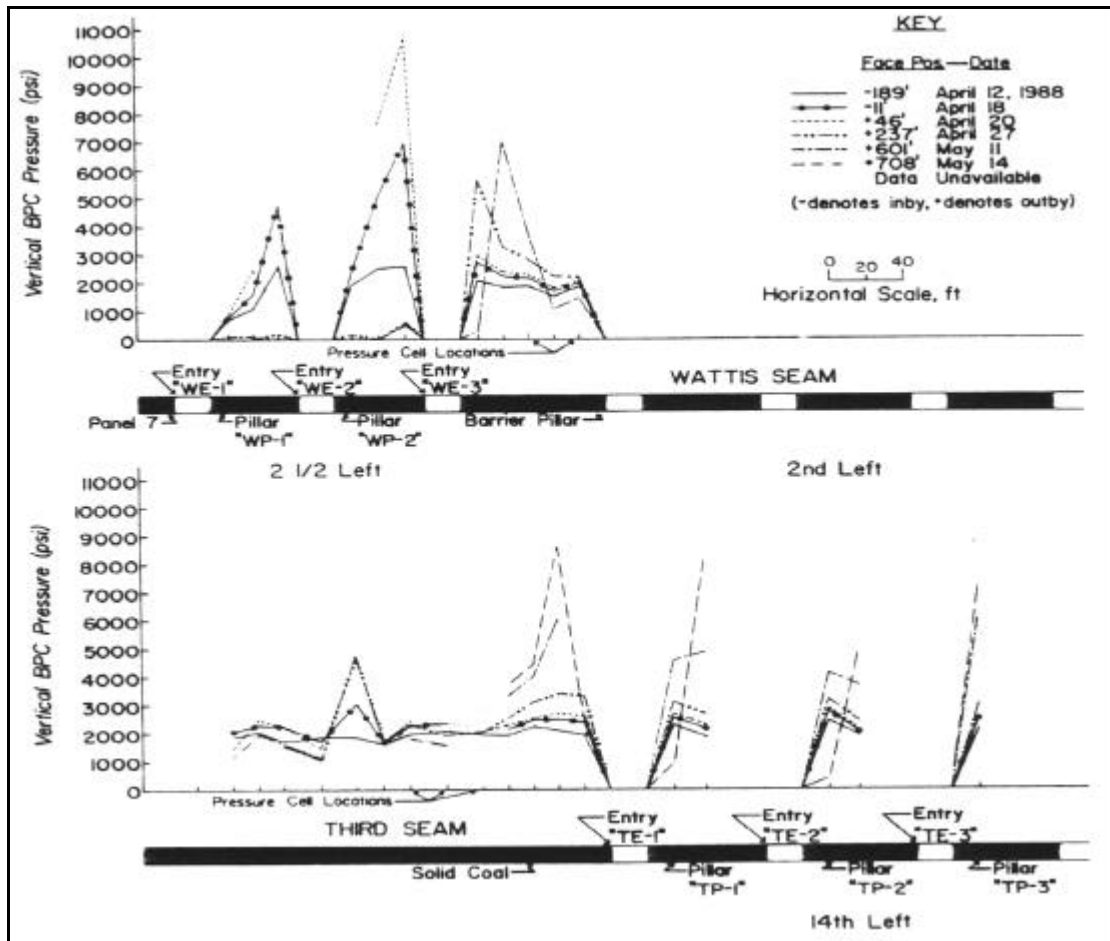


Figure 8: -Vertical BPC pressure profiles across study area for selected longwall face positions-looking inbye (Koehler et al. 1989).

-11 ft FPs indicating pillars WP-1 and WP-2 shielded the barrier and lower workings from a majority of the forward abutment. At +46 ft FP, pillar WP-1 experienced the full forward abutment, while the north rib and core of pillar WP-2 carried the side abutment and loads transferred from the WP-1 row of pillars. Again, barrier and 14th left pillar loading rates did not accelerate between -11 ft and +46 ft FPs.

From +46 ft FP to +237 ft FP, barrier pillar stress continued to build up. Pressure increases in the BCP's in the solid coal underlying the barrier pillar confirm a build-up of load on the south rib of Entry TE-1. Shortly after +237 ft FP, barrier pillar BPC W7 recorded a peak pressure of 6200 psi: cell pressure then began to drop, apparently due to failure of the south rib. Evidently, progressive failure of the barrier's north rib also began shortly +237 ft FP. Progressive failure of the barrier's ribs continued until at least +601 ft FP with load redistributing inward. At +601 ft FP, Wattis seam data collection was terminated due to hazardous conditions. To evaluate the performance of the Wattis barrier pillar it was necessary to determine at which phase of extraction the maximum integrated pillar load changes occurred, and the distribution of that load change across the pillar width. Total integrated load change due to mining was calculated for face positions from +46 ft to +601 ft by comparing mining-related BPC pressures to equilibrium pressures. The result of analysis is presented in Figure 9.

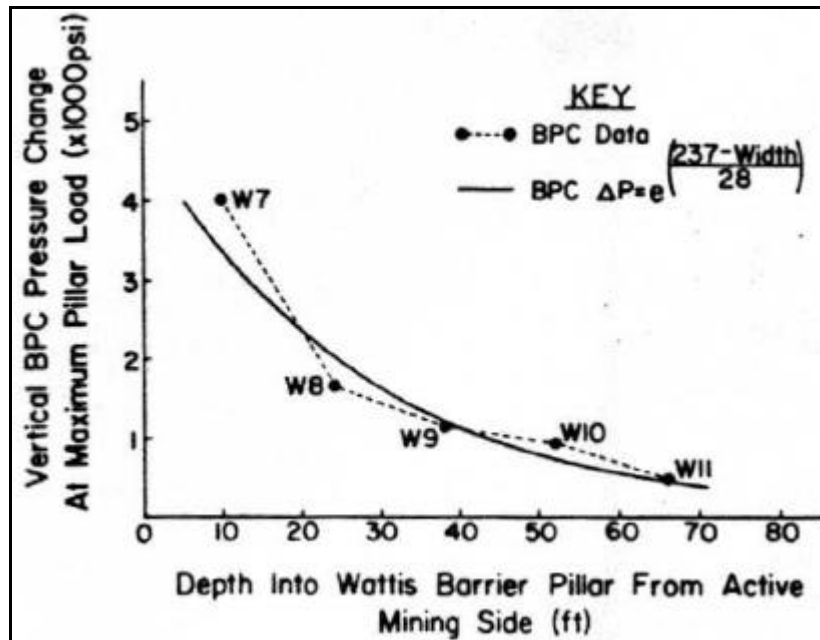


Figure 9: - Vertical BPC pressure change at maximum pillar load versus depth into Wattis barrier pillar from active mining side.

As evidenced by field data, the barrier was of insufficient width at the study site to support the mining-induced loads. Conducting a regression analysis on collected data, a natural log-based pillar pressure equation was determined as a function of pillar width. This equation is shown on Figure 9. Due to the load decaying nature of the obtained equation, a value of BPC $\Delta p=0$ psi predicts infinite barrier width. For absolutely no load transfer to the opposite mining site (BPC $\Delta p=1$ psi), the barrier pillar width was predicted to be 237 ft. A more realistic yet less conservative approach was to allow small load changes on the rib opposite mining. Substitution of BPC $\Delta p=10$ psi into the equation resulted in a pillar width of 172 ft. It should be realised that the produced equation is a mathematical representation of monitored data in a single barrier pillar subjected to specific set of mining conditions and can not be used as a general design equation. However, it shows that mine-specific loading conditions can be incorporated into the design of barrier pillars, thus minimising unwanted losses of reserve due to unsafe, under- or over-sized barrier pillars.

2.1.2.2 Numerical methods and monitoring

The width of a barrier pillar is the most important parameter governing pillar performance. An undersized pillar results in excessive load transfer to adjacent mine workings and leads to ground instability problems. Conversely, oversized pillars eliminate the instability problems, but can substantially reduce the available ore reserve. The objective of barrier pillar design is to maximise the ore recovery while maintaining safety. The barrier pillar design methods discussed in this report are all empirical methods and have been developed from field measurements and observation of pillar behaviours at various mine sites.

Laboratory measurements of physical properties of coal and scaling of lab results to the prototype have been used in the development of some empirical approaches. Most of the barrier pillar design methods that have been presented ignore certain important design parameters such as coal strength, coal permeability and its variation as a function of depth and stress. Their use thus requires engineering

judgement and perhaps more sophisticated analyses such as numerical modelling. Furthermore, the effect of water pressure on pillar stability has been ignored by most empirical methods or taken into consideration in a vague manner. Therefore, the use of empirical method is advisable if the design is supported by on-site monitoring. This means that the barrier pillar should be redesigned based on continuous observation of pillar behaviour, although it is recognised that this is impractical in many cases.

The numerical approach to barrier pillar design offers significant advantages over empirical methods. Numerical codes are useful tools to build models of mining structures, which have complex geometry, geology, and boundary conditions. For example multi-level mining in coal mines, which add more complexity to the design, can be very well handled when using numerical methods. This method is more accurate because it takes into account the effects of variations in material properties in the roof and floor areas, which significantly affects the stress distribution within the pillar. Additionally, more complex material constitutive law and failure criterion can be incorporated for the pillar and surrounding regions as well as pillar-roof/floor interfaces.

Moreover, numerical codes can be used for parametric studies analysing the effects of various factors (such as material strength, variations in material property due to water inflow into the material and major geologic structures, mining sequence) on structure response. Therefore, numerical techniques, once calibrated against field observations for a given ground condition, can be successfully used in other similar ground conditions to model/simulate different mining scenarios.

2.1.3 Design parameters for water barrier pillars

The aim of this section is to review the important design parameters to be considered in the design of water barrier pillars in coal mines if the design is done by conventional engineering methods, as opposed to empirical design. Water barrier pillars are generally designed to provide stability, protect the active mine work areas from water inflow, and eventually act as an air seal for ventilation purposes. Important issues that should be considered in the design of water barrier pillars are; stability of entries, maximum water head to be accumulated behind the pillar, overburden depth and in-situ stress, variation of coal strength and hydrologic parameters (such as permeability) as a function of depth, intensity of weathering, distribution of coal cleat and major discontinuities, and the location and orientation of geological contacts in the area of interest. The following are further discussions of the most important parameters in the design of water barrier pillars.

2.1.3.1 Pillar size

It is very difficult to propose a general equation applicable to the design of water barrier pillars. Section 1 presented a comprehensive review of all available barrier pillar design equations. None of the empirical equations discussed in sections 1.2 to 2.3 consider the important geomechanics and hydrologic parameters mentioned above. In addition, the equations are generally based on mining experiences at relatively shallow depths (say less than 1000 ft). This means that the effects of higher in-situ stress level, further complexity of mine structure as mining goes deeper, change in overall rock mass behaviour due to extensive mining and higher stresses, and increased height of hydrostatic water head have been ignored in all the empirical equations. Therefore, the use of the empirical equations discussed earlier in the report, is not recommended for determining the appropriate water barrier pillar size, in particular at greater mining depths. Instead, 3D and 2D numerical codes can be employed to incorporate the effects of mine geometry, mining sequence, vertical confinement offered to the pillar, high in-situ stress, varying material properties, to successfully determine the optimum pillar size. Nevertheless, the optimum pillar size alone does not offer assurance against water seepage into the pillar and possible serious water inflows. Coal hydrologic parameters and orientation of discontinuities must be taken into consideration in the design of ultimate pillar size.

2.1.3.2 Permeability and porosity of coal formations as a function of depth/stress

Conventionally, a rock mass is assumed to be a naturally porous medium. Therefore, the flow of water through a rock mass can be assumed to obey Darcy's law, which has the following form:

$$Q = AKi \quad (12)$$

where Q = discharge rate, A = discharge area, K = coefficient of permeability, i = hydraulic gradient.

Permeability is a measure of the ease with which a fluid will flow through a porous medium. Permeability also depends on fluid properties such as fluid density, fluid viscosity, and medium characteristics. The following equation defines permeability as a function of these parameters:

$$K = Cd^2 \frac{\gamma}{\mu} \quad (13)$$

where C = dimensionless constant, d = characteristic dimension of the medium, γ = fluid density, and μ = fluid viscosity.

The most commonly used relation, which relates permeability to the physical properties of porous media, is the Carman-Kozeny permeability equation. This expression, which is detailed in Carman (1937) and McKee et al (1988), clearly illustrates the relative importance of porosity, pore nature, and fluid properties on the rate of discharge in a medium. Further analytical treatment of coal hydrologic parameters is avoided here and the reader is referred to McKee et. al. (1988) for an interesting analytical treatment of stress dependency of coal permeability and porosity. Instead, some of their correlation of field data with analytical results will be presented here.

The objective of the McKee et. al. (1988) study was to develop relationships for permeability, porosity, and density of coal formations as a function of effective stress. Using the Carman-Kozeny permeability equation, the equations were developed for both constant and variable pore compressibility and the material grains were assumed to be incompressible. These relations, then, were fitted to laboratory and field data. Eight laboratory core tests (four coal, one granite, two sandstone, and one clay) were used to illustrate the applicability of the theory. Also more than 40 field permeability data points from the Piceance, San Juan, and Black Warrior basins (USA) were collected and fitted to the theory with a correlation coefficient of 0.8 to 0.95. While some scatter was evident, the data indicated that permeability decreased with depth. Some initial success was achieved by drawing an empirical straight line correlation between depth and permeability of log-log plots, and led to the search for more fundamental theory to explain the data and correlation. Moreover work at the Institute of Gas Technology documented the strong stress dependence of core sample permeability in the laboratory. These and other laboratory studies have shown that coal permeability decreases by one or two orders of magnitude when effective stress is increased by 2000 psi (13.8 MPa) (Rose et al., 1984).

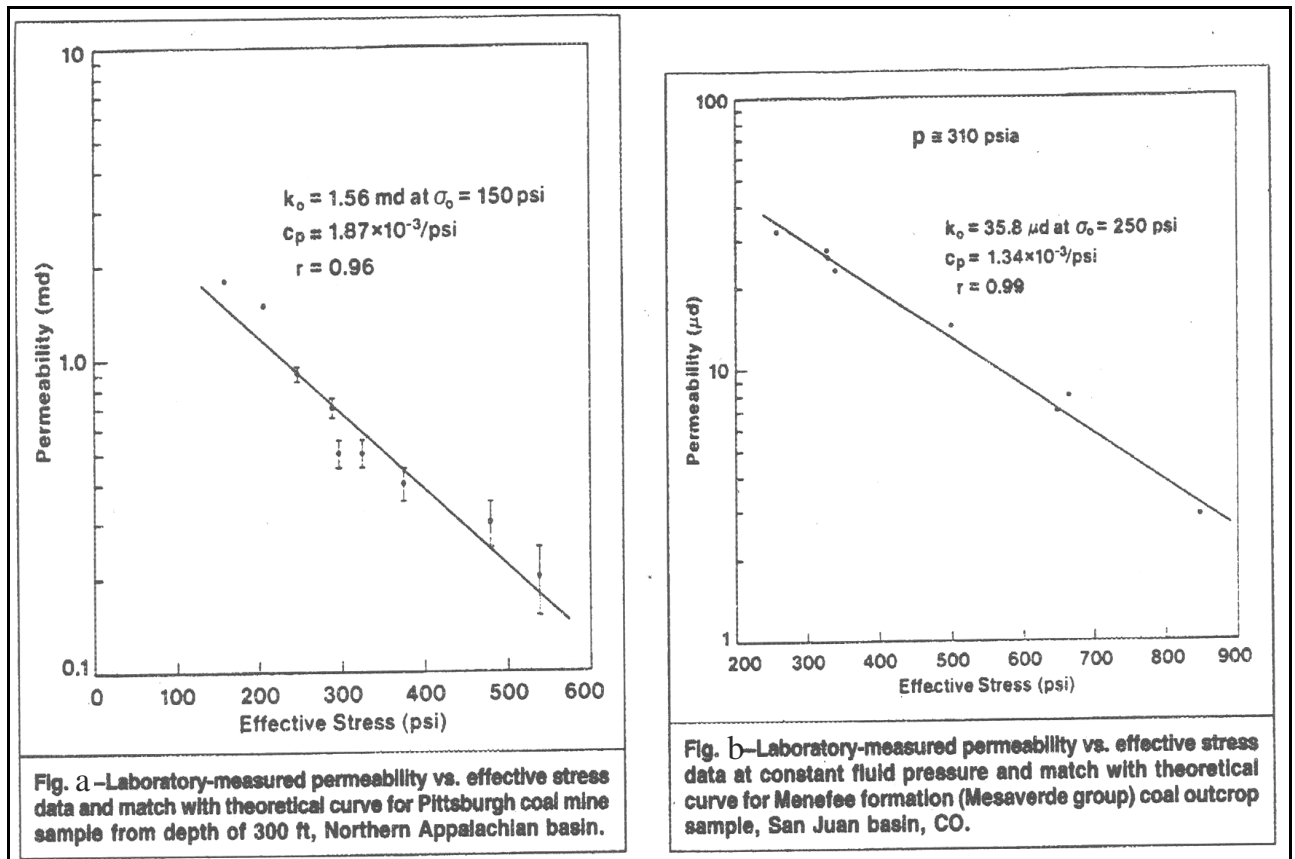


Figure 10: -Variation of permeability as a function of stress-constant pore compressibility (McKee et al., 1988).

Figure 10 demonstrates permeability versus stress for two coal samples tested in the laboratory. Figure 10-b is the result of the test that confining pressure was varied. The permeability of this sample was more than two orders of magnitude less than the test result in which confining pressures were kept constant (Figure 10-a). A relatively good correlation coefficient obtained between lab and theoretical data justifies the assumption of constant pore compressibility. However, Somerton et al. (1974) showed that compressibility is unlikely to remain constant over the entire stress history. Instead, it will approach the rock (or grain) compressibility as effective stress increases, because small asperities on the cleat face resist closure and must be deformed or crushed before further reduction in porosity is achieved. The result is a departure from linearity (constant pore compressibility). The constant compressibility that was observed for the tested samples (Figure 10) implies that the material was initially relatively consolidated (McKee et al., 1988). As a general rule, compressibility declines with increasing stress, although on some samples it may increase. Since a stress-dependent compressibility can be sample-specific, a general function can not be determined. Assuming an exponentially declining compressibility, theoretical curves were fitted (McKee et al., 1988) to the laboratory data. Further correlation of theory with lab and field data from greater depths can be seen from McKee et al. (1988). Figure 11 shows the variation of specific density as a function of depth for shale.

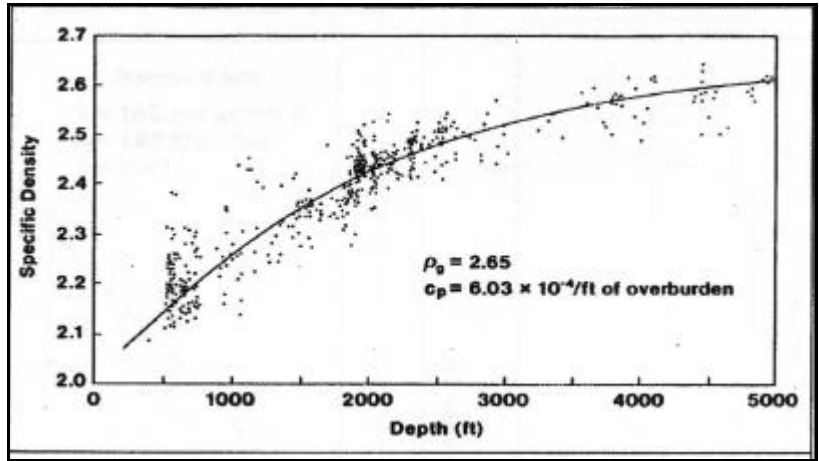


Figure 11: -Laboratory-measured density versus depth data and theoretical match for shale core samples from northern Oklahoma (McKee et al., 1988).

Figure 12 shows the variation of permeability versus lithostatic depth/effective stress for Piceance, San Juan, and Black Warrior basins. Because of scarcity of data on depth dependence of compressibility a constant value was used for pore compressibility when using the theoretical approach. Nevertheless, a good data fit to theory was obtained.

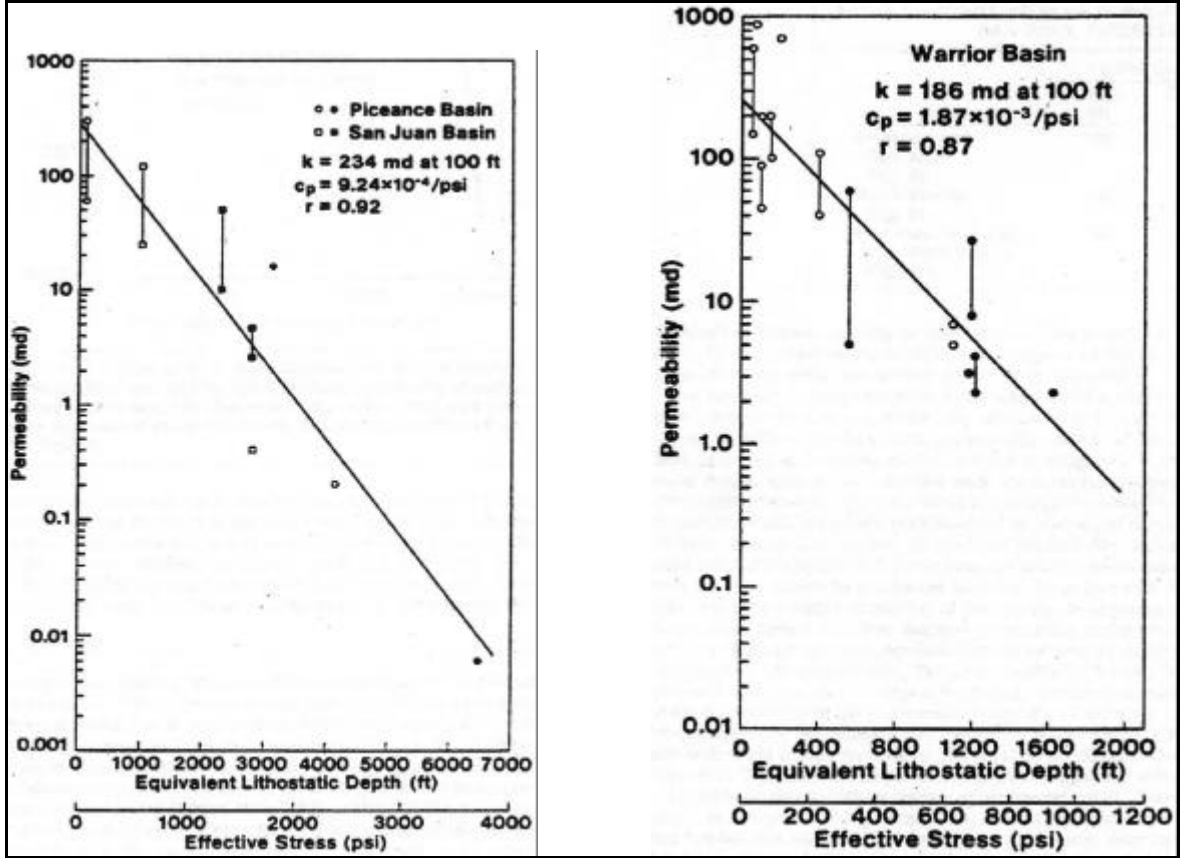


Figure 12: - Semilog plot of field-test-derived and estimated permeabilities with equivalent lithostatic depth (and effective stress) and match with theoretical curve for coal seams in the Piceance, San Juan, and Black Warrior basins (McKee et al., 1988).

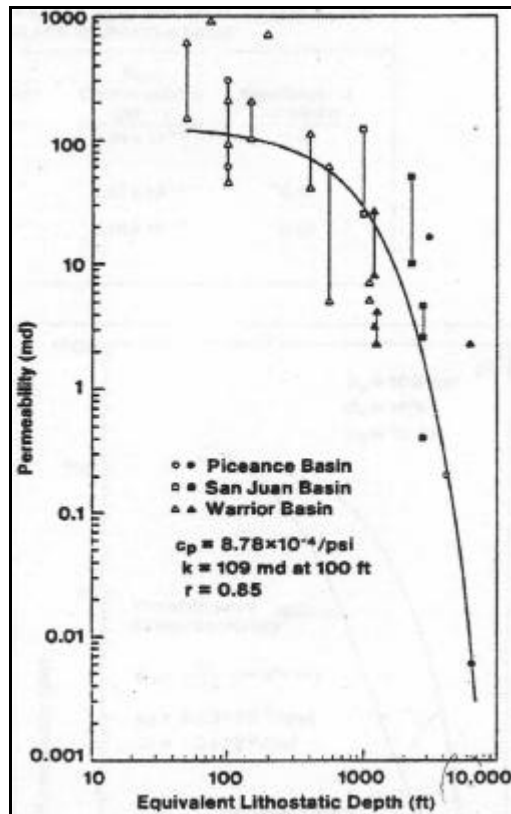


Figure 13: -: Log-log plot of field-test-derived and estimated permeabilities with equivalent lithostatic depth (and effective stress) and match with theoretical curve for combined data from coal seams in the Piceance, San Juan, and Black Warrior basins (McKee et al., 1988).

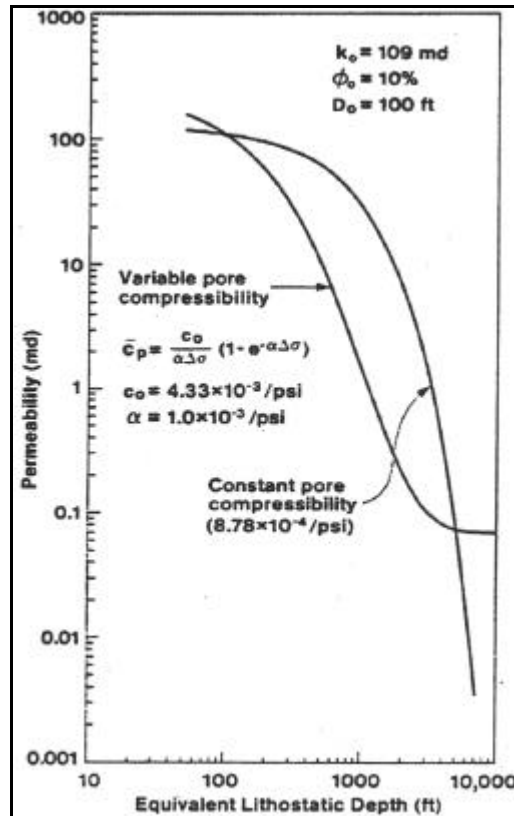


Figure 14: -Variations in geologic log-derived permeability with depth and match with theoretical curve for Miocene mudstone, Nagaoka plain, Japan (McKee et al., 1988).

Figure 13 shows a log-log plot for all the coal permeability results, as a function of depth, obtained to date from the Piceance, San Juan, and Black Warrior basins, except for unknown anomalies. A good correlation of data with the theory is seen in the figure and pore compressibility for all data combined is nearly the same as that for an individual basin. Again, constant pore compressibility was used as the simplest assumption. Figure 14 compares constant pore compressibility versus exponentially declining pore compressibility. The curve for constant pore compressibility is the same as Figure 13. For variable pore compressibility, initial compressibility was selected such that average pore compressibility represented the data presented in Figure 13. The constant defining rate of decline of compressibility, α , was taken as the average value determined from lab data. Figure 14 shows that with exponentially declining pore compressibility, permeability will eventually become constant. However, the current field data available for these basins do not warrant use of exponentially declining pore compressibility.

The presented correlations outline a useful approach in order to determine the permeability variations as a function of depth/lithostatic stress. This approach gives an overall picture of rock mass permeability at a macro scale and can be cautiously used in the design of barrier pillars if the rock mass is in good condition, has a uniform distribution of discontinuities, and the lithostatic stress is the only governing stress. However, this is not generally the case. There are always anomalies of discontinuities and geologic structures in the rock mass and increased permeabilities caused by these local anomalies are much larger than permeabilities obtained from core drilling and laboratory testing. Structural deformation, folding, and faulting cause secondary or fracture permeability. Moreover, high horizontal in-situ stress can also

enhance or reduce permeability. Also, water pressure can act against in-situ stresses and this implies that effective stress should be always considered in the design. According to Noel et al (1989), while impounded water will gradually seep through a coal barrier in minor quantities the greatest leakage will occur along bedding planes just above or below the coalbed or along localised geologic structures such as faults, joints, paleochannels, and slickensides. Thus, in laying out barriers every possible precaution should be taken in order to avoid anomalous geologic conditions.

2.1.3.3 Pillar rock mass properties and distribution of major geological structures within the pillar

It is obvious that rock mass properties govern a barrier pillars behaviour against applied loading and also affects the flow parameters of the rock medium. Distribution of and orientation of the discontinuities defines the water flow path and potential instability problems due to water inflow. It appears that coal formations are more uniform, from a structural and fracture distribution point of view, than other rock formations. Hence, the contact between various formations (in a coal basin) and flow properties of contacts and their filling material are the most important issues that must be considered in the design of water barrier pillars. Miller and Thompson (1974) investigated various factors that influence the retardation of seepage by barrier pillars in the Appalachian Plateau coal region and found that water usually flows along bedding and other separation planes such as slickensides and localised geologic structures rather than through intergranular spaces.

Thus, when designing barrier pillars, care must be exercised to avoid bad geologic conditions (such as contacts and localised porous structures) and pillar geometry/configuration should be selected such that detrimental effects of these structures (from a water flow viewpoint) should be minimised. In addition to identification of these anomalous geologic conditions, attention must be paid to the seepage through the pillar, because it may lead to dissolution and piping of the coal and surrounding rock mass and threat the long-term pillar stability. Furthermore, seepage may result in pumping and treatment costs.

2.1.4 Summary and conclusions

In addition to the “rules of thumb” presented earlier, the following brief summary points cover actual practice in selected countries, and suggestions for carrying our pillar design by “conventional methods”.

For most UK mines, coal barrier pillars should be not less than 120 ft (37m) in width, according to Whittaker and Singh (1978). This seems to provide an “ample margin of safety” for most UK conditions, even though the original design rule ignored the permeability of the coal (or mining depth).

In Eastern Canada, no coal mines are currently in operation, but at the time that the Westray Mine was operational (up till 1992) the Nova Scotia mining regulations required 100m (328 ft) barrier pillars between new mines and older flooded workings. This was probably needed to account not only for the actual barrier, but also for inaccuracies or errors in locating old workings, possibly because of incomplete records, or inaccurate survey techniques used at the time. Westray was also a relatively deep coal mine, at over 300m.

In Illinois, the law requires barrier pillars of at least 200 ft (61m) wide to be left between coal mines.

The Kentucky Department of Mines and Reclamation requires mines to design outcrop barrier pillars with a width of at least 50 ft plus the maximum hydrostatic head that can build up on the outcrop barrier, i.e. $W = 50 + H$. This is not appropriate for barrier pillars at depth.

India seems to have had more problems with water barrier pillar failures than most other countries. It is thus instructive to learn from the experience of that country. In India, the 200 ft (61m) 'optimum' width would appear to be adequate in mines up to 240m deep, although it seems that some mines use water barrier pillar widths of only 80 ft (24.4m). Failures have occurred at widths less than 80 ft, and there is some evidence that these may have been caused by survey error or lack of up-to-date records.

If conventional engineering design is to be done, then it will be necessary to carry out formal analyses of coal and rock stresses and strength. It is evidently very important to account for the presence of discontinuities, since these can control the stability of and flow through water barrier pillars.

It is also necessary to make some estimates of the permeability of the coal seam and host rock. It is suggested that Figure 12 and Figure 13 can be used to estimate the permeability of the coal, provided appropriate in-situ test measurements are done to confirm the general applicability of the plot. A good correlation of data with the theory is seen in the figure and pore compressibility for all data combined is nearly the same as that for the individual coal sample.

In most countries, modern legislation has changed to requiring the barrier pillars (as for other parts of the mine) to be "designed to accepted engineering standards, by competent persons". This means that owners are able to use new methods as technology changes, and this also relieves the legislators of the responsibility for the design. If an equation is written into law, and the pillar subsequently fails, then it is possible for the authority to be sued for the loss. Instead, modern practice in most countries places the onus on a "competent person" to do the design.

Water barrier pillars in South African collieries seem to roughly lie between the North American and Pennsylvania mine inspector's rules of thumb. No distinct correlation can be made to any of the existing international hydraulic barrier pillar formulae as shown in Figure 15. In South African collieries, the mechanical design of barriers is used to govern the hydraulic performance of these pillars.

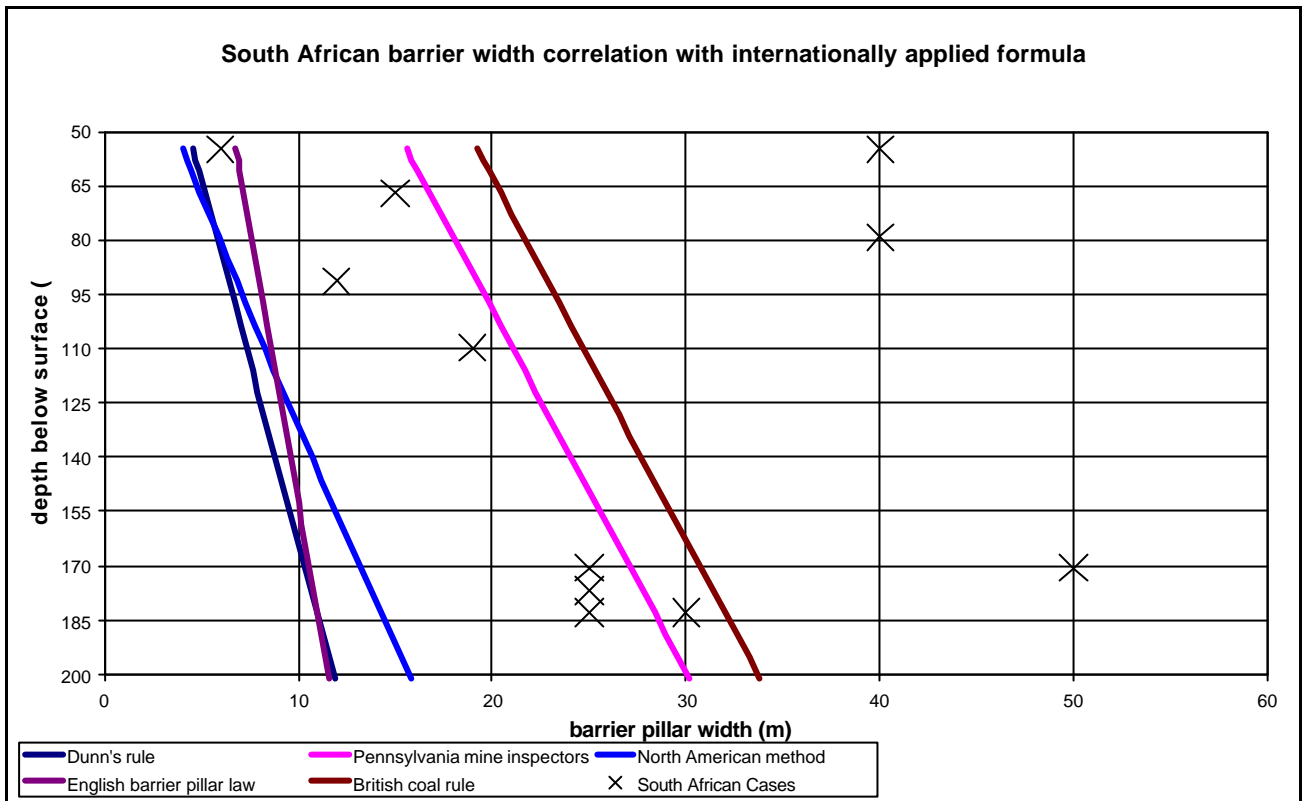


Figure 15: -Correlation of South African colliery barrier widths with internationally applied formulae

2.2 National literature review

Very little research has been done on the design of water barrier pillars in South African Collieries.

The most significant work done (*Cook et al., 1969 and McKinnon, 1998*) concerns the design of water barriers in hard rock mines. Although some common design criteria exist in these research reports, the stress regime at great depths and rock that is far more competent does render them impractical for coal. The limited research into barrier pillar design for both soft and hard rock exclusively deals with the mechanical stability of these pillars. Cook et al, 1969 attempted to address the hydraulic stability of barrier pillars in hard rock after the flooding of the West Driefontein mine. Key issues addressed by Esterhuizen (1991) and Cook et al, 1969 on the design of barrier pillars for soft and hard rock, respectively, are discussed below.

2.2.1 Coal barrier pillar design

Esterhuizen (1991) found that there were lack of guidelines for the designing of barrier pillars in South African collieries. The only guideline that existed stated that substantial barriers were required to isolate mining areas from one another. Different approaches and methods were applied to design barrier pillars.

He studied the circumstances that led to the collapse of barrier pillars, monitored their behaviour, and applied numerical modelling to assess their strength and loading.

His main conclusions were:

- Confinement provided by initial failure around the perimeter of a pillar played an important role in the strength of pillars.
- Continuous rib pillars are about 37 percent stronger than a square pillar of the same width if the W:H ratio is less than 5.
- For a greater W:H ratio the percentage increase in strength is greater.
- For stable conditions, the stresses in barrier pillars are considerably lower than the stress in the surrounding panel pillars. However, if the surrounding panel pillars fail, the stress transferred to the barrier pillar depends entirely on the ability of the overlying strata to cave. If caving of the strata occurs regularly, the loading of the barrier pillar does not increase significantly. Conversely, if the overlying strata bridge over the failed pillars, the barrier pillar will experience a significant increase in stress. (This is shown in the numerical modelling on the loading conditions done for this project)
- The width of the barrier has an important effect on the stress that it will be subjected too.

For slender barriers, Esterhuizen recommended the calculation of the strength by applying Salamon's equation (*Salamon et al, 1967*) for a pillar of the same width even if the equivalent results in a W:H ratio greater than 5. The result is multiplied by 1.37 to give the strength of a slender barrier of the same width.

For squat pillars, he recommends that one should look at the strength of the interface between the coal and the surrounding strata. If the interface is strong, he recommends the Wilson approach (*Wilson 1972*).

If the interface is weak, numerical modelling is applied to assess the effect of the weak layer.

A factor of safety of at-least two (2) is recommended for slender and squat barrier pillars.

2.2.2 Metalliferous barrier pillar design

After the flooding at West Driefontein Mine, Cook *et al*, 1969 questioned the ability of an 18m wide continuous barrier (between adjacent mines as required by law), to prevent flooding under high pressure heads (13.8MPa in the case of West Driefontein Mine).

A study was conducted into the effectiveness of Witwatersrand quartzite acting as a barrier at a depth of between 1800m and 3600m assuming a stopping width of 1m on either side. (Cook *et al*, 1969)

It was said that the stability of boundary pillars was unlikely to deteriorate rapidly with increasing depth and that experience gained at moderate depths was relevant to the design of pillars at much greater depths.

It was further said that the effectiveness of a boundary pillar as a water barrier depends both on the strength of the pillar and on the ability of the surrounding rock to withstand pillar stresses.

It was difficult to determine the nature of the stress distribution across the highly stressed pillars or the fracture zone in their vicinity. To be able to assess the effect of pillar loads on the surrounding rock, it was assumed that the average pillar stress was distributed uniformly across the width of the pillar.

It was concluded that intact quartzite is virtually impermeable to water at pressures insufficient to cause hydraulic fractures of the rock, that is, at pressures less than its tensile strength, namely about 14MPa. Jointed and failed rock resist the flow of water through it, provided that the normal stress in the rock across joints and fractures exceeds the pressure of the water.

The high compressive stresses induced by a pillar generate sufficient normal stress across joints and fractures in any direction to preclude the possibility of water flowing through these discontinuities

2.2.3 Current Practices

Barrier pillars on most of the collieries were reported to be related to the width of the pillars in the adjacent workings. Current practices do not account for the design of barriers based on their ability to retain water contained in reservoirs. Of more concern is the carrying capacity of compartments or dams and the civil designed structures (plugs or seals built into the pillars). Water leakage through and around the barriers is controlled by pumping programs that reduce compartment water heads through recycling. In mines conducting total extraction, the purpose of the barrier pillars is to form the limit for goafing and to define the boundaries of the reservoirs. The mechanical design of the barrier pillars seems to incorporate the hydraulic design.

3 Mechanical design of coal pillars

Since coal barrier pillars fulfill the dual functions of providing mechanical stability and hydraulic stability to collieries, it is worth noting the parameters that influence the mechanical stability of these pillars.

3.1 Square pillars

Salamon and Munro, 1967 defined the safety factor as:

$$SF = \frac{\textit{strength}}{\textit{load}} \quad (14)$$

The load is calculated using the tributary area load theory. This can be applied provided pillars are of uniform geometry and panel width is greater than depth below surface. Every pillar is assumed to carry the weight of overburden immediately above it.

$$\textit{load}_{\textit{Pillar}} = \textit{stress}_{\textit{virgin}} \cdot \frac{\textit{area}_{\textit{original}}}{\textit{area}_{\textit{new}}} \quad (15)$$

$$\therefore \textit{load}_{\textit{Pillar}} = 25H \cdot \frac{c^2}{w^2} \quad (16)$$

The pillar strength formula is given by:

$$\textit{strength} = 7176 \cdot \frac{w^{0.46}}{h^{0.66}} \quad (17)$$

They found the values 7176 (coal strength empirically derived), 0,46 and 0,66 from statistical analysis.

From studying these cases it was found that a safety factor of 1,6 would have been acceptable in most mining situations, but other influences and experience could adjust it up or down.

3.1.1 Applications and limitations:

A limitation of this pillar strength formula is that it assumes that the strength of a pillar increases proportionally with a power of the width to height ratio, which is less than unity. This limitation was not evident in the statistical study because the collapsed pillar case histories only included pillars with width to height ratios of 3.6 or less.

Salamon, cautioned against mining at depths shallower than 40m as it had been noted that pillars with width to height ratio's less than 1.75, having an areal percentage extraction in excess of 75% and a width less than 6m are prone to collapse despite safety factors in excess of 1,6. Some of the limitations of the Salamon pillar strength formula are listed below:

- A safety factor states the stability of the pillar and not the bord
- Pillar widths should be in excess of 5m
- W:H ratio should exceed 2.
- At shallow depths (< 40m) it is very sensitive to even small variations in pillar widths.
- Width to height ratio less than 5
- Seams shallower than 150m. At greater depths the pillars are stronger than calculated.
- Blast fracture damage and continuous miner pillars.

Most pillar failures, according to Madden (1991), occur when:

- Mining depth = 20 - 60m - most at 30 & 60m
- Pillar widths = 3 - 6m - most at 6m
- percent areal extraction > 75 percent - most at 80 percent
- W:H ratio = 1 - 3 - most at 1
- Safety factor = 0,9 - 1.3 - most at 1.0

3.2 Rectangular pillars

Where the calculation of strength of pillars of rectangular cross-section must be done, Wagner (1980) suggested the use of equivalent width for substitution of the width in the strength calculation:

$$W_e \approx 4 \cdot \frac{A_p}{c_p}$$

$$Width_{equivalent} \approx 4 \cdot \frac{Area_{pillar}}{length_{perimeter}}$$

(18)

3.3 Continuous miner cut pillars

Madden (1986) found that due to the absence of blast damage, which is allowed for in the Salamon and Munro formula, continuous miner cut pillars will have a larger safety factor. Thus the pillar width can be reduced to have the same nominal safety factor by:

$$h_o = h \cdot \left(1 + \frac{2 \cdot \Delta w_o}{w}\right)^{2.46} \quad (19)$$

where : h_o = safety factor for pillars cut by CM
 h = safety factor originally calculated
 Δw_o = blast damage (change in width) - avg. 0,2 – 0.3 deep
 w = original pillar width

3.4 Squat pillar strength formula

The safety factor design formula of Salamon and Munro (1967) has been used very successfully in designing stable pillar geometries in SA collieries. This formula was based on collieries having a depth of mining ranging between 20m and 220m with the majority of the collieries shallower than 150m. In the past most collieries operated at depths of less than 150m and the problem of designing squat pillars never arose.

A limitation of the pillar strength formula is that it assumes that the strength of a pillar increases proportionally with the power of the width to height ratio, which is less than unity. However, most of the newer collieries and some of the reserves currently being mined on the older collieries are situated at depths in excess of 150m and up to 580m.

These cases extend beyond the empirical range of Salamon and Munro's (1967) statistical analysis. It was for this reason that Salamon (1982) extended his pillar strength formula to take notice of the increasing ability of a pillar to carry load with the increasing width to height ratio.

Salamon and Wagner (1980) suggested that in the design of coal pillars, the squat pillar formula could be used with the critical width to height ratio taken at 5,0 and, although more difficult to make a realistic estimate, that e (rate of strength increase) can be taken as 2,5. The assumption of the critical width to height ratio equal to 5 is based on the fact that no pillar has collapsed with a width to height ratio greater than 3,75.

The squat pillar formula is given by:

$$s_p = k \frac{R_o^b}{V^a} \left\{ \frac{b}{e} \left[\left(\frac{R}{R_o} \right)^e - 1 \right] + 1 \right\} \quad (20)$$

Where : s_p = pillar strength
 k = strength of coal - unit strength of a cube

V = pillar volume
 R_o = critical width to height ratio
 R = pillar's width to height ratio
 e = rate of strength increase
 a = constant - statistically determined
 b = constant - statistically determined

3.5 Mining method influence on pillar fracturing

Madden (1991) found that for a restricted bord width, the mining method practised influences the depth and frequency of fractures.

In conventional drill and blast sections, the blast damage zone extends 0.25m to 0.3m into the pillar.

From about 100m depth, stress induced fractures occur in pillars mined to a SF of 1.6. Slabbing starts occurring at around a depth of 175m for a 1.6 safety factor.

3.6 Ageing of pillars

Van der Merwe (1998) states that the safety factor concept as set out by Salamon, Munro and Madden does not explicitly cater for long term stability and thus can not be used to predict the life of the pillar.

Progressive pillar scaling models calculate the distance that a pillar has to scale to initialise failure and then assign a rate of scaling to that distance.

From Salamon and Munro statistical data, for the Vaal Basin coalfields, a 0.3 safety factor with an *in-situ* pillar strength of 4.5 MPa would have a 100 percent probability of failure.

For the Witbank and Highveld coalfields, the coal pillar strength was 7.2 MPa with an observed minimum safety factor of 0.5 (100 percent probability of failure).

By substituting the mining parameters, one can calculate the minimum width of a pillar to ensure failure, for a specific set of data. The difference between original mining dimensions and the critical width to ensure failure is the scaling distance.

The rate of scaling is influenced mainly by three parameters: The mining height, the age of the pillar at failure and atmospheric weathering.

Atmospheric weathering includes:

- water logged areas, contaminated with various minerals as in the case with water compartments
- changes in ambient air temperature
- changes in humidity

4 Water flow in rock

4.1 Flow equations

Miller and Thompson (1974) investigated various factors that influence the retardation of seepage by barrier pillars in the Appalachian Plateau coal region and found that water usually flows along bedding and other separation planes such as slickensides and localised geologic structure rather than through the intergranular spaces. This finding was strengthened by underground observations of flow mechanisms in five South African collieries (Appendix II). Fracture dominated flow was demonstrated (section 6) through numerical modelling to closely correlate with actual underground measured flow. Water flow in most rocks can thus be assumed to obey Darcy's law for laminar flow, which is expressed as:

$$q_x = k \frac{dh}{dx} A \quad (21)$$

where:

- q_x is the flow rate ($L^3 T^{-1}$) in the x direction
- k is the permeability coefficient that has dimensions of velocity (cm/s)
- h is the hydraulic head with dimension L
- A is the cross-sectional area normal to x (dimension L^2)

for calculations which involve water at about 20° Celsius.

The unit for permeability is Darcy, where 1 Darcy = 9.87×10^{-9} cm² and k corresponds to approximately 10^{-3} cm/s.

Where permeability was determined in a laboratory through using a radial flow test the following formula was used to calculate permeability:

$$k = \frac{q \ln\left(\frac{R_2}{R_1}\right)}{2pL\Delta h} \quad (22)$$

where:

- k is the permeability coefficient that has dimensions of velocity (cm/s)
- q_x is the volume rate of flow
- L is the length of the specimen
- R_2 and R_1 are the outer and inner radii of the specimen
- Δh is the head difference across the flow region corresponding to DP , the change in pressure

This formula is applicable to the in-situ borehole tests conducted for this project.

4.2 Ground water in South African Coalfields

In South African coalfields, groundwater is associated mainly with the dolerite dykes, dolerite sills and sandstones.

4.2.1 Groundwater associated with dolerite dykes

The porosity and permeability of this igneous rock are zero. Where cracks or discontinuities penetrate these dolerite dykes the circulation of groundwater creates zones of chemical weathering along the sides of the dyke. Vast amounts of water can be associated with these weathered zones. Typical yield from boreholes in these weathered zones ranged from 10 to 30l/sec or 36 to 108kl/h.

The weathering along the sides of the dykes is a function of the depth of groundwater circulation, which tend to pinch out at depths beyond 60m.

4.2.2 Groundwater associated with dolerite sills

Sills as undulating intrusive bodies, follow specific horizons in the Karoo sediments and occasionally penetrate into the sediments at angles up to 85°. Very little water is usually encountered along the horizontal portions of the sill, but where it cuts at steep angles through the overlying sediments, the same weathering as with dykes occurs along the sides, with the subsequent groundwater stored in these weathered materials.

4.2.3 Groundwater associated with sandstones

The permeability of sandstone is very low and the rate at which ground water can be released from intact sandstone, which was measured from boreholes collecting water from pores in the sandstone, is less than 0.05l/sec or 180l/h.

The permeability of the discontinuities in the sandstone is much higher than that of the pores and yields from boreholes intersecting such discontinuities ranged from 0.1 to 15 l/sec or 0.36 to 54kl/h. The deeper the mining the less permeable these discontinuities will be as they tend to close up under the weight of increased cover depth.

Where the sandstone is underlain by shale, the groundwater in the sandstones can be regarded as separate occurrences, each with its own hydraulic potential.

4.2.4 Groundwater associated with shales

The shales in the vicinity of the coal seams tend to be impervious to groundwater and water in shales is normally associated with discontinuities in the shales.

4.2.5 Groundwater associated with underlying Karoo sediments

Due to the crystalline nature of most of the coalfields' underlying rock, no primary porosity is present. Whatever water may be encountered in these rocks, must be contained in discontinuities. It would not have any influence on the charge and re-charge rates of underground workings.

However, if the base material consists of sandstone, the groundwater may be derived from this source during mining operations.

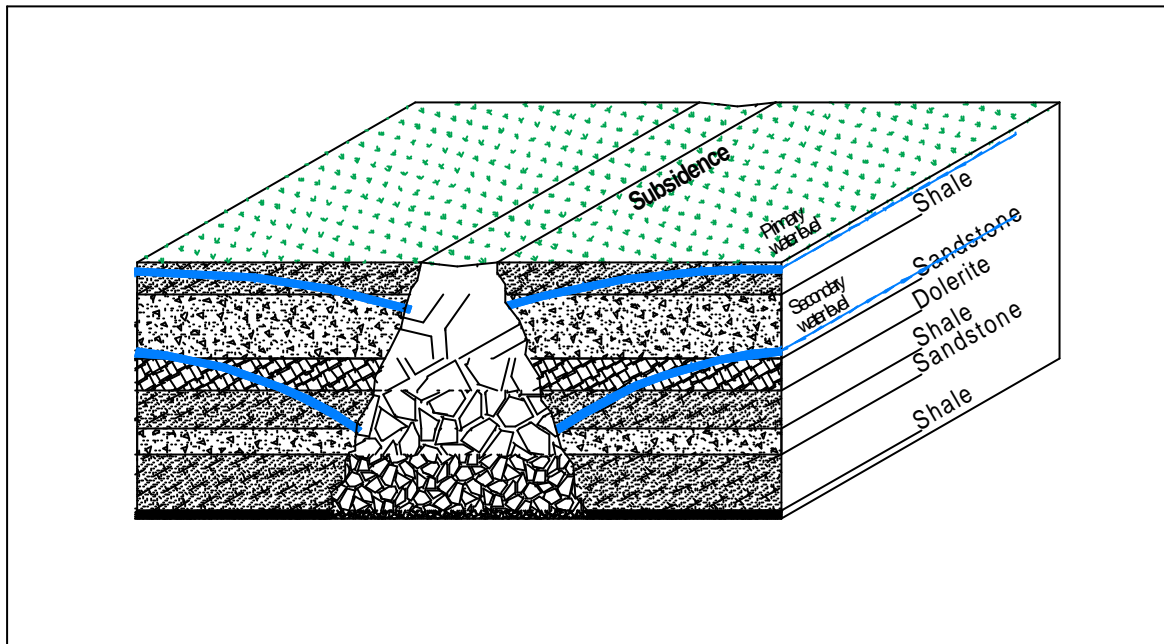


Figure 16: –Groundwater dewatering in total extraction area (after Hodgson)

4.2.6 Water storage in South African Collieries

Storage of run-off water is done in three ways:

- Compartments
- Dams
- Ponds

4.2.6.1 Compartments

Compartments are totally sealed areas, bordered by a combination of continuous barrier pillars and panel pillars with civil engineered seals constructed in-between. Seam dip and seam floor contours, have a major influence on the head vs. capacity of the compartment. Most are laid out so that the maximum capacity can be obtained within the set maximum head as stipulated in the code of practice. This head of water can vary from 0 to 40m or 0 to 400kPa. A disadvantage of compartments is that when applied to areas where total extraction has been done, the head of the water can increase exponentially without a dramatic increase in volume of water. Each site is unique as to the amount of water stored for a set maximum water head.

4.2.6.2 Dams

Dams are flooded areas with retainer walls around the perimeter. These walls are purely there to retain the water up to a set maximum head (in most instances 2m) and after that, the water decants over the wall. The seam floor contours effect the capacity of water storage but the water head is always fixed at below the height of the retainer wall. A few collieries operate their underground water storage in such a way. Very little total extraction is practised at these collieries.

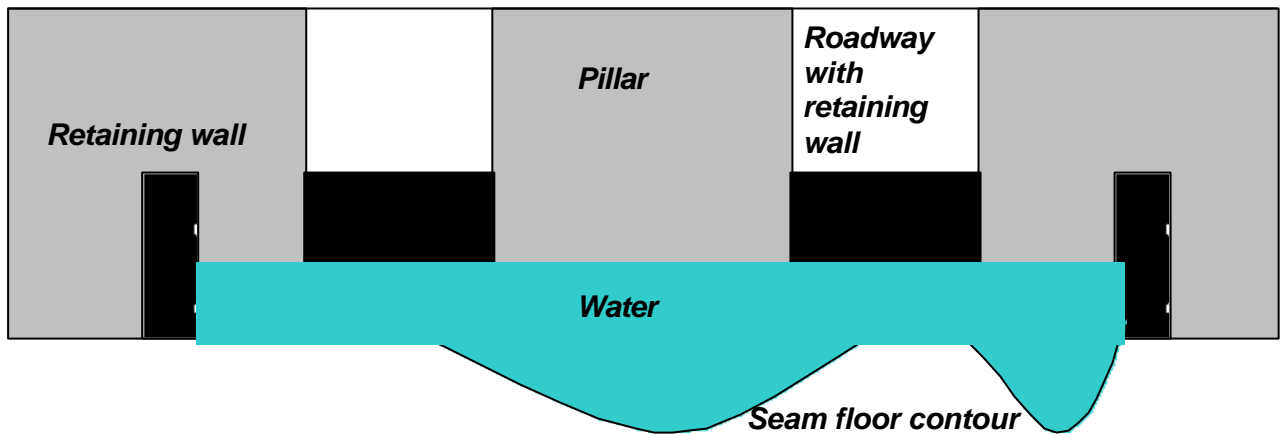


Figure 17: Retaining walls forming a dam

4.2.6.3 Ponds

Ponds can be classified as water taking its natural course, governed by the seam floor contours. Depending on the dip of the seam it can create a quite significant head of water. From the questionnaires there was one such case. Another prime example of this is old abandoned mines.

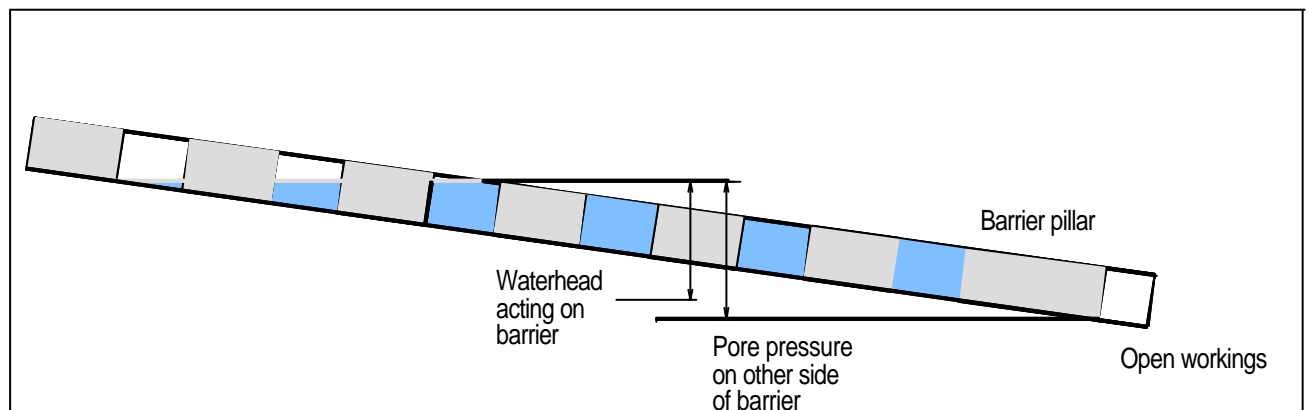


Figure 18: Water accumulating against barrier due to dip of seam

The primary factor affecting the selection, design and construction of underground water compartments and seals is the anticipated water head or hydraulic pressure that the boundaries of the compartment will have to withstand when sealing is completed.

For total extraction panels, as shown in figure 19, the pressure increase is slow at first as the seam workings fill with water. After full capacity is reached, where the volume of water is equal to volumetric extraction taking floor contours into consideration, the pressure increase is exponential for a very small increase in volume. This is because the water fills the cavities created by the subsided overburden.

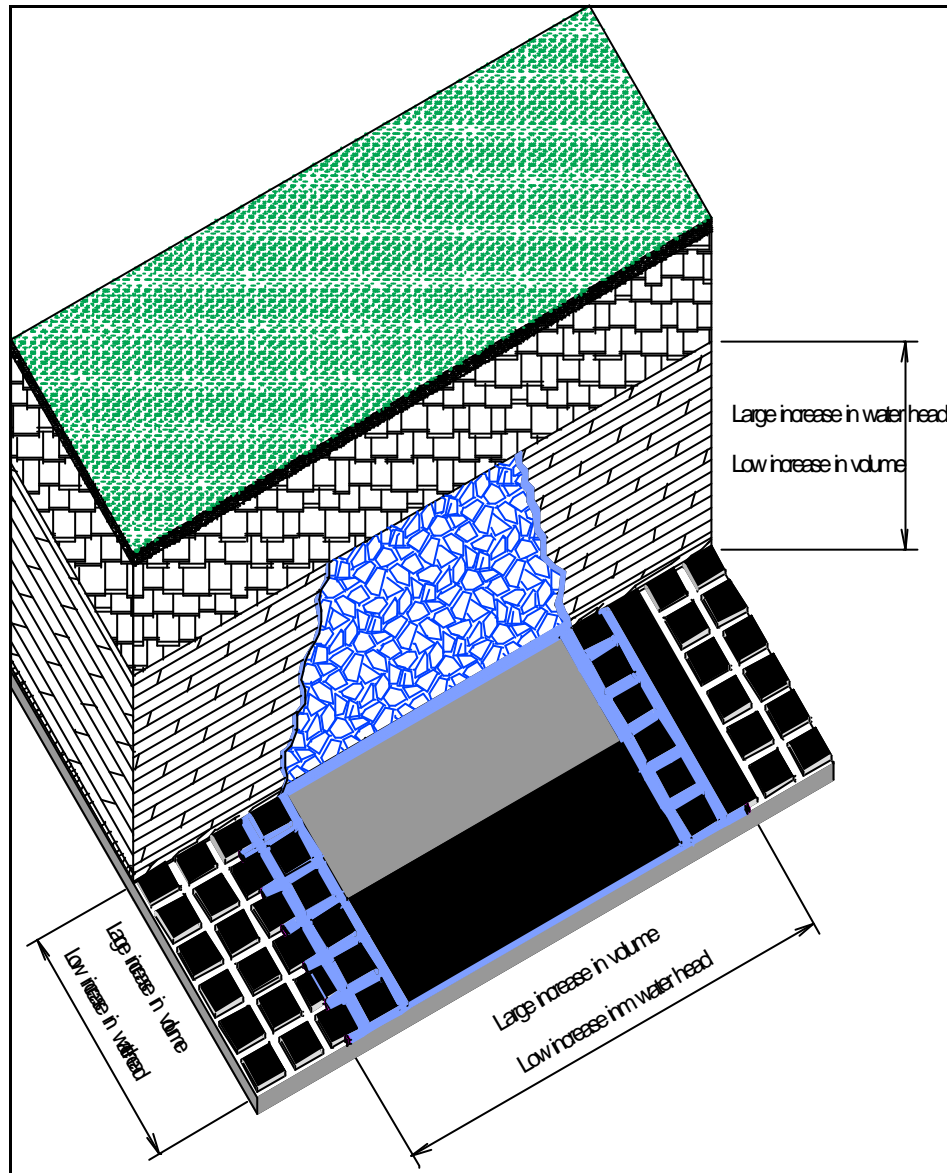


Figure 19: - volumetric vs. pressure increase

If this water connects to an overlying extracted seam filled or partially filled with water or to the natural water table, the increase in water pressure can increase dramatically while storage capacity is lost due to unaccounted groundwater filling the compartment.

5 Data gathering for numerical models

Three methods of data acquisition were used to gather data that would form the primary input for the numerical models. The methods and use of the data are discussed below.

5.1 National industry questionnaire

Questionnaires (Appendix I) were circulated to 52 operating South African collieries to obtain information on the occurrence and management of water. Fourteen collieries responded to the questionnaire.

The data supplied by the collieries was used to establish operating ranges for input into numerical models. The four significant operating ranges derived from the questionnaires are as follows:

- (1) Mining depth range
- (2) Seam height range
- (3) Water barrier width range
- (4) Range of reservoir water heads

Rates of compartment dewatering were used to correlate (discussed in section 7) actual results with the modelled results.

Figures 20 to 23 show the predominant ranges for mining depth, seam height, barrier width and water head derived from the questionnaires.

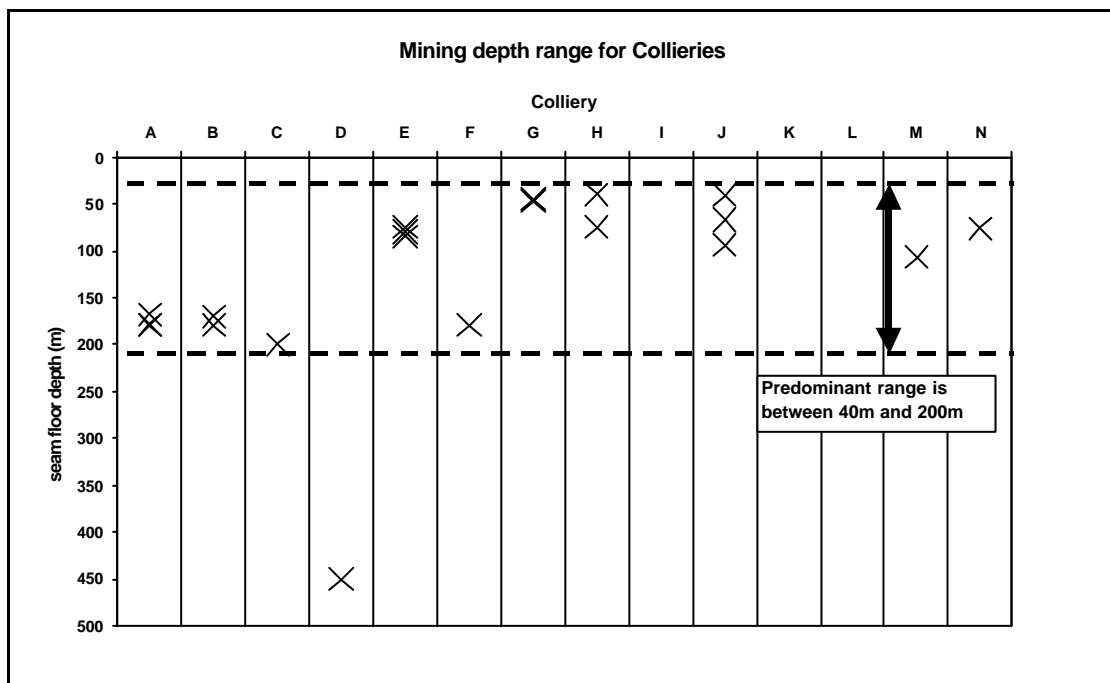


Figure 20: Mining depth range for South African collieries based on questionnaire data

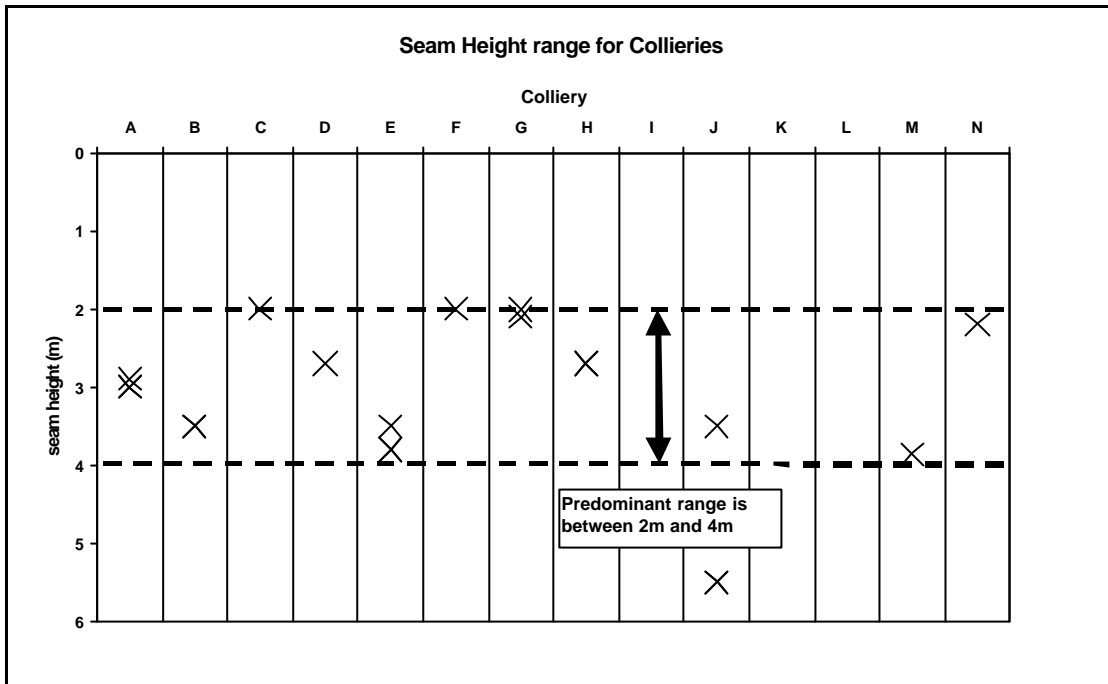


Figure 21: Seam height range for South African collieries based on questionnaire data

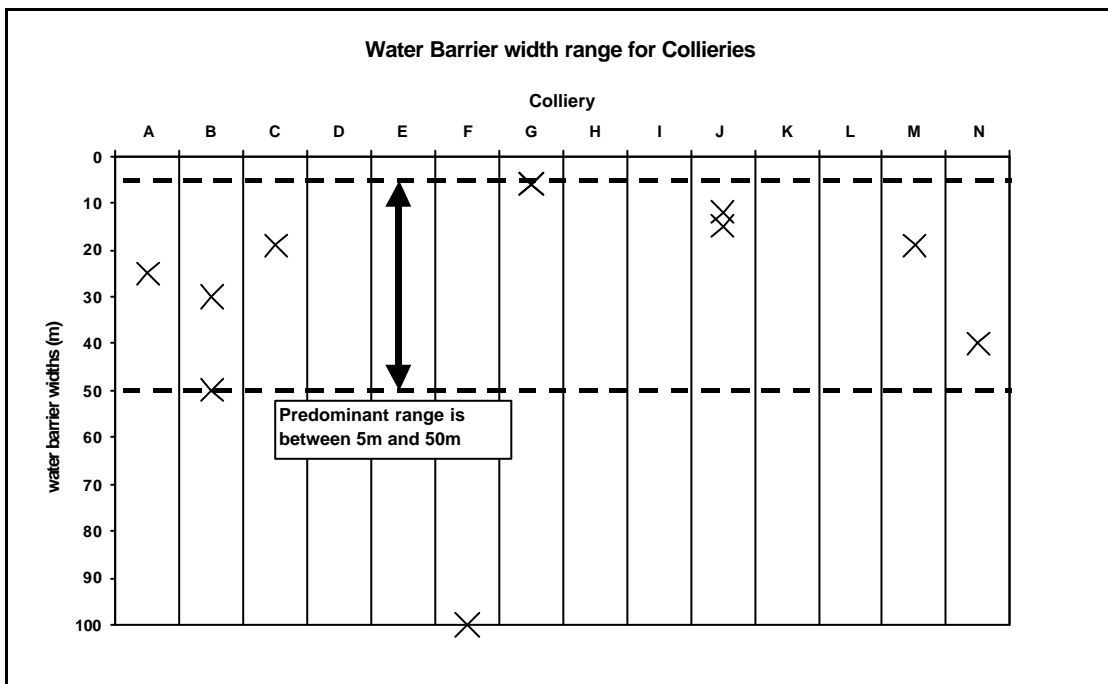


Figure 22: Barrier pillar width range for South African collieries based on questionnaire data

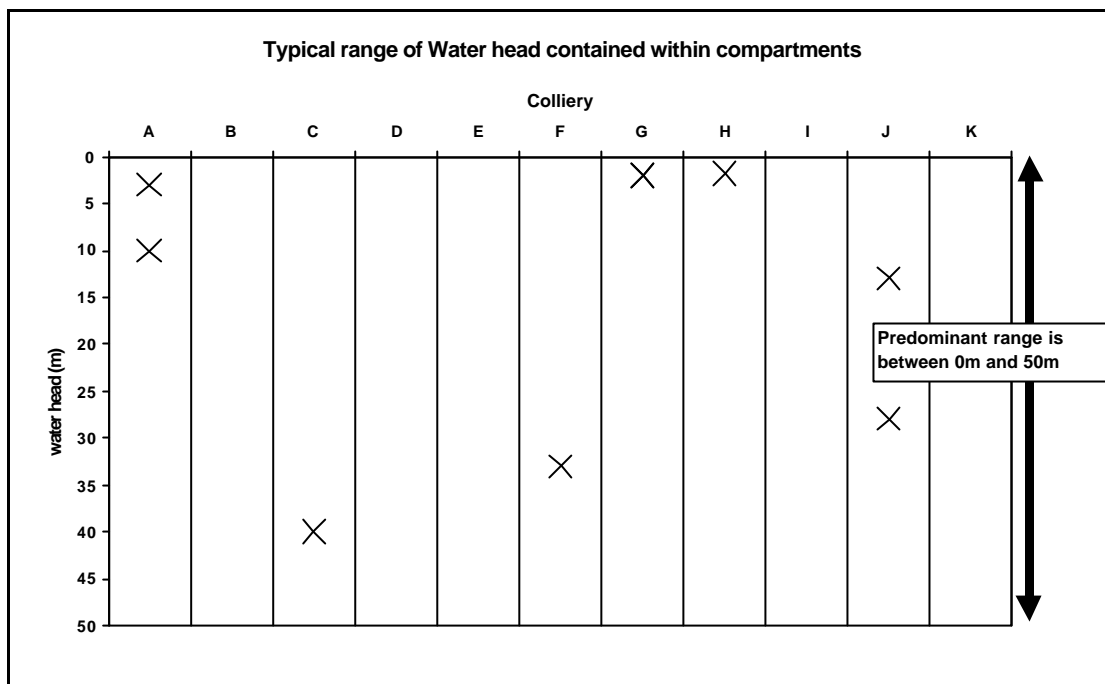


Figure 23: Compartment water head range for South African collieries based on questionnaire data

5.2 In situ monitoring

Two sites were equipped with pressure and flow monitoring equipment to correlate the models with actual conditions. Boreholes were drilled into roof and floor strata at predetermined distances and patterns in relation to the barrier pillars. The holes were sealed in pre-selected strata horizons to collect water flowing from the compartments through the strata. Borehole pressures and flow rates were monitored over time and used to calibrate effective permeabilities. These permeabilities were used to adjust model outputs to actual flow rates and pressures. Permeability calculations are discussed in section 6 (Numerical modelling).

Details of the in situ monitoring are contained in Appendix II.

5.3 Geotechnical Survey

Four collieries were visited to assess the hydrological condition of the rock mass in the vicinity of water compartments. The in situ observations included assessments of rock mass condition, primary conduits for flow, rates of water leakage, pillar responses to loading and influence of mining and pillar geometry on the water flow. A brief outline of the main conclusions of the in situ investigations for two instrumented collieries follow (detailed descriptions of the assessments are contained in Appendix II):

Colliery A

- The roof is generally a competent and massive sandstone with occasional bedding partings and locally the presence of coal fossils provide additional horizontal discontinuities of limited extent.

- Jointing is very sparse in the roof, tension cracks in bords occur more frequently.
- Water leakage appeared to be mainly through horizontal bedding and joints, leaving iron-stained pillar surfaces.
- Water was only observed from the hangingwall where joints, faults or tension cracks occurred.
- At the southeast corner of the compartment seven concrete seals were constructed to fill splits in the barrier. Up to 0.5m scaling was apparent from the sidewall coal of the pillars adjacent to the seals. Water leakage occurred principally around the seals.

Colliery B

- The immediate 5m of roof consisted of well-laminated siltstones and gritstones. Distinct open partings define the laminations of the immediate 0.5m of siltstones.
- Discontinuities observed to influence water flow are the interfaces between the coal bands and the laminations of the siltstones. Flow along the above mentioned structures were limited to the first stress fracture intersected in the roof or floor.
- Water flow from the roof seemed to be limited to the first 0.5m of the roof. This distance represented the densely laminated siltstones.
- Persistent flow of water from the roof and floor strata was observed.

The in situ investigations revealed that water flow is predominantly through discontinuities rather than porous media. The type (sandstone, siltstone, gritstone) and characteristics (bedded, massive or laminated) of the roof and floor rock mass influences the flow rate. Geological logs of 8 collieries were examined to ascertain the condition of the immediate roof and floor strata. The predominant range of laminated or bedded strata was used as the input for the representation of horizontal discontinuities in the UDEC models. Figures 24 and 25 show the depth of laminated or bedded strata for the 8 collieries.

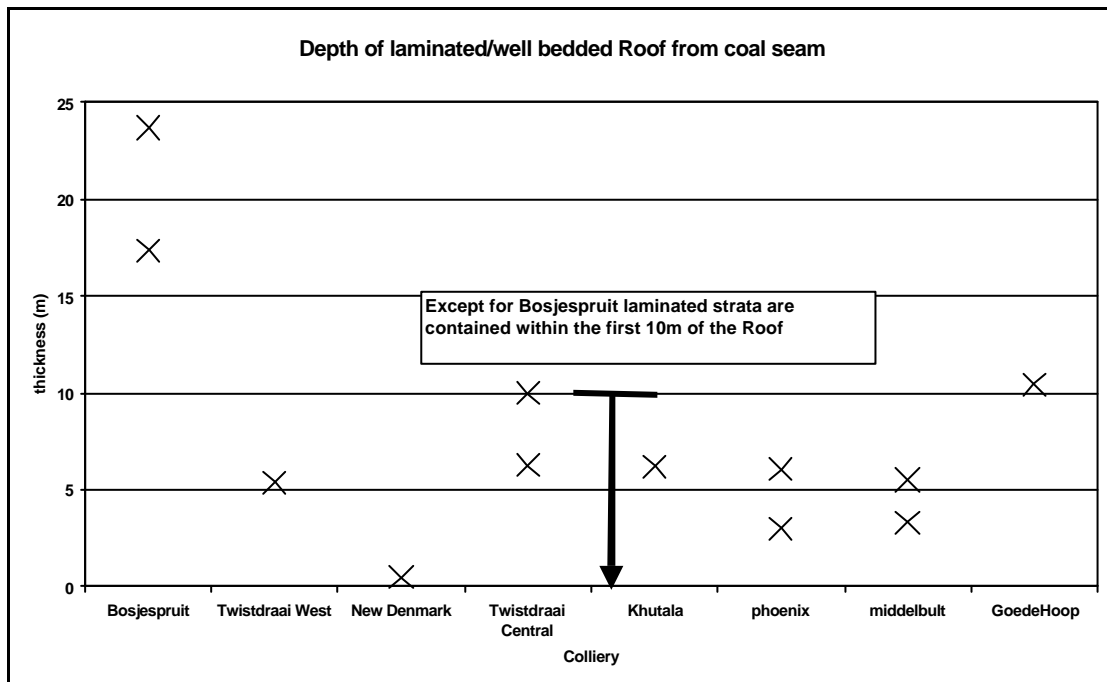


Figure 24: Extent of laminations/bedding into the roof ascertained from geological logs

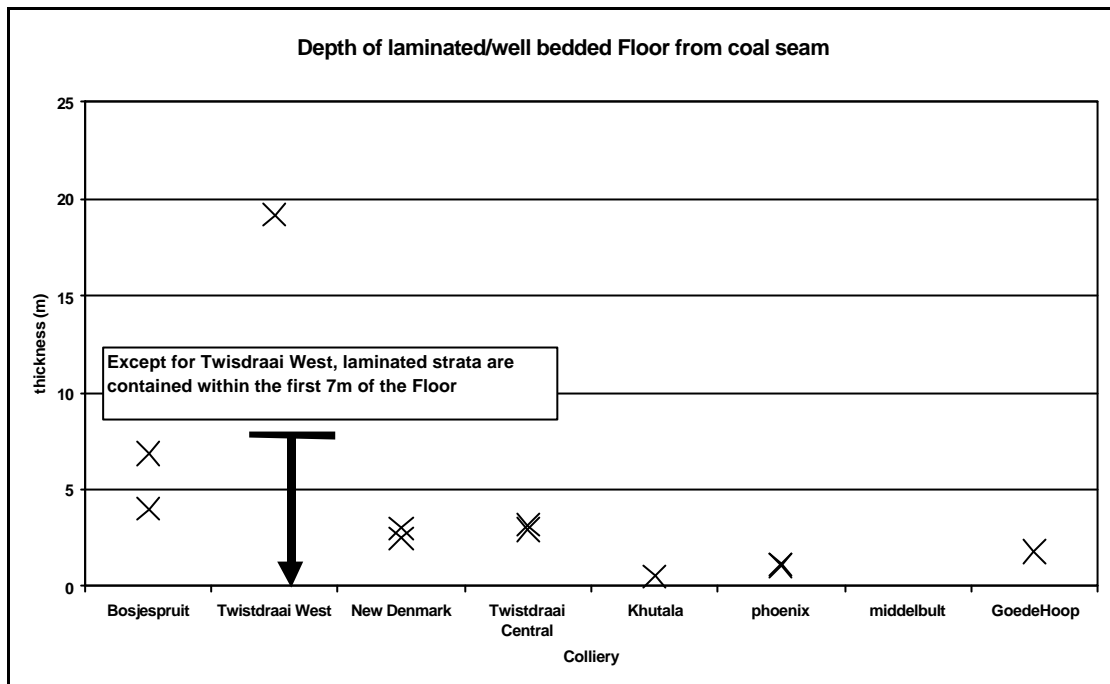


Figure 25: Extent of laminations/bedding into the floor ascertained from geological logs

5.4 Geotechnical classification of flow regimes

Water flow through and around coal bound barrier pillars can be classified according to the rock type hosting the discontinuities that allow water leakage. Discharge of water onto the dry side of a barrier pillar from a flooded or partially flooded area will normally be a combination of water seeping from the roof, coal or floor. The geohydrological condition of the immediate roof, coal and floor will determine the type of flow regime pertinent to a particular mine. The bulk of local underground collieries can be classed into the seven flow regimes depicted in Figures 26a to 26g. These flow regimes account for the type and competence of the strata constituting the roof and floor and the influence of the barrier pillar or roadways in forming vertical fractures.

<p align="center">Figure 26a</p>	<p align="center">Figure 26b</p>
<ul style="list-style-type: none"> • Leakage of water occurs through the coal seam and discrete vertical joints in bedded sandstone roof and floor strata • Go to design chart 	<ul style="list-style-type: none"> • Leakage of water occurs through the coal seam only • The roof and floor strata are massive and impermeable • Go to design chart

<p align="center">Figure 26c</p>	<p align="center">Figure 26d</p>
<ul style="list-style-type: none"> • Leakage of water occurs through the coal seam and discrete vertical joints in bedded sandstone roof and soft, damaged, laminated siltstone/gritstone floor • Go to design chart 	<ul style="list-style-type: none"> • Leakage of water occurs through the coal seam and soft, damaged, laminated siltstone/gritstone roof and floor • Go to design chart

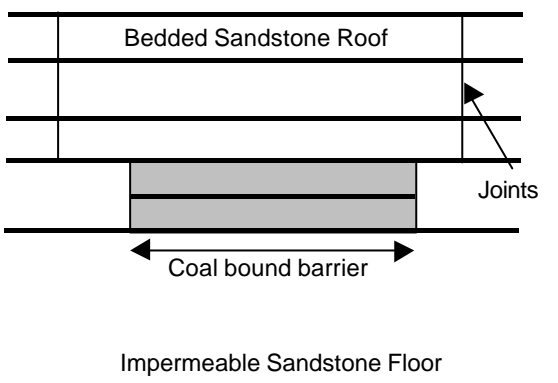
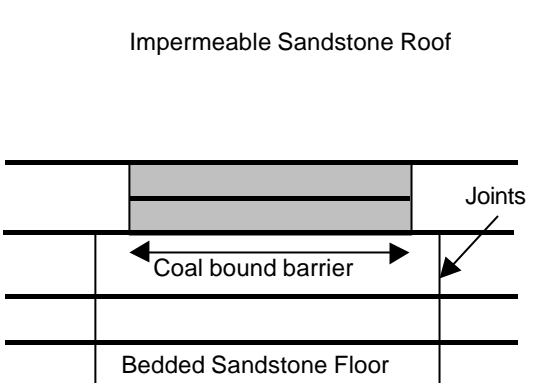
Figure 26e	Figure 26f
	
<ul style="list-style-type: none"> • Leakage of water occurs through the coal seam and discrete vertical joints in bedded sandstone roof. • The floor is massive and impermeable. • Go to design chart 	<ul style="list-style-type: none"> • Leakage of water occurs through the coal seam and discrete vertical joints in bedded sandstone floor. • The roof is massive and impermeable. • Go to design chart

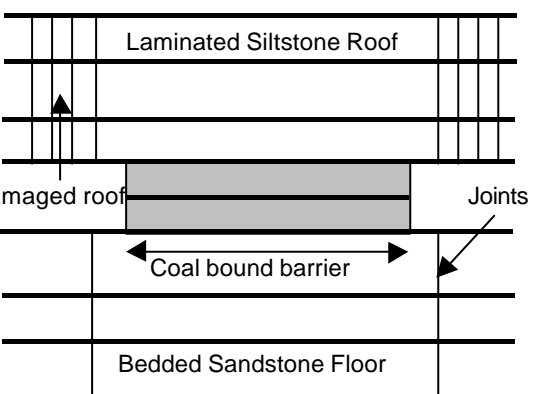
Figure 26g

<ul style="list-style-type: none"> • Leakage of water occurs through the coal seam and soft, damaged, laminated siltstone/gritstone roof and discrete vertical joints in bedded sandstone floor. • Go to design chart

Figure 26: Geotechnical classification of flow regimes according to condition of roof and floor strata i.e. massive, few vertical joints in competent strata, shear damaged zones in incompetent strata

The relationship established between rock type and hydraulic condition is shown in Table 2.

Table 2 Hydraulic condition of rock mass derived from characteristics of the roof, coal and floor strata

Rock type and characteristic	Vertical fractures	Hydraulic condition
Massive sandstone	None	No leakage into roadways since no horizontal or vertical tapping fractures exist
Competent bedded sandstone	Few discrete joints spaced at centre of roadways	Flow into roadways occurs through natural joints or tensile fractures formed in roadways
Incompetent siltstone/gritstone/sandstone	Multiple vertical fractures at pillar edge due to shear damage of roof and floor	Multiple leakage points in roadway
Discretely laminated coal	None	Leakage into roadway occurs through horizontal roof/floor contact planes and central horizontal discontinuity in coal
Combinations of the above roof and floor characteristics have been used to formulate the seven geotechnical flow regimes depicted in Figures 26a-g		

The flow paths for 33 South African collieries were classed according to the condition of the roof and floor strata to ensure that the full spectrum of geotechnical flow regimes were captured in the numerical models (Figure 27). The classification was done by obtaining information on the condition of the roof and floor strata in the vicinity of water reservoirs from the mine's rock engineers and geologists.

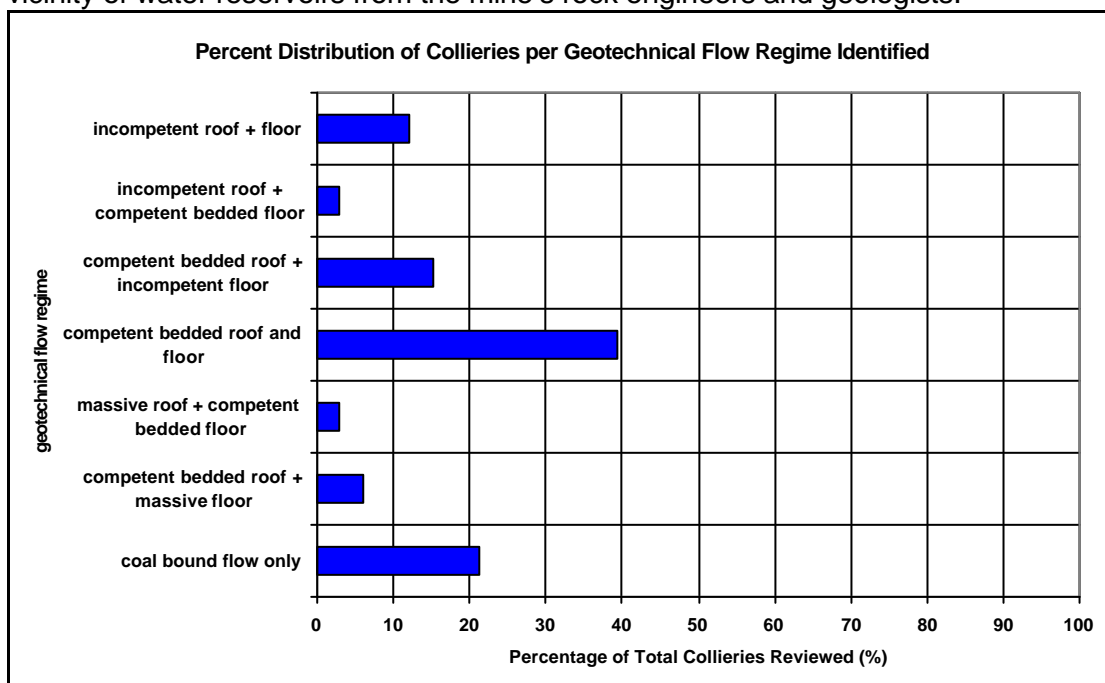


Figure 27: Classification of 33 South African collieries by geotechnical character of the roof and floor strata

Seventy-five percent of the collieries surveyed fall into three geotechnical categories for flow. These, in decreasing percentage are:

- (1) Competent bedded roof and floor strata with few discrete vertical joints in the roof and floor that form conduits for water leakage. Additionally, flow of water occurs at the interface of the coal and the roof and floor strata. The roof and floor strata are generally, well bedded sandstones.
- (2) Massive, impermeable roof and floor strata occur in approximately 20% of the collieries thus resulting in flow only at the contacts of the seam with the roof and floor strata. Roof and floor strata are generally massive sandstones.
- (3) Competent bedded roof with few discrete vertical joints and an incompetent floor with shear damaged (multiple fractured) pillar edges. Additionally, flow of water occurs at the interface of the coal and the roof and floor strata. The roof, is generally well-bedded sandstones and the floor laminated siltstones and gritstones.

5.5 Conclusions

Information gathered from the questionnaire, in situ monitoring and geotechnical investigations formed the basis for determining operating ranges for the numerical models. These are summarized below:

1. The bulk of South African collieries operate between surface and a depth of 200m.
2. Barrier pillar width's range from 5m to 50m.
3. Individual seam heights range between 2m and 4m.
4. The maximum compartment water head is approximately 50m.
5. Ninety percent of collieries can be classified into the seven geotechnical flow regimes defined.
6. The geological logs of collieries suggest that soft laminated strata are usually confined to the first 10m of roof and floor strata.
7. The measured rock mass permeabilities can be obtained by using a discontinuity residual aperture of 0.15mm (section 8.2.1.1) in the numerical models.
8. Only 40% of mines may be faced with water problems related to barrier pillars since 60% of water compartments are confined by either competent roof and floor or massive roof and floor strata.

6 Ground penetrating radar scan

The aim of the ground penetrating radar (GPR) tests conducted at an underground colliery was to determine whether GPR is a viable tool for examining fractures in coal pillars to depths of 2m or more. A detailed discussion of the test site, the procedures employed and the results obtained from the GPR scans are contained in Appendix VI.

GPR has not been successful in this case in coal. In the pillars at the test Colliery, the overall conductivity of the coal appeared to be too high to make any meaningful measurements.

7 Effect of water quality on coal strength

Coal core samples were submerged in solutions of varying pH over a four-week period. It was expected that the change in pH of the solution would influence the point load strength of the coal. Nothing conclusive could be drawn from the analysis. No correlation between point load strength and water quality was derived.

8 Numerical modelling

The predominant spectrum of geotechnical flow regimes in and around barrier pillars for South African Collieries was simulated with numerical models to assess the influence that pillar width, pillar loading, discontinuity location, persistence, spacing and hydraulic condition has on rates of water leakage on the dry sides of barrier pillars. The formulation of the geotechnical flow regimes (discussed in section 5) was done by a local colliery survey of rock conditions that form the predominant host for water flow.

8.1 Suite of Numerical Models

Miller and Thompson (1974) investigated various factors that influence the retardation of seepage by barrier pillars in the Appalachian Plateau coal region and found that water usually flows along bedding and other separation planes such as slickensides and localized geologic structures rather than through the intergranular spaces. This finding was strengthened through underground observations of flow mechanisms in five South African Collieries (Appendix II).

Based on the predominant mechanism of flow (fracture driven) that exists in South African Collieries, the program Universal Distinct Element Code (UDEC) that models the behaviour of discontinuums was chosen as the primary tool for analysis. UDEC is described as a 'distinct element' program. This numerical method falls within the general classification of discontinuum analysis techniques. A discontinuous medium is distinguished from a continuous one by the existence of contacts or interfaces between the discrete bodies that comprise the system.

Since the type of flow in South African coal measure strata is predominantly fracture rather than porous medium driven, a continuum analysis was viewed as unnecessary. UDEC has the capability to perform the analysis of fluid flow through the fractures of a system of impermeable blocks. A fully coupled mechanical-hydraulic analysis or a steady state analysis can be performed, in which fracture conductivity is dependent on mechanical deformation and conversely joint water pressures affect the mechanical computations. Since only the final steady state mechanical influence on flow is of interest, the steady state flow algorithm was used for this analysis.

8.1.1 Model hydraulic behaviour of rock fractures

Fluid pressure is assumed to vary linearly according to the hydrostatic gradient. Flow is governed by the pressure differential between adjacent domains (area between model contacts). The flow rate is calculated in two different ways depending on the type of contact created in the model. For a point contact, the flow rate from a domain with pressure p_1 to a domain with pressure p_2 is given by:

$$q = -k_c \Delta p \quad (23)$$

where k_c is the point contact permeability factor, and

$$\Delta p = p_2 - p_1 + r_w g (y_2 - y_1) \quad (24)$$

where p_w is the fluid density,
 g is the acceleration of gravity
 y_1, y_2 are the y-coordinates of the domain centres

Where a contact length can be defined, the flow rate is given by:

$$q = -k_j a^3 \frac{\Delta p}{l} \quad (25)$$

where k_j is the joint permeability factor
 a is the contact hydraulic aperture, and
 l is the length assigned to the contact between the domains

8.2 Establishing modelling parameters

8.2.1 Hydraulic modelling parameters

8.2.1.1 Hydraulic aperture

In section 6.1.1 it is shown that Darcy's Law for laminar flow between parallel plates governs fluid flow. A relationship exists between the mechanical state of the model and fluid flow by the response of assigned hydraulic apertures of discontinuities to loading. For a known pressure difference or flow rate between two points in the model, the hydraulic aperture can be adjusted to give the required results.

The calibration of hydraulic aperture was done using the results of in situ testing conducted at underground collieries. UDEC models simulating a 40m cross-section of the barrier pillar were set up to best represent the mechanical geometry of the barrier pillar that yielded the state of pillar loading derived from elastic modelling (obtained from the program Lamodel-Appendix II). The Lamodel program was setup to represent the regional setting of the barrier pillar. The UDEC calibration model is shown in Figure 28.

Having established the correct mechanical stress state for the barrier pillar (Figure 29), the domain water pressures across the pillar were monitored by varying the residual hydraulic apertures across a coal bound horizontal joint. These water pressures were matched to the underground measured results to obtain the input residual hydraulic aperture for the models (Figure 30). The residual hydraulic aperture is the minimum aperture of discontinuities permitting fluid flow. Fluid flow will be less influenced by mechanical joint displacement that results in joint closure than the residual aperture. The minimum rate of fluid flow will thus occur if for a given length of a discontinuity, the entire length is at residual aperture.

Based on the calibration models, **a residual aperture of 0.15mm** was used for the models. The chosen residual aperture was further verified by comparing the mine's compartment pumping rate to the theoretically derived flow rate as a function of aperture. Figure 31 shows that a residual aperture of 0.15mm for a single horizontal fracture with length 20m, subject to an end pressure of 250kPa, yields a flow rate of $3 \times 10^{-6} \text{m}^3/\text{sec}$. For 10m of bedded roof and floor strata and a barrier length of 1km, this flow rate can be expressed as 6ML/day. This flow rate correlates well with the mine's rate of pumping from the compartment (7ML/day to maintain a compartment pressure of 200kPa).

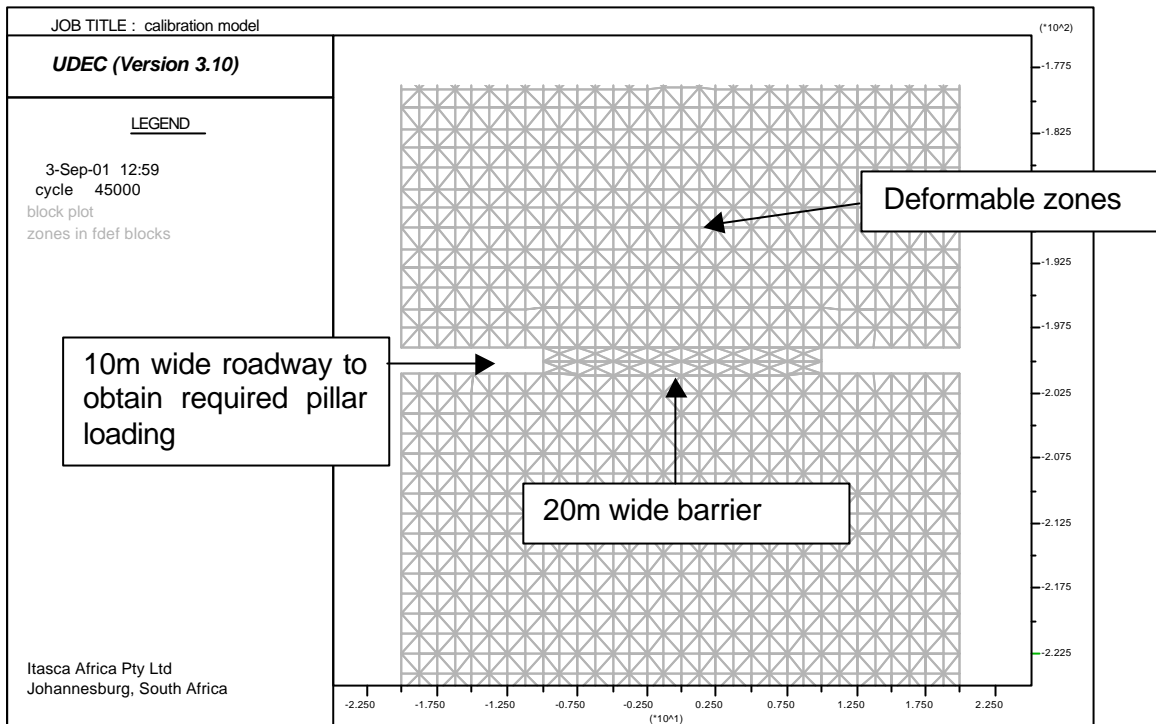


Figure 28: Geometry of calibration model used to obtain correct barrier pillar loading and required residual aperture to produce measured time dependent degradation in water pressure across the barrier pillar.

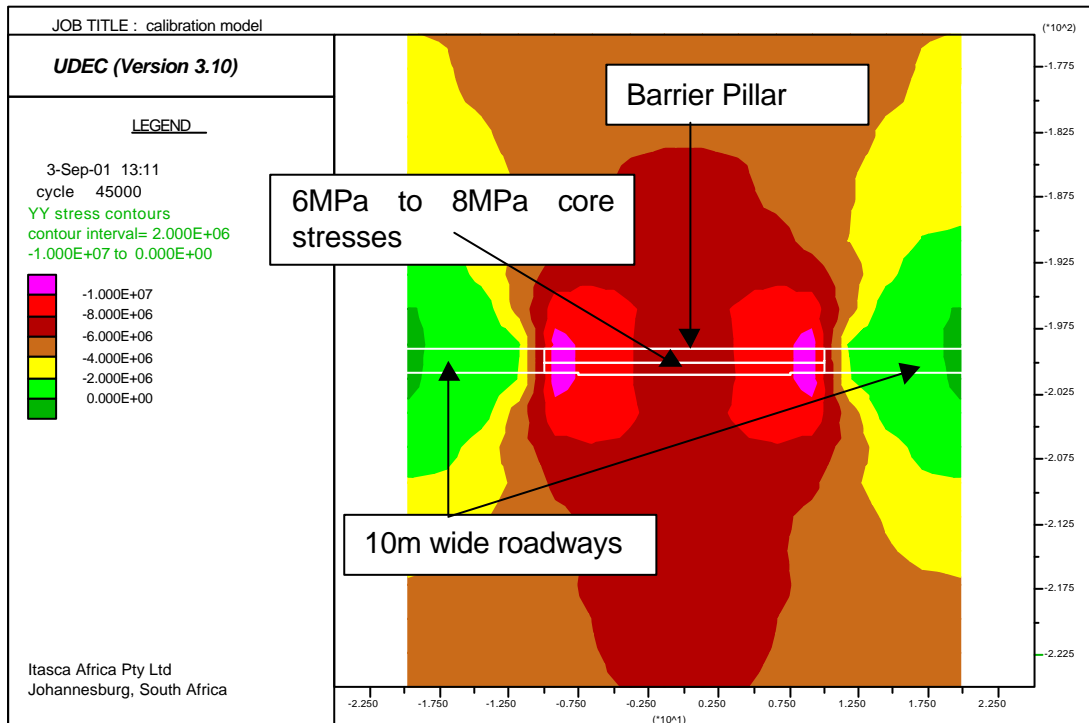


Figure 29: Vertical stress state across 20m wide barrier pillar with 10m wide roadways (Roadway width chosen to obtain an average pillar stress of 7MPa)

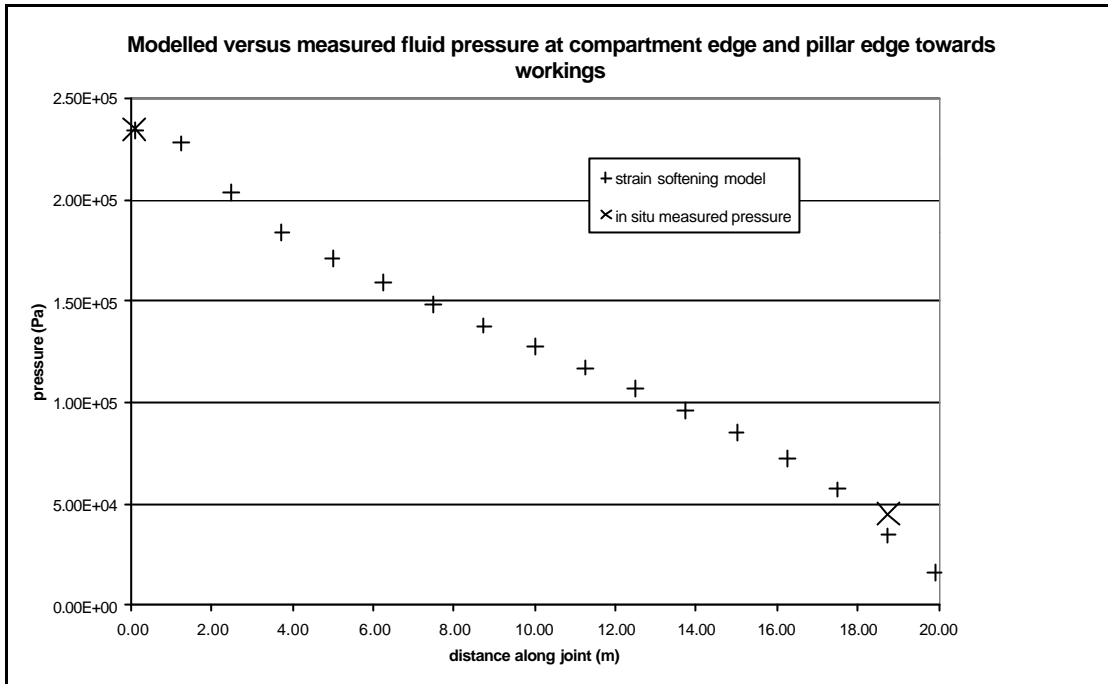


Figure 30: Worst measured water pressure degradation correlated against modelled distribution of water pressure along horizontal model joint for a residual aperture of 0.15mm.

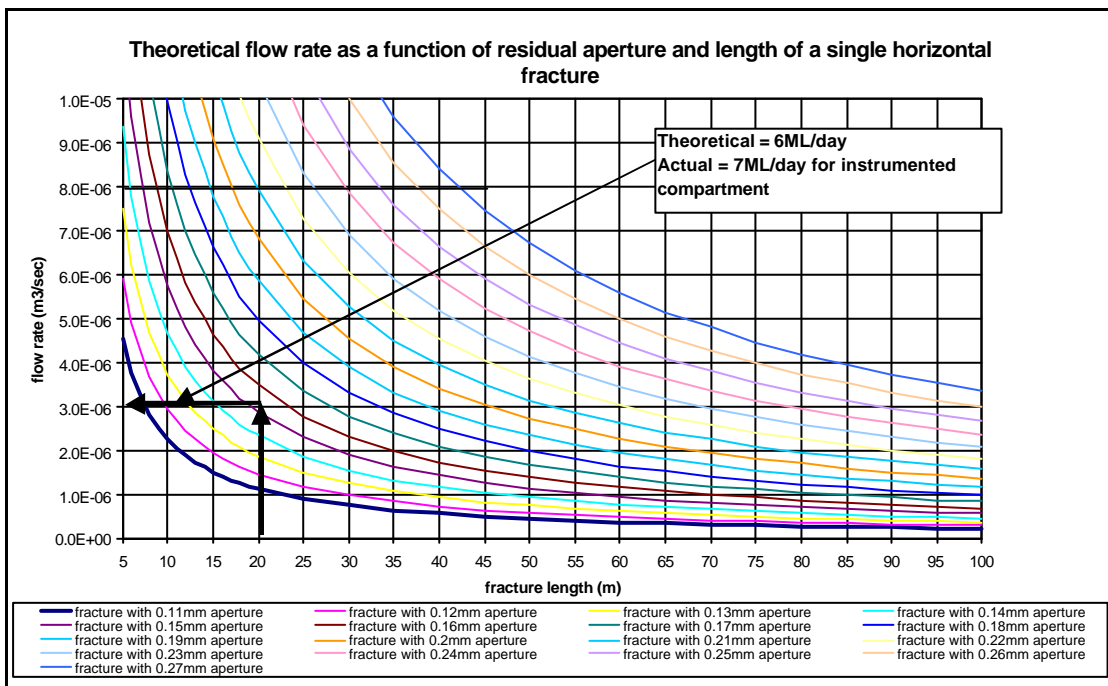


Figure 31: Modelled flow rate for in situ tested mine as a function of residual aperture and single horizontal fracture length.

8.2.1.2 Joint permeability factor

The theoretical value $\frac{1}{12m}$ for the joint permeability factor k_j was used in the models, where m is the dynamic viscosity of the fluid. For water at 20°C, m is 1×10^{-3} Pa.sec, hence k_j is $83.3 \text{ Pa}^{-1}\text{sec}^{-1}$.

8.2.1.3 Explicit flow fractures

Fractures modelled that permit the flow of water were broadly subdivided into three classes (Figure 32).

- I. Horizontal bedding planes and laminations – the spacing and depth of horizontal planes modelled were derived from the examination of geological logs of collieries (Section 5.3).
- II. Vertical joints – discrete vertical joints were placed 2m on either side of the barrier pillar to represent the entry and exit points of water from the flooded compartment to the ‘dry’ side of the pillar. These joints are representative of cracks formed in competent roof or floor strata as a result of tensile cracking through beam bending (flexure).
- III. Shear fractures – for models simulating flow through soft, incompetent strata, a series of vertical fractures representing shear fractures (damaged areas) were placed at the edges of the barrier pillar.

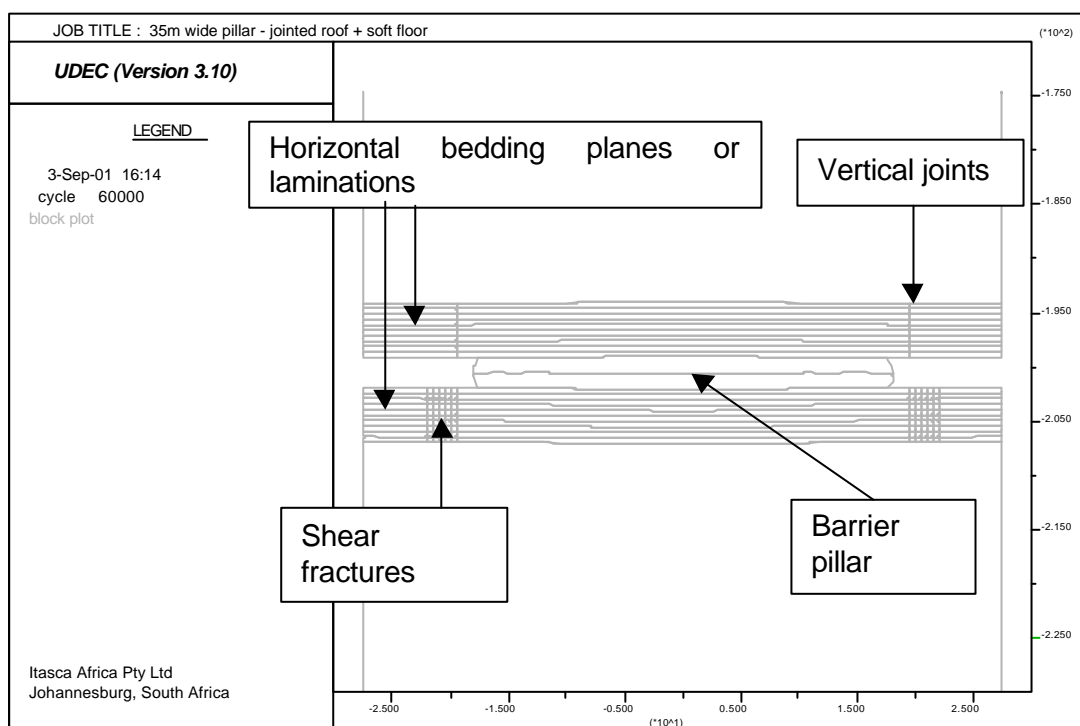


Figure 32: The three classes of fractures that form flow paths as represented in the UDEC models

8.2.1.4 Incorporation of reservoir water pressure

Responses from the questionnaire data (section 51) indicated that the water head in underground compartments vary between 0 and 50m. Models were run using a 25m and 50m compartment water head, which is incorporated into the numerical models by input as a linear hydraulic pressure gradient. The conversion from head (m) to pressure (Pa) is governed by the following equation.

$$p = \rho g h \quad (26)$$

where p and h are the water pressure and head

8.2.2 Mechanical modelling parameters

Properties are assigned to all blocks and planes in the models. The blocks represent the rock bounded by the planes and the planes represent the artificial and geological features represented in the models. Properties assigned to the various deformable zones in the model govern the rock mass response to applied stresses. The sections that follow describe the properties assigned to the deformable blocks (rock mass) and planes (joints, bedding planes, shear fractures, constructional partings).

8.2.2.1 Rock properties

The rock types and properties governing the behaviour of the roof, coal and floor strata is listed in Table 3.

Table 3 Rock type and properties used in UDEC models (after van der Merwe, 1998)

Rock type	Sandstone	Coal	Siltstone/Gritstone
Elastic modulus (GPa)	5	3	2.6
Poisson's ratio	0.15	0.35	0.13
Mass density (kg/m ³)	2400	1500	2300
Bulk modulus (GPa)	2.4	3.3	1.2
Shear modulus (GPa)	2.2	1.1	1.2
Cohesion (MPa)	10	1	10
Friction (°)	46	24	35
Tensile strength (MPa)	3.5	0	3

8.2.2.2 Fracture properties

Properties assigned to planes (fractures) were grouped into three categories viz. Constructional, realistic and residual. The realistic properties are those assigned to fractures which best represent their mechanical state before failure.

Table 4 lists the properties assigned to the different fracture categories.

Table 4 Properties assigned to categories of fractures

Fracture category	Constructional	Realistic	Residual and new contacts
Normal stiffness (Pa/m)	1×10^{11}	1×10^{11}	1×10^{11}
Shear stiffness (Pa/m)	1×10^{11}	1×10^{11}	1×10^{11}
Cohesion (MPa)	10000	10	0
Friction ($^{\circ}$)	30	30	30
Tension (MPa)	10000	0	0

Constructional parting planes were created in the models to dictate the position of change in zone sizes (Figure 33). The modelled areas, incorporating the coal seam were zoned using an edge length of 1m. Areas beyond the coal seam and up to the constructional partings were zoned with edge lengths of 2m. The remaining modelled areas were zoned with an edge length of 4m. The decrease in edge length towards the coal seam allows for greater resolution and accuracy of plotted model parameters. The constructional partings merely form zone positional boundaries and are hence assigned very stiff properties, which inhibit their influence (no slip permitted) on modelled results.

All other discontinuities in the models are assigned realistic properties, which permit slip. Depending on the shear and normal loading regimes, fractures may progress beyond their peak strengths towards residual behaviour. Fractures that attained residual behaviour were governed by the residual properties assigned. All new contacts developed in the models were permitted to slip using the residual fracture properties.

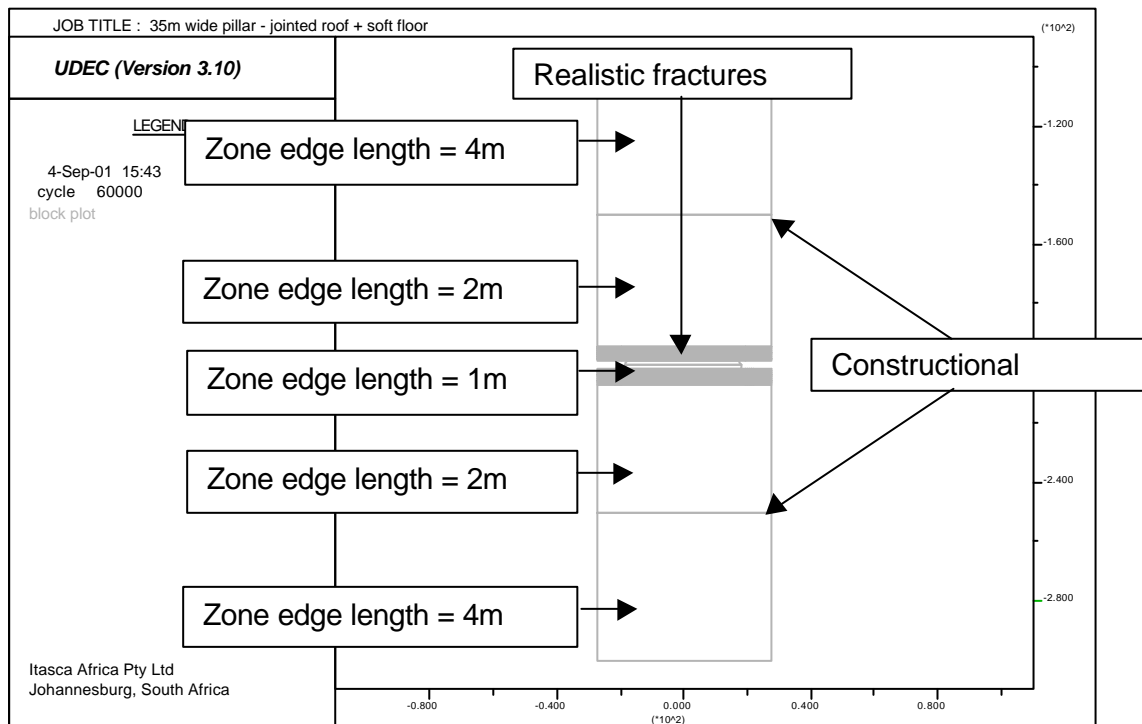


Figure 33: Assigned deformable zone edge lengths and position of category of fractures

8.2.3 Constitutive behaviour of models

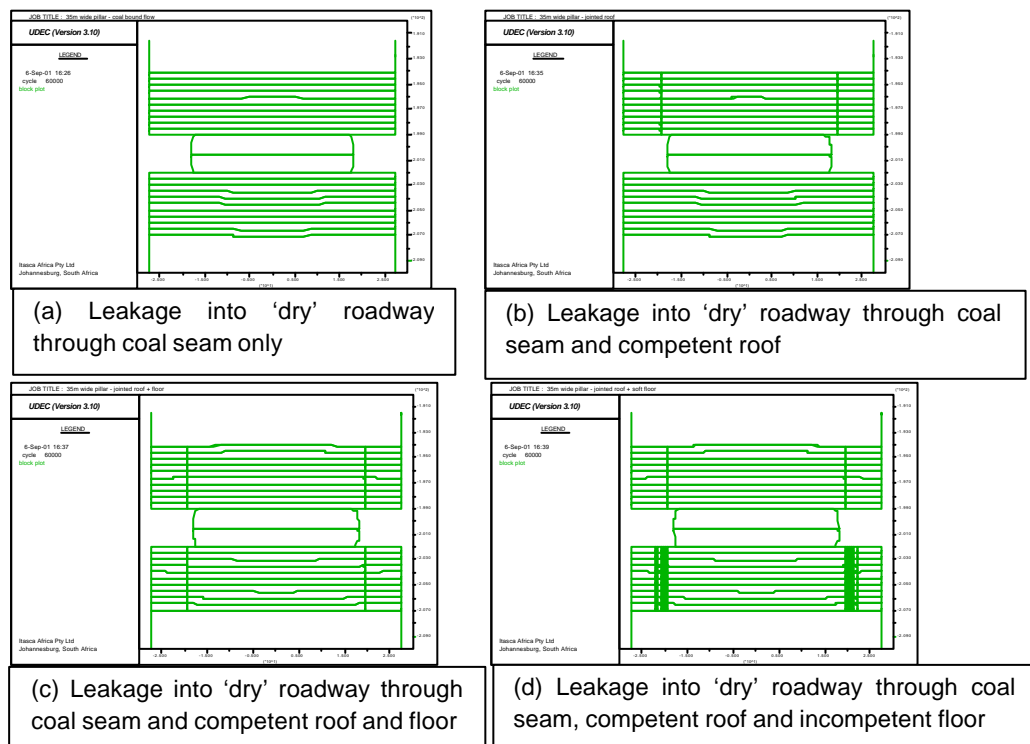
The roof and floor strata represented in the models were governed by the Mohr Coulomb block constitutive model used to represent shear failure in the rock mass. The coal seam was strain-softened by reducing the cohesion to zero over 1% plastic strain.

The standard Mohr Coulomb joint model was applied to all discontinuities. The internal fracture flag was set for each joint segment when the joint shear or tensile strength was exceeded. This allowed all residual values to be used (Table 4) for friction, cohesion and tension in all subsequent calculations.

8.3 Representing Geotechnical flow regimes

If vertical fractures (discrete joints and shear fractures) which form the entry and exit points for water flow are located beyond the barrier pillar edges, then the roof, coal and floor strata behave as independent flow regimes. The rate of discharge of water on the dry side of the barrier pillar is thus the cumulative flow rates from each of these regimes.

Five generic fluid flow models were used to analyze the full spectrum of geotechnical flow regimes discussed in section 5.4 The contribution of the roof, coal and floor strata to the cumulative flow rate was separated for a particular geotechnical condition. For variations in barrier pillar width or compartment water head, permutations of the individual contributions to flow of the roof, coal and floor strata could thus be used to produce the desired influence of a geotechnical flow regime on the rate of water discharge. Figure 34 show the geotechnical flow regimes as represented in the UDEC models.



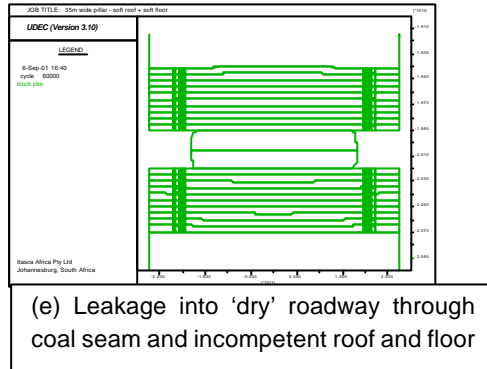


Figure 34: Representation of geotechnical flow regimes in UDEC where vertical fractures are indicative of the condition (competent or incompetent) of the roof and floor strata.

8.4 Modelling methodology

Fifteen UDEC models representing the 5 generic geotechnical flow regimes (section 6.3) for barrier pillar widths of 50m, 35m and 20m were set-up and run to mechanical and hydraulic steady states. For the aforementioned range of barrier pillar widths, additional models were constructed, and solved to establish the influence of changing compartment water head and depth on the rate of water leakage. Table 5 briefly outlines the primary outputs derived from the models.

Table 5 Primary outputs derived from UDEC models

Model	Figure 34	50m wide barrier	35m wide barrier	20m wide barrier
Coal bound flow only	A	Establish coal contribution to flow only		
Competent roof and coal flow	B	Establish competent roof contribution to flow		
Competent roof, floor and coal flow	C	Establish competent floor contribution to flow		
Competent roof, incompetent floor and coal flow	D	Establish incompetent floor contribution to flow		
Incompetent roof, floor and coal flow	E	Establish incompetent roof contribution to flow		
Depth change of model (d)	D	Influence of pillar loading on geotechnically classified flow		
Water head change of model (d)		Influence of water head on geotechnically classified flow		

8.4.1 Model size

Models were constructed to represent the upper limit (50m), lower limit (20m) and average (35m) barrier widths for the predominant range used in South African Collieries (section 51). A roadway width of 20m was found to best estimate the barrier pillar loading derived from elastic boundary element modelling of the underground test sites. The elastic modelling (Appendix II), was done on a regional scale thus incorporating asymmetrical loading of the pillar.

Upper and lower horizontal model boundaries were placed 100m away from the coal seam to prevent the influence of edge effects on results. For variations in barrier pillar widths, model vertical boundaries were shifted to accommodate the 20m roadway. All other boundaries remained unchanged. Figure 35 shows the model size for the simulation of a 35m wide barrier pillar.

Flow through and/or around the barrier pillars was generically modelled for a seam floor depth below surface of 200m. A set of models for the range in barrier widths and the most common geotechnical flow condition [Table 5(d), Figure 34(d)] was then chosen, the seam floor depth altered to 100m and rerun to establish the influence of depth on the rate of water discharge.

Based on the local colliery survey discussed in section 51, an average seam height of 3m was used for all models.

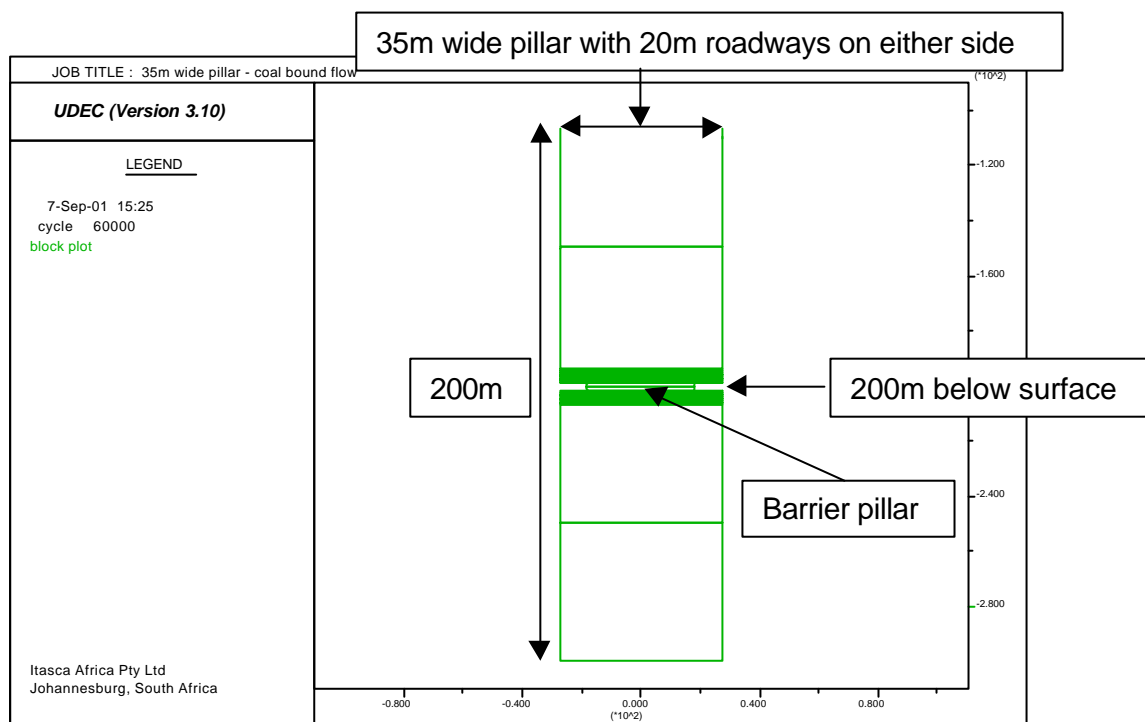


Figure 35: Size of UDEC model for the simulation of a 35m wide barrier pillar

8.4.2 Boundary conditions

The boundaries are assigned conditions that govern the behaviour of the entire model. These conditions are formulated and applied to the boundaries to best represent the in situ stress state of the rock mass. A linear increasing stress gradient representing a k-ratio of 2 was applied to the top horizontal boundary of the model. The velocities and displacements for all other boundaries were fixed at zero.

A pressure representing the water head was applied to the edges of the excavated roadway that represented the water compartment and the vertical left model boundary. The water pressure gradient is governed by the following equation:

$$p = fp + (fpx \cdot x) + (fpy \cdot y) \quad (27)$$

Where p is the water pressure, fp the fluid pressure at the boundary, fpx the fluid pressure gradient along the x-axis, fpy the fluid pressure gradient along the y-axis, x the x-coordinate at a desired point in the model and y the y-coordinate.

The vertical model boundary on the 'dry side' of the pillar above and below the coal seams were made impermeable (Figure 36).

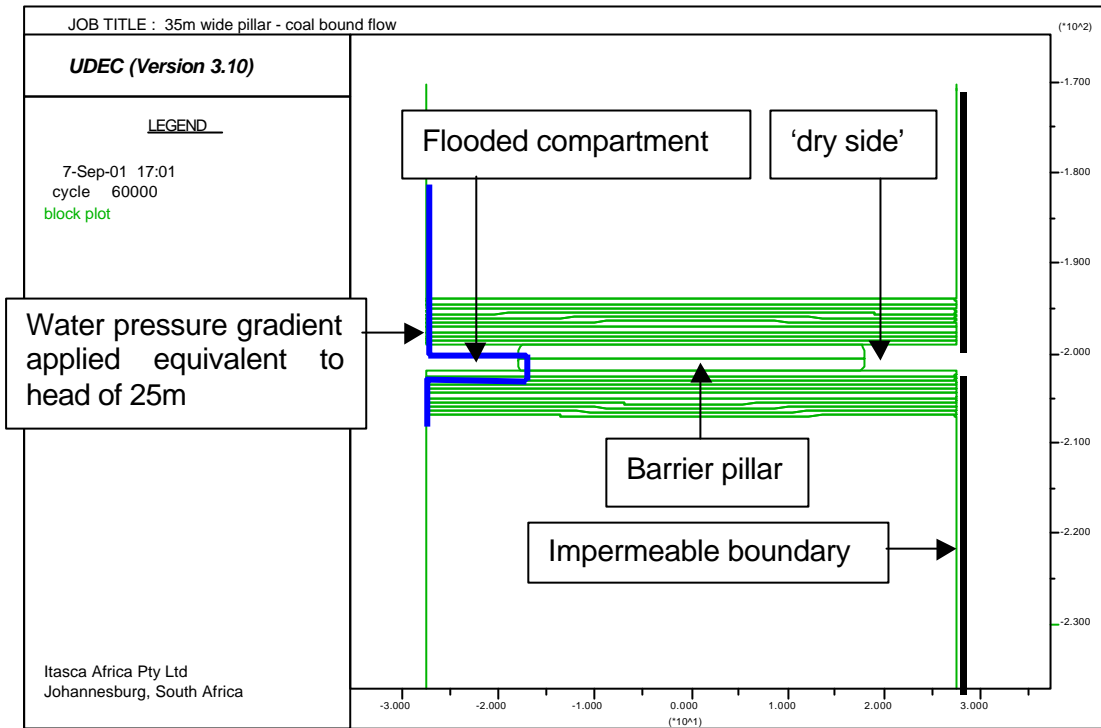


Figure 36: Hydraulic model boundary conditions

8.4.3 Modelling strategy

1. The virgin stress state was generated in the block models with no excavations being made, by stepping the model to equilibrium i.e. close to zero velocities and nil out of balance forces. Indicators such as the state of unbalanced forces, velocities and far field displacements were assessed to determine the stability of the models.
2. After excavating the 20m wide roadways to create the barrier pillar, the models for a range of pillar widths and a particular geotechnical condition were initially run with elastic block constitutive behaviour. Mohr Coulomb and strain softening behaviour (section 8.2.3) was progressively introduced into the models thus enabling controlled understanding of results.
3. Mechanical equilibrium was established prior to applying a water pressure gradient to the models since only the final steady state flow was of interest.
4. For the geotechnical conditions modelled, the flow rates and paths of water flow along discontinuities was noted.

8.5 Modelling Results

The primary objective of the project was to create a series of design charts that will enable easy estimation of the required hydraulic width of a barrier pillar considering factors such as manageable rates of water leakage and tolerable compartment water heads. Methods for establishing the mechanical stability of the barrier pillars are outside the scope of this project. An important aspect of the analysis is that mechanical design of the barrier pillars must be conducted prior to designing for hydraulic stability. Since the hydraulic analysis is the focus of the research, the results will concentrate on parameters and methods used to quantify flow rates or leakage in the predefined geotechnical flow regimes.

Publications (not exhaustive) such as van der Merwe (1998), Salamon (1983), McKinnon (1988), Esterhuizen (1998), Goodman (1980), Budavari (1983) deal with the mechanical response of barrier pillars to loading.

8.5.1 Response of Hydraulic Aperture to Loading

The hydraulic aperture of discontinuities has the largest influence on the rate of discharge of water. Since, in Darcy's equation for laminar flow, the flow rate is directly proportional to the cube of the aperture, small changes in aperture will greatly influence the flow rate. The hydraulic aperture of discontinuities in the UDEC models is given, in general, by

$$a = a_0 + u_n \quad (28)$$

where a_0 is the joint aperture at zero normal stress, and

u_n is the joint normal displacement (positive denoting opening)

The minimum value, $a_{res} = 0.15\text{mm}$, was calibrated for the aperture using results (section 8.2.1.1) from underground testing. Below this value, mechanical closure of the joint does not influence the contact permeability. An increase in normal compressive stress increases the joint normal closure (negative denotes closing), thus decreasing the hydraulic aperture from the a_0 value. If the normal stress along a discontinuity in a confined block of ground is high enough, the aperture along the joint will tend towards its residual value.

Since joint normal stress is directly proportional to depth below surface, it follows that the hydraulic aperture and hence the flow rate decreases with increasing depth for a constant head of water. Figure 37 shows the hydraulic aperture along a coal bound discontinuity after mechanical loading for a depth of 200m and 100m below surface. Due to the edges of the pillar being unconfined (Figure 38), hydraulic apertures tend to remain high (a_0 values). The rock mass poisson's ratio influences the degree of lateral pillar spalling and hence the hydraulic aperture. Unconfined pillar edges will thus always have higher hydraulic apertures than the pillar centres.

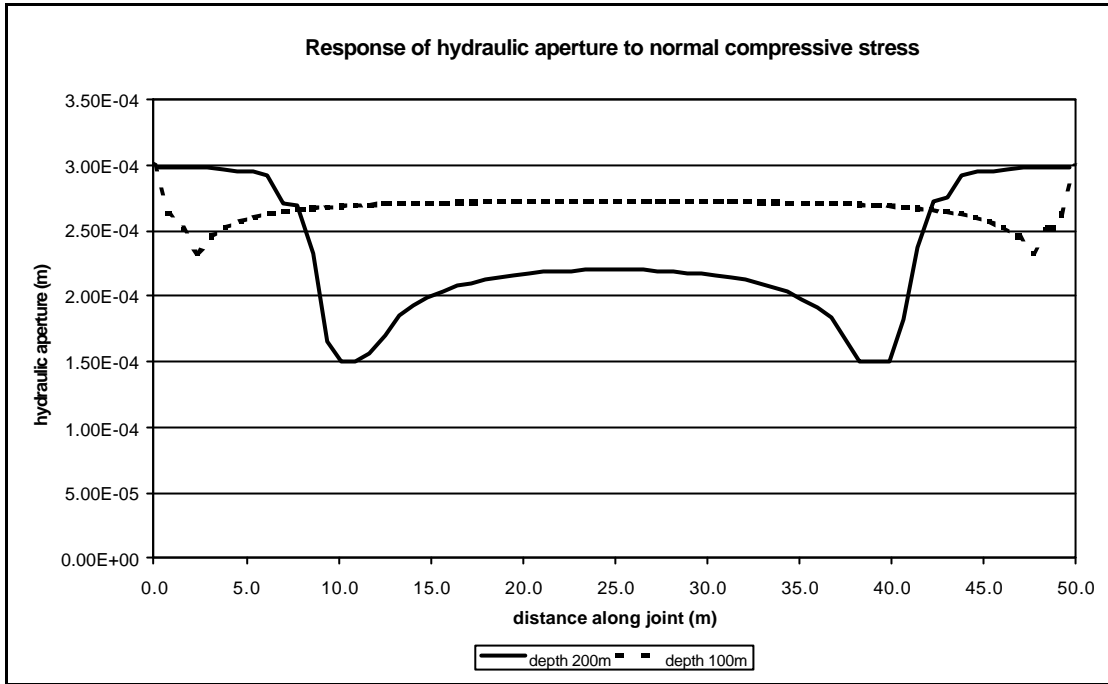


Figure 37: Response of hydraulic aperture to variations in depth (stress)

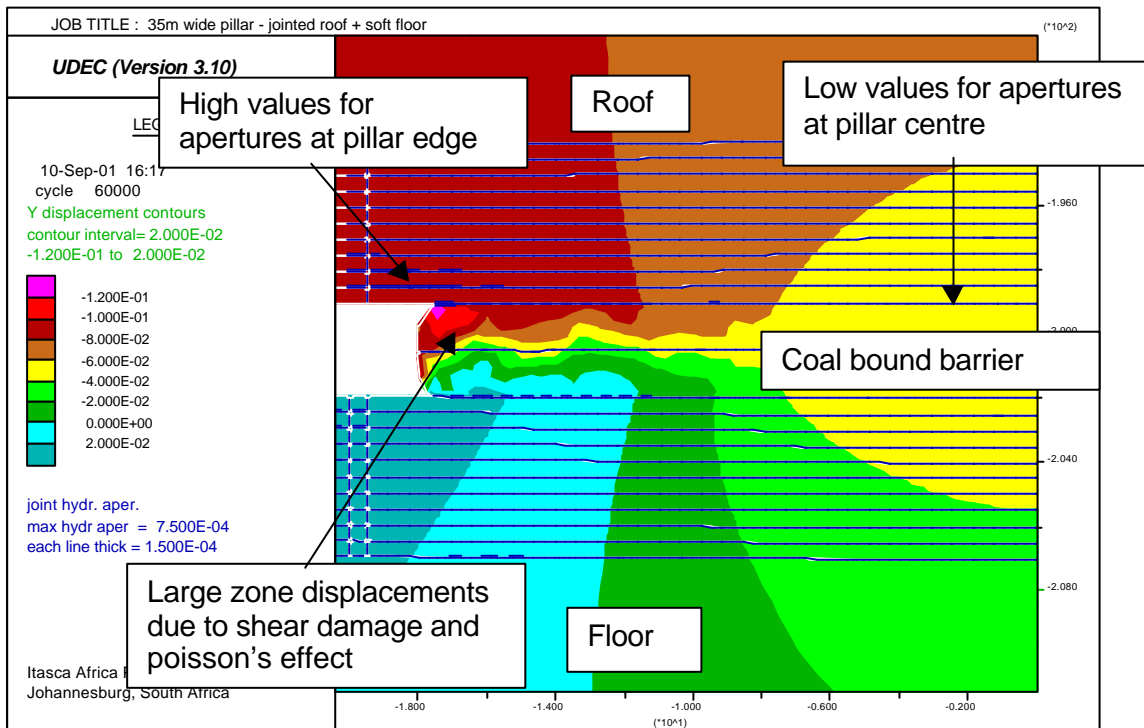


Figure 38: High degree of pillar edge displacement (area of shear damage) results in reduced closure of discontinuity apertures at the edge of the pillar.

In section 3 it is shown that the strength of a pillar is directly proportional to its width to height ratio. It follows that for a particular extraction ratio, the average pillar stresses are higher for smaller pillars and hence joint normal closure greater. The average hydraulic aperture for a horizontal discontinuity thus decreases with

decreasing pillar width as shown in Figure 39. When the pillar width is decreased to a value approaching the lateral edge spalling, the average apertures tends to increase.

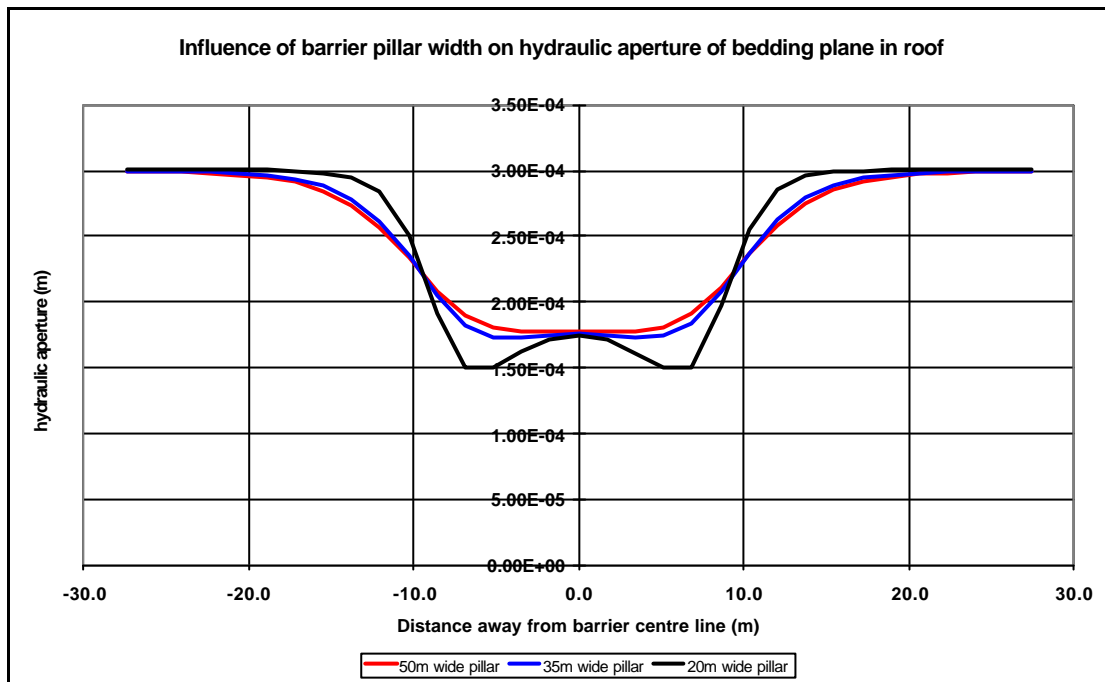


Figure 39: Distribution of hydraulic aperture in a roof bound bedding plane as a function of barrier pillar width

8.5.2 Flow paths

The flow path for a particular geotechnical regime is governed by the location, number and frequency of discontinuities and the difference in water head between flow points. Flow along horizontal discontinuities (bedding planes) will progress until equilibrium in water pressure is reached i.e. pressure in all domains of the discontinuity for the entire length is equal to the input pressure. Leakage of water onto the dry side of the barrier pillar will only occur if the inclination of roof and floor beds results in their ends 'daylighting' in the roof and/or floor of the roadway. Since most roof and floor strata lie conformable to the coal seam, it follows that flow along bedding planes will result in no water leakage unless they are intersected by vertical or sub-vertical fractures.

These tapping fractures (vertical/sub-vertical fractures that connect bedding planes to the excavated roadway) have been simulated to represent either discrete joints in competent strata or shear damaged incompetent strata (section 8.2.1.3). These fractures form the egress point for water resulting in accumulated roof and floor leakage into the roadway. Horizontal fracture planes in the coal seam contribute directly to the flow rate (rate of leakage) on the dry side of the pillar due to the finite width of the pillars modelled. Figures 40 and 41 illustrate the flow paths for competent and incompetent strata, respectively.

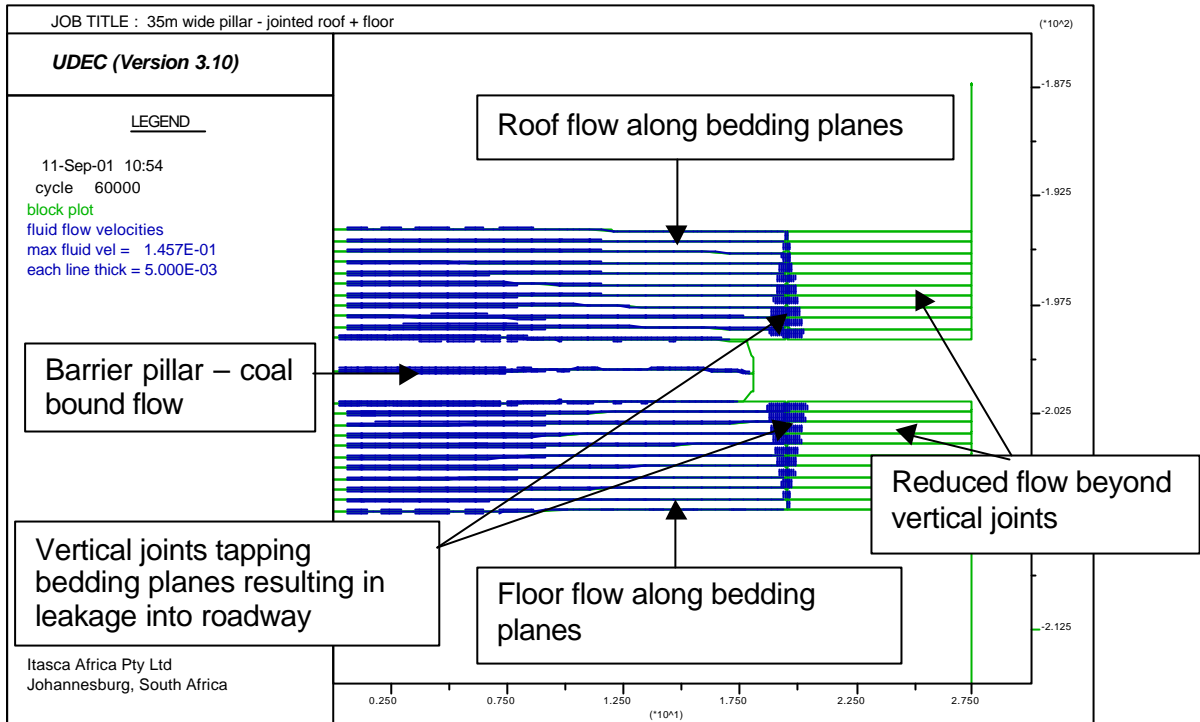


Figure 40: UDEC fluid flow velocity lines showing the tapping effect of a discrete vertical roof and floor joint

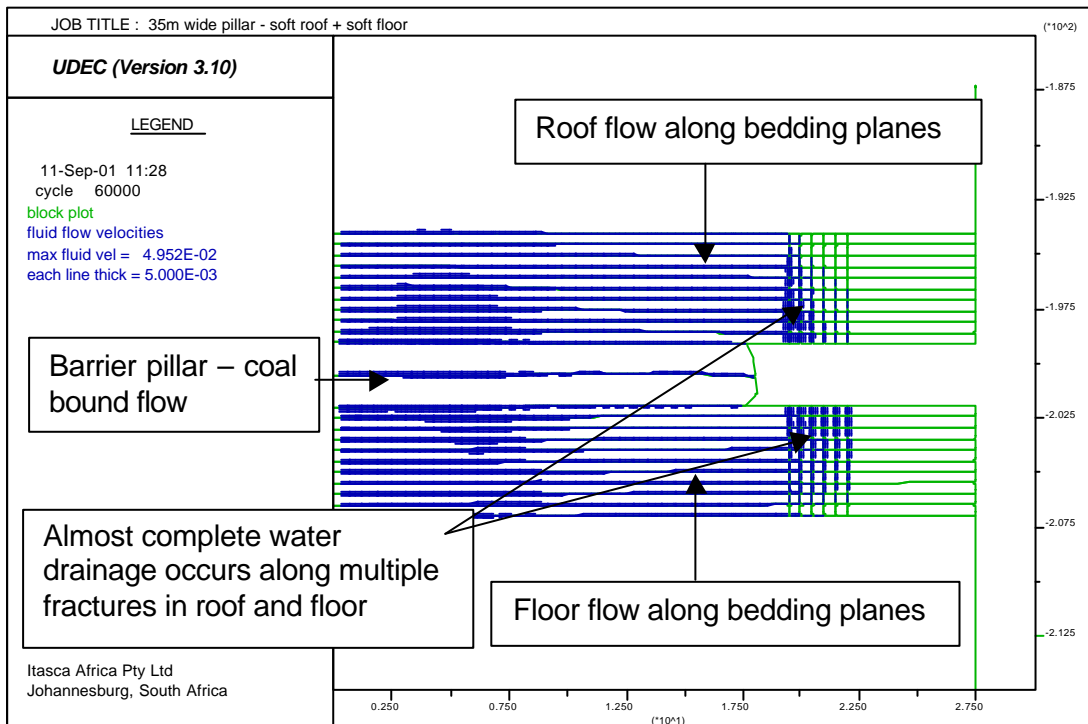


Figure 41: UDEC fluid flow velocity lines showing the tapping effect of multiple vertical joints that represent shear damaged areas of incompetent roof and floor strata

Figures 40 and 41 illustrate the influence that the number of vertical fractures has on water leakage into the roadway. The greater the number of vertical fractures that 'daylight' in the dry roadway, the greater is the rate of discharge into the dry side of the barrier pillar. Competent roof and floor strata (sandstones) are generally not prone to shear damage resulting from the indentation effect of pillars. Naturally occurring vertical and horizontal cracks (joints and bedding planes) thus govern the flow through these strata. Underground investigations revealed very low frequencies of natural or artificially induced vertical cracks (roadway tension cracks) in well-bedded sandstones.

Siltstones and gritstones are less siliceous than sandstones and hence lower strength. Underground observations (Appendix II) support the broad view that these strata are more prone to shear damage than sandstones. In all UDEC models constructed, multiple vertical joints thus represents incompetent strata and discrete vertical joints, competent strata. If incompetent sandstones bound the coal seam in a particular mine, then the user of the design charts (section 9) will classify his/her flow regime using the siltstone/gritstone charts.

8.5.3 Formulating expressions for modelled flow

The rate of flow for the different geotechnical flow regimes is dependent on the hydraulic aperture along discontinuities, the water head and length of fractures. The aperture in turn is dependent on the width of the pillar and the depth below surface (loading regime).

Using the modelled flow rates for the five generic flow regimes, a relationship was established between barrier pillar width and cumulative hydraulic aperture. The hydraulic aperture in Darcy's equation could thus be expressed in terms of barrier width. This enabled a set of governing equations to be derived for the seven geotechnical flow regimes that contained two independent variables (barrier width and water head). The flow diagram depicted in Figure 42 shows the methodology adopted to establish the governing equations using Darcy's law.

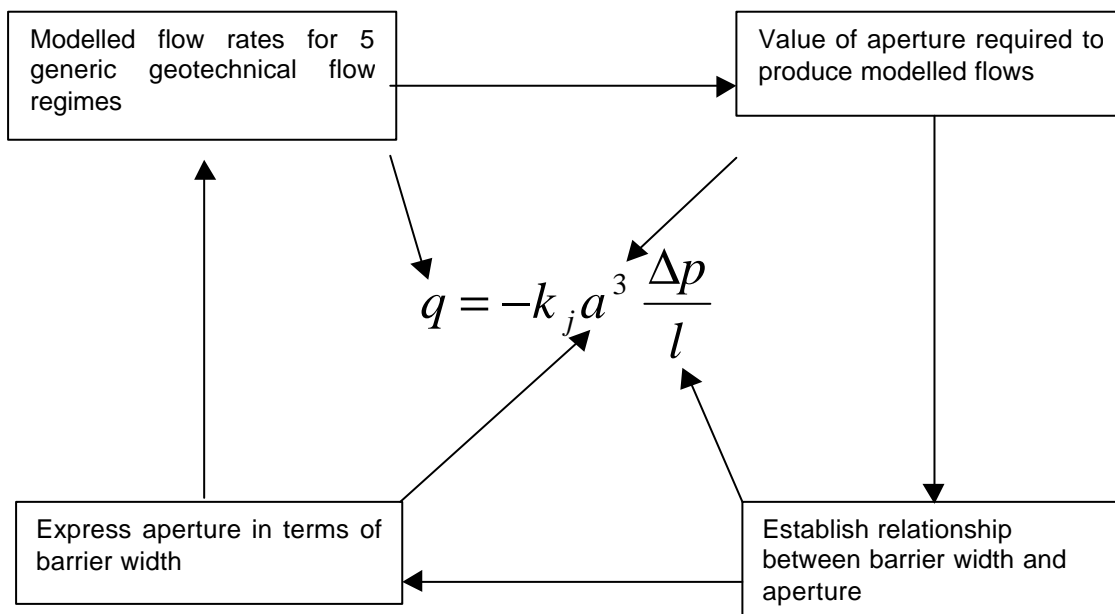


Figure 42: Flow chart showing the methodology adopted to establish governing equations for flow using modelled flow rates and Darcy's equation

8.5.3.1 Modelled flow rates

The cumulative flow rates into the roadways on the 'dry side' of the barrier pillars for the 5 generic geotechnical flow regimes is shown in Table 6.

Table 6 Rate of water leakage on the dry side of the barrier pillar for variations in pillar width at a depth of 200m below surface

Geotechnical flow regime	50m wide barrier (m ³ /sec)/m	35m wide barrier (m ³ /sec)/m	20m wide barrier (m ³ /sec)/m
Coal bound	1.132E-05	1.222E-05	2.457E-05
Competent roof + coal bound	3.813E-05	3.910E-05	6.206E-05
Competent roof and floor + coal bound	6.708E-05	6.904E-05	1.033E-04
Competent roof + incompetent floor + coal bound	7.591E-05	7.880E-05	1.219E-04
Incompetent roof + floor + coal bound	8.110E-05	8.418E-05	1.350E-04

8.5.3.2 Geotechnically classified fluid flow expressions

Rearranging Darcy's equation, the cumulative aperture required to yield the modelled flow rate can be derived.

$$a = \left(\frac{q_m l}{k_j \Delta p} \right)^{\frac{1}{3}} \quad (29)$$

where q_m is the modelled flow rate (m³/sec.m) and l the barrier width (m)

The cumulative apertures obtained as a function of barrier pillar width for the 5 geotechnical flow regimes is shown in Figure 43.

Over the 20m to 50m barrier pillar width operating range established from the industry survey, equations governing the relationship between aperture and barrier width can be obtained. Since aperture and barrier widths are exponentially related in Darcy's equation, best fit exponential rather than linear functions were used to equate the two parameters. The curves with derived functions are shown in Figure 44 for roof and floor geotechnical conditions and Figure 45 for coal bound flow.

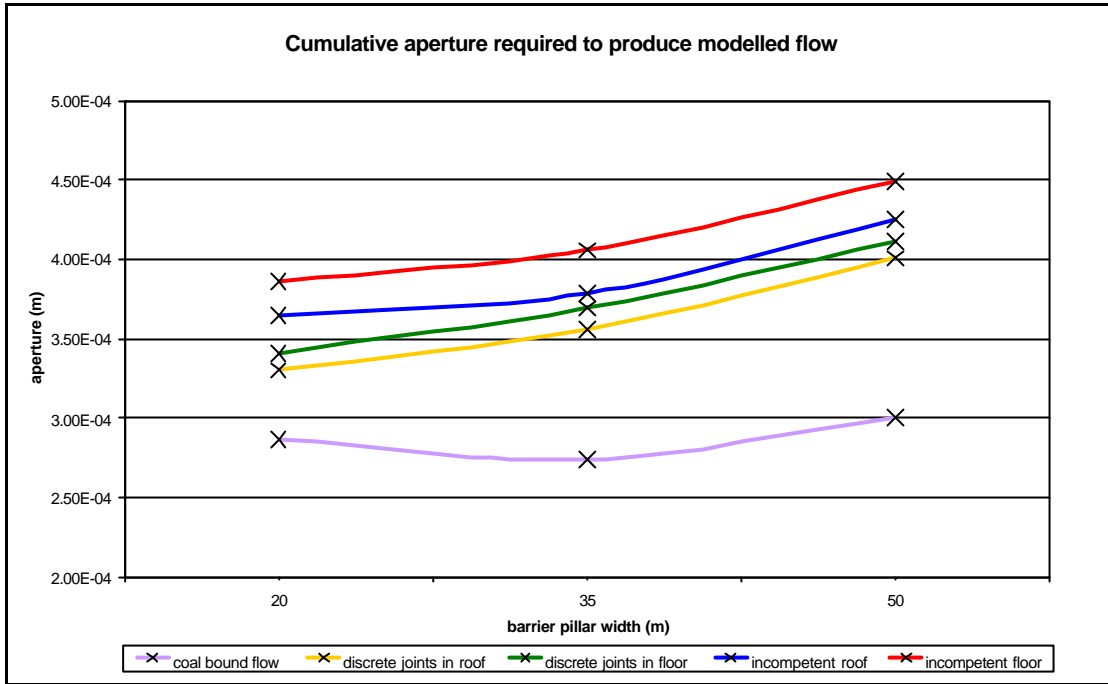


Figure 43: Cumulative hydraulic aperture as a function of barrier pillar width for geotechnical conditions of the roof, coal and floor

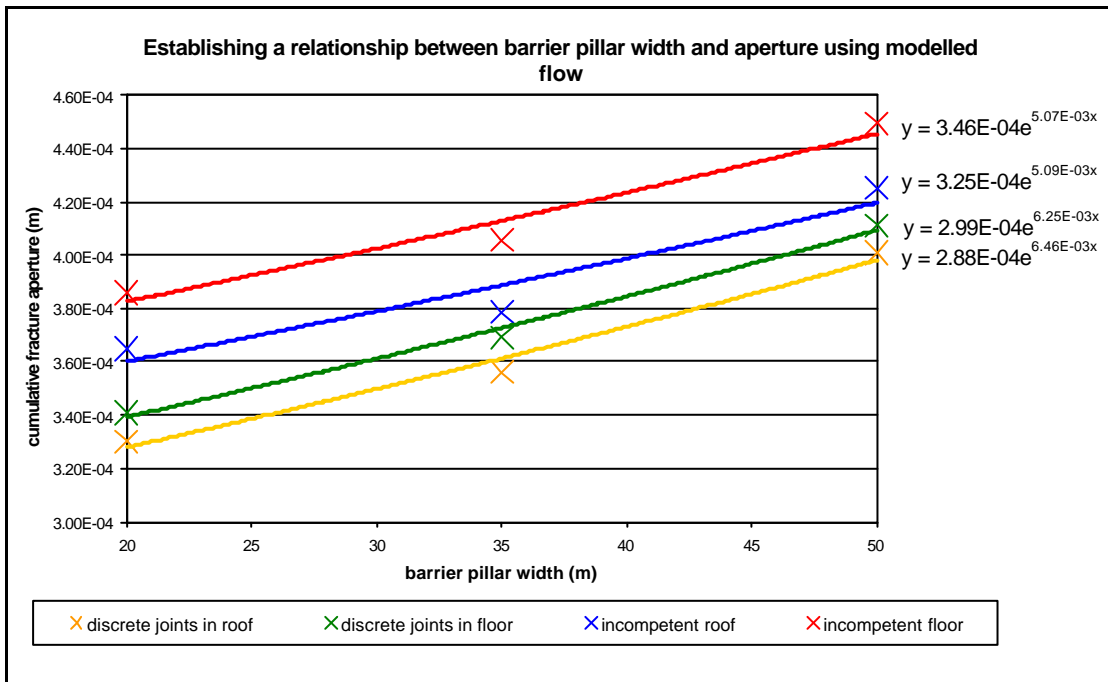


Figure 44: Best fit exponential functions for cumulative aperture as a function of barrier width using modelled flow rates for roof and floor geotechnical conditions

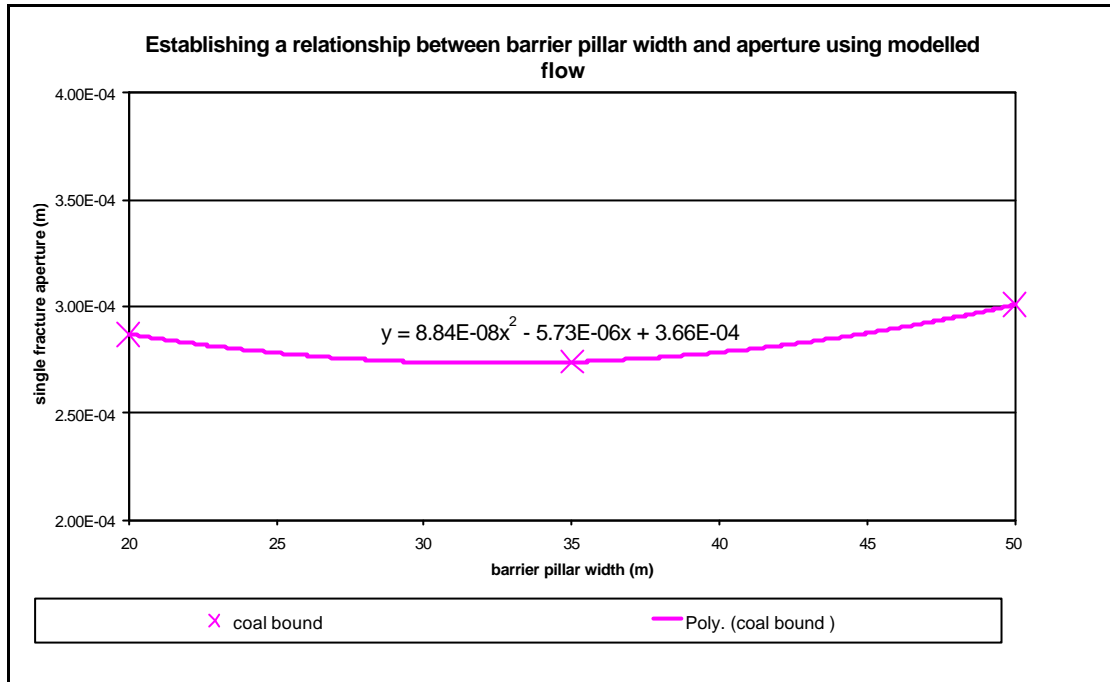


Figure 45: Best fit polynomial for cumulative aperture as a function of barrier width using modelled flow rates for coal bound flow only

Using the expressions defined for geotechnical conditions of the roof, coal and floor strata, Darcy's equation can be simplified, requiring the input of 2 independent variables to solve for flow rate for any barrier width between the operating ranges.

Combinations of the flow rates for roof, coal and floor conditions can be made to produce the flow attributable to the seven geotechnical conditions classified in section 4. These combinations are simply the addition of flow rates from the roof, coal and floor strata depending on condition. The expression for aperture in terms of barrier width relevant to the condition of the roof, coal or floor strata is shown in Table 7. Combinations of flow condition (Table 7) to produce the geotechnical flow regimes are shown in Table 8.

Table 7 Replacement of aperture in Darcy's equation for conditions of roof and floor strata

Number	Flow Condition	Replace (a) in Darcy's equation with:
1	Coal bound only	$8.84 \times 10^{-8} l^2 - 5.73 \times 10^{-6} l + 3.66 \times 10^{-4}$
2	Competent roof	$2.88 \times 10^{-4} e^{6.46 \times 10^{-3} l}$
3	Competent floor	$2.99 \times 10^{-4} e^{6.24 \times 10^{-3} l}$
4	Incompetent roof	$3.25 \times 10^{-4} e^{5.09 \times 10^{-3} l}$
5	Incompetent floor	$3.46 \times 10^{-4} e^{5.07 \times 10^{-3} l}$
6	Massive strata	$a = 0$

Graphs depicting the uncombined flow rates for the roof, coal and floor strata based on condition described in Table 7 are attached in Appendix III.

Table 8: Combinations of strata conditions listed in Table 4 to produce flow for seven geotechnical flow regimes

Geotechnical flow regime	Combination for a given width of barrier (Table 7)		
	roof	coal	Floor
Coal bound flow only	6	1	6
Competent roof + coal + massive floor	2	1	6
Massive roof + coal + competent floor	6	1	3
Competent roof + coal + competent floor	2	1	3
Competent roof + coal + incompetent floor	2	1	5
Incompetent roof + coal + competent floor	4	1	3
Incompetent roof + coal + incompetent floor	4	1	5

Fluid flow from a fully or partially flooded water compartment to a dry roadway seldom occurs in an isolated layer of strata (e.g. only through the roof). Some additive combination will be required to depict the cumulative influence of roof, coal and floor flow depending on the permeability of the strata. It is obvious that incompetent strata is more permeable than competent strata and that flow from the floor will be higher than that from the roof for consistent roof and floor strata due to the linear relationship between depth and water head.

9 Design charts

Using the fluid flow equations formulated in section 6.5.3.2, design charts were developed for the seven predominant geotechnical flow regimes. These charts (Appendix IV) relate barrier pillar width, water head, depth below surface and rate of water leakage into roadways adjacent to the barrier pillar. Important aspects to be considered when operating the charts are discussed below.

9.1 Correction factors for depth below surface

The influence of depth below surface on flow rates for a given pillar geometry can be expressed using Darcy's Law as follows:

$$q \propto a^3 \text{ but } a^3 \propto \frac{1}{s} \text{ since } s = \gamma h \therefore q \propto \frac{1}{h} \quad (30)$$

where h is the depth below surface and s the virgin state of stress

It is clear from the above expressions, that an inverse relationship exists between flow rate and depth below surface i.e. the deeper the barrier for a uniform loading state, the less the flow. Running UDEC models for exactly the same geometrical settings but varying the depth below surface enabled a correction factor chart to be formulated that adjusts flow rate for depth below surface (Figure 46).

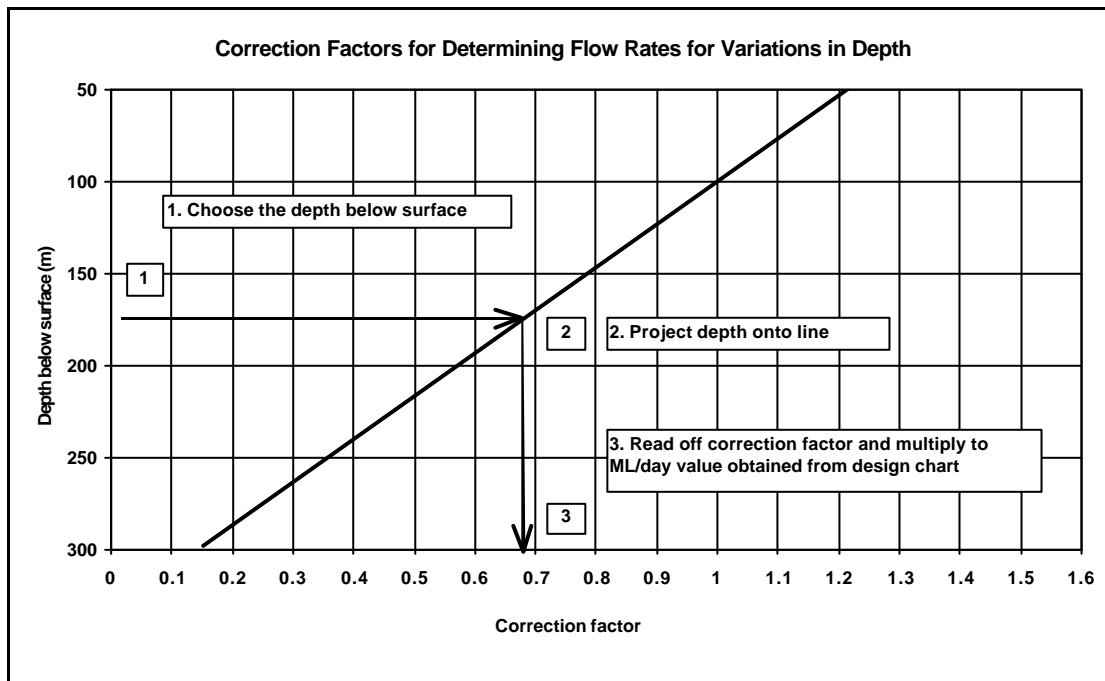


Figure 46: Correction factor for rates of leakage (flow rate) for depth below surface

The correction factor for depth related rate of leakage has been incorporated into the design charts.

9.2 Rate of water leakage

A practical way of relating water flow for the geotechnical flow regimes was devised by portraying the rate of water accumulation on the dry side of the barrier (first two roadways) to a set ponding height. The time taken for water to pond to knee depth height (approximately 1m) was calculated and related to the volume in ML/day. Drawing flow lines of quantity/time could thus easily be related back to known rates of ponding or pumping cycles employed on collieries.

The realistic time-based leakage was calculated using the dimensions depicted in Figure 47.

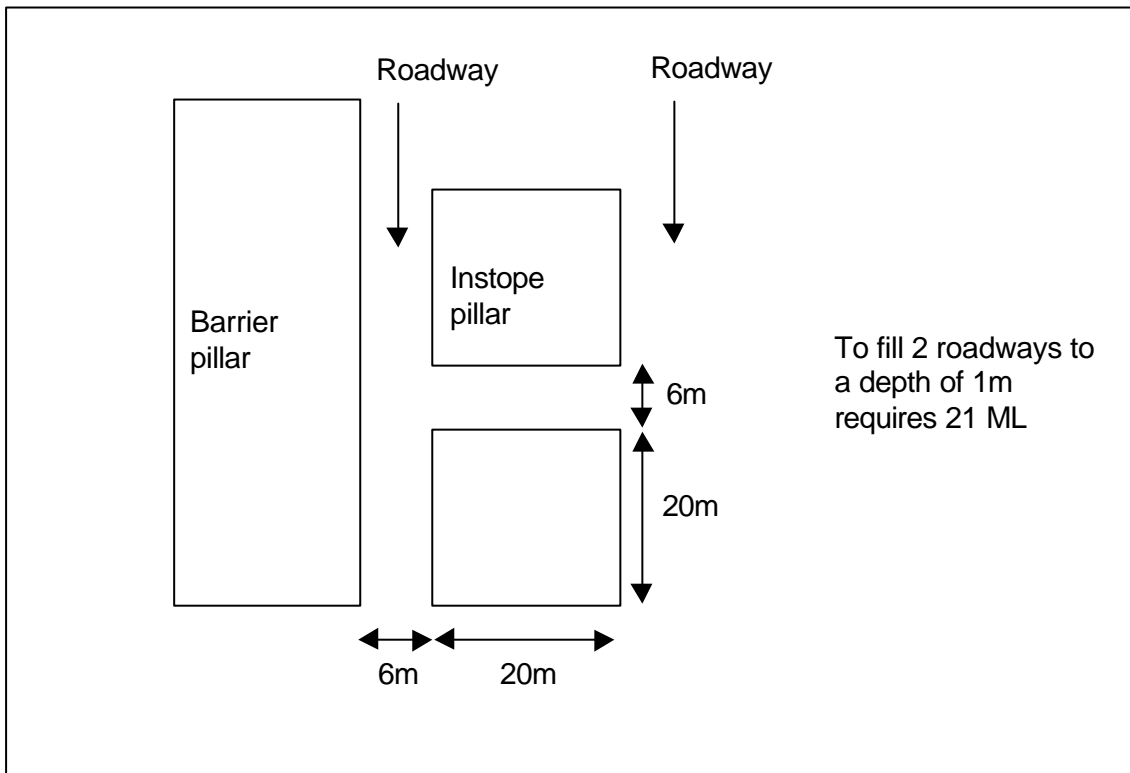


Figure 47: Dimensions used to calculate rate of leakage resulting in knee depth ponding (1m)

For the five categories of leakage depicted in Figure 48, the time taken for water to reach knee depth ponding in two roadways is shown in Table 9.

Table 9: Relating leakage rates for knee depth ponding to categories of leakage

Approximate time for water to reach knee depth ponding	
Rate of leakage category or required pumping rate (ML/day)	Time (hr)
Very high	< 10
High	10 - 20
Moderate	20 - 72
Low	72 - 192
Very low	> 192

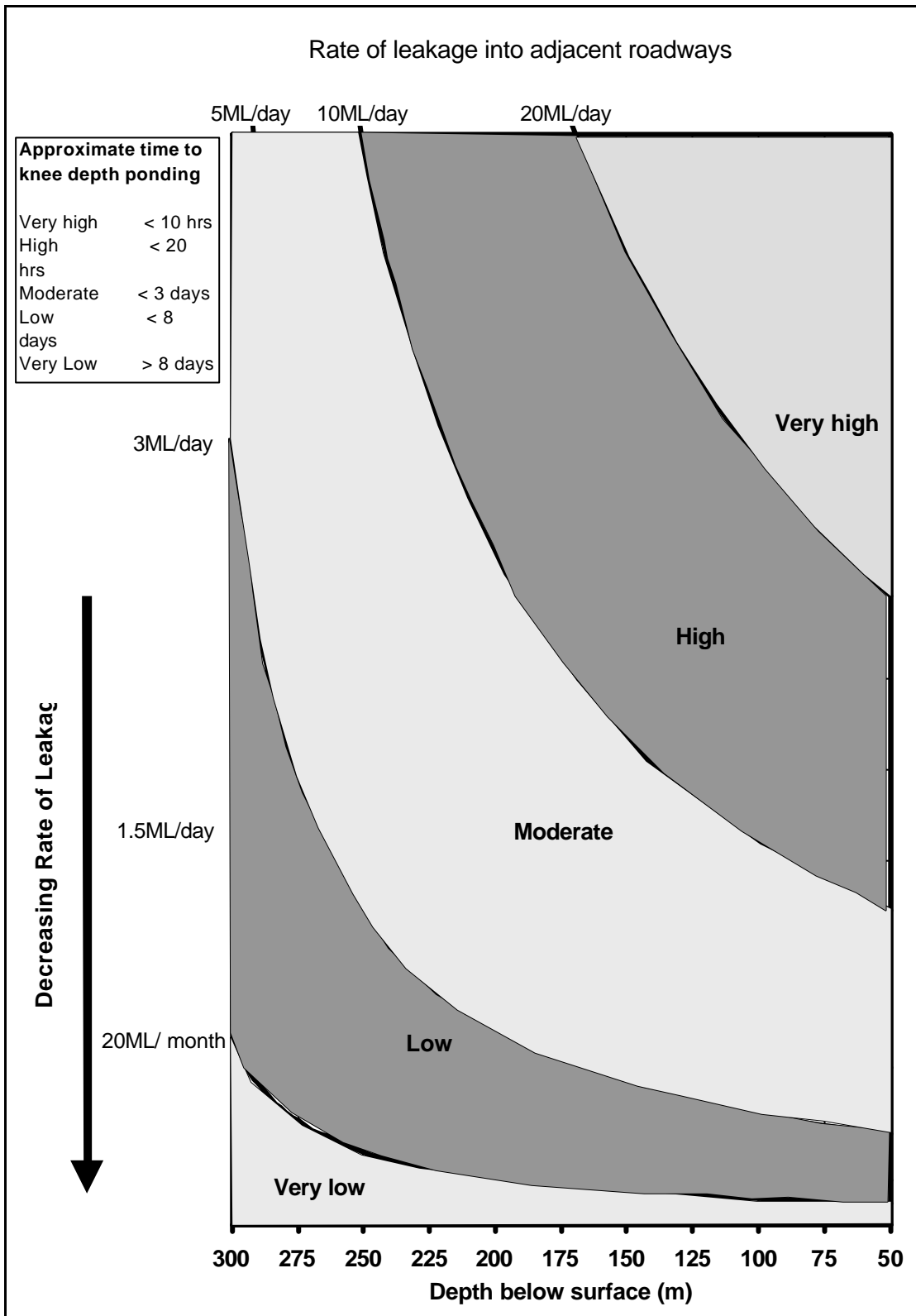


Figure 48: Five categories for rate of leakage and time taken for knee depth ponding

9.3 Correction factor for length of barrier pillar

The design charts applicable to the seven geotechnical flow regimes defined have been normalized for a 1km long barrier pillar. This normalization has an influence on the rate of water leakage or rate of roadway pumping determined from the charts. For a specific length of barrier pillar applicable to a particular mine the actual rate of water leakage or roadway pumping rate required can be determined from the following simple correction factor.

$$Lk_{actual} = Lk_{chart} \times \frac{L}{1000} \quad (31)$$

where Lk_{actual} is the actual rate (ML/day) of water leakage or pumping rate
 Lk_{chart} is the rate (ML/day) of water leakage or pumping rate determined from the design charts, and
 L is the length of pillar (m) applicable to a particular mine

9.4 Design chart operating ranges

Operating ranges for the design charts have been determined from local industry wide surveys of collieries that store water underground. These ranges are shown in Table 10.

Table 10: Operating ranges for geotechnically classified hydraulic design charts

Operating range	Reservoir floor depth below surface (m)	Seam heights (m)	Barrier pillar widths (m)	Water head (m)	Reservoir dewatering (ML/day)
	40 - 200	2 - 4	5 - 50	2 - 50	0.25 - 30

Operating conditions for the design charts exclude:

- (1) Water seepage associated with seals (observations indicate that seepage associated with seals could be significant).
- (2) Geotechnical conditions different from the seven most common described in Section 4.
- (3) Water seepage associated with geologically anomalous features (faults, dykes).
- (4) Significant water seepage beyond 5m (modelling parameter) into the roof and floor (industry survey indicates flow confined to the first 10m and 7m of the roof and floor, respectively).

9.5 Classification of flow regimes

Water flow through and around coal bound barrier pillars can be classified according to the rock type hosting the discontinuities that allow water leakage. Discharge of water onto the dry side of a barrier pillar from a flooded or partially flooded area will normally be a combination of water seeping from the roof, coal or floor. The geohydrological condition of the immediate roof, coal and floor will determine the type

of flow regime pertinent to a particular mine. The bulk of local underground collieries can be classed into the seven flow regimes depicted in Figures 49a-g.

Figure 49a	Figure 49b
<ul style="list-style-type: none"> • Leakage of water occurs through the coal seam and discrete vertical joints in bedded sandstone roof and floor strata • Go to design chart 5a 	<ul style="list-style-type: none"> • Leakage of water occurs through the coal seam only • The roof and floor strata are massive and impermeable • Go to design chart 5b

Figure 49c	Figure 49d
<ul style="list-style-type: none"> • Leakage of water occurs through the coal seam and discrete vertical joints in bedded sandstone roof and soft, damaged, laminated siltstone/gritstone floor • Go to design chart 5c 	<ul style="list-style-type: none"> • Leakage of water occurs through the coal seam and soft, damaged, laminated siltstone/gritstone roof and floor • Go to design chart 5d

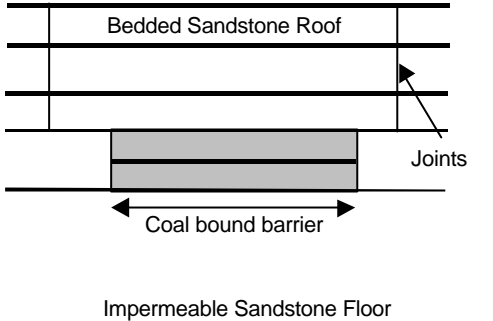
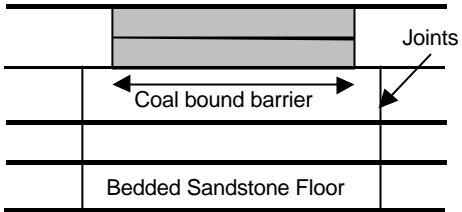
Figure 49e	Figure 49f
	
<ul style="list-style-type: none"> • Leakage of water occurs through the coal seam and discrete vertical joints in bedded sandstone roof. • The floor is massive and impermeable. • Go to design chart 5e 	<ul style="list-style-type: none"> • Leakage of water occurs through the coal seam and discrete vertical joints in bedded sandstone floor. • The roof is massive and impermeable. • Go to design chart 5f

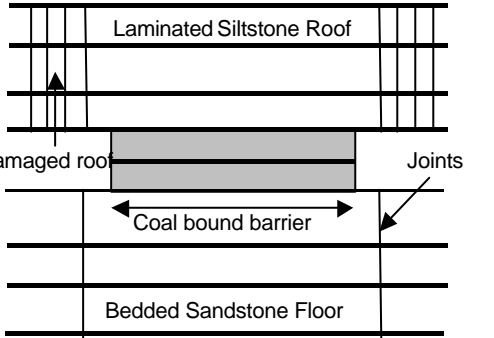
Figure 49g

<ul style="list-style-type: none"> • Leakage of water occurs through the coal seam and soft, damaged, laminated siltstone/gritstone roof and discrete vertical joints in bedded sandstone floor. • Go to design chart 5g

Figure 49: Geotechnical classification of flow regions

9.6 Requirements and use of the design charts

9.6.1 Basic information required

Basic generic and mine specific information is required to enable use of the hydraulic design charts. The flow chart illustrated in Figure 50 depicts the inputs required to determine the optimum hydraulic pillar width for planned barriers and the maximum tolerable head for existing barriers.

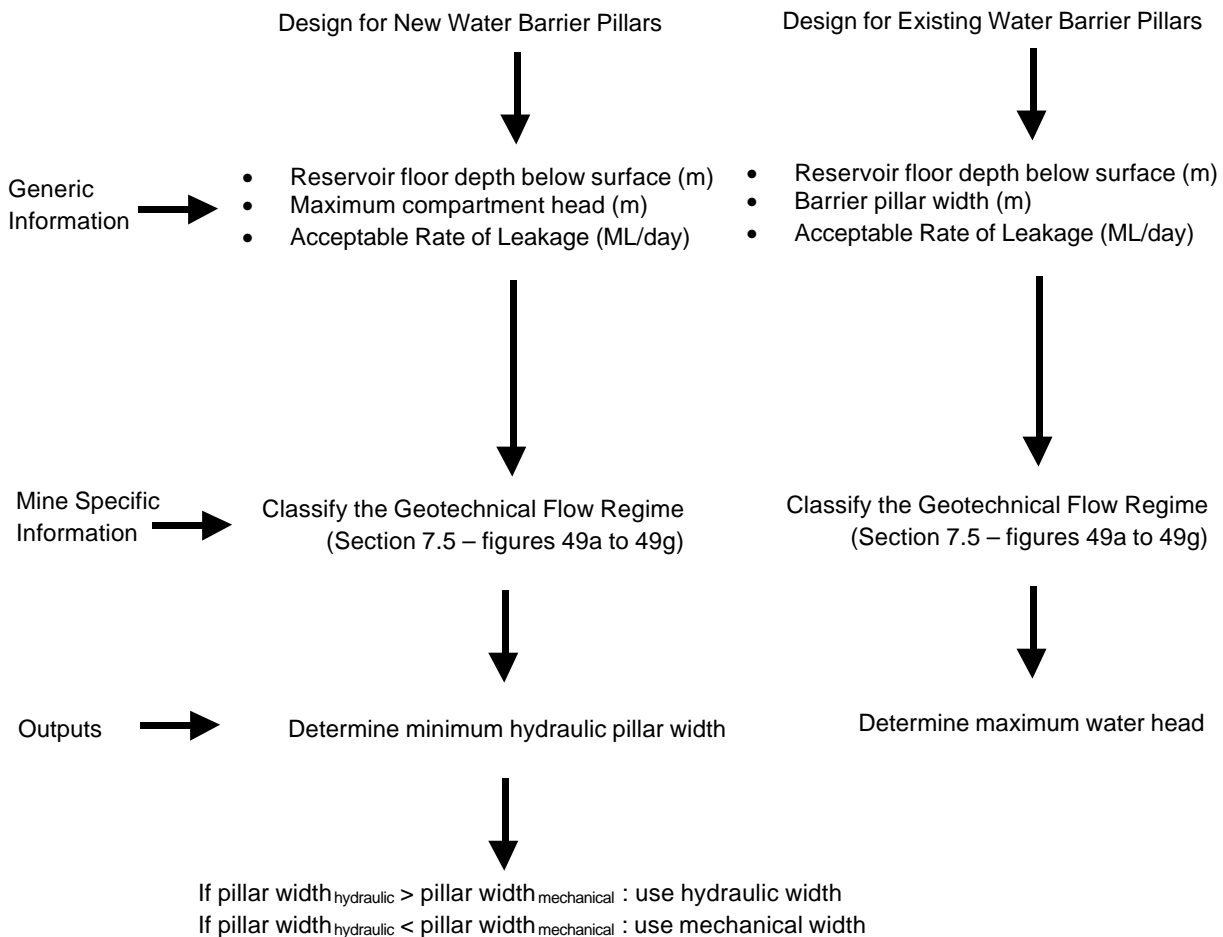


Figure 50: Flow chart illustrating the information required to determine the minimum hydraulic barrier width for new water reservoirs and the maximum tolerable head for existing barrier pillar bound water reservoirs

9.7 Operation of Design Charts

The primary use of the design charts is to determine the minimum hydraulic pillar width for new pillars and the maximum manageable water head for existing compartments (barrier pillar width established). The versatility of the design charts also allows for their use in water management feasibility planning. These additional uses are demonstrated in **Appendix V: EXAMPLE APPLICATIONS**.

9.7.1 Determining the Minimum Hydraulic Barrier Width – NEW BARRIERS

The steps outlined below must be read in conjunction with the design chart depicted in Figure 51.

Step 1: Choose the **geotechnical flow regime** applicable to the roof, coal and floor strata at the position of the proposed barrier pillar from **Figures 49a to 49g**.

Step 2: Go to the **appropriate design chart** depicted in **Appendix iv**. Confirm the choice of design chart by matching the boxed schematic of the geotechnical flow regime with that chosen from **Figures 49a to 49g**.

Step 3: Mark the floor depth of the proposed barrier pillar on the design chart x-axis titled: **Depth below surface (m)**.

Step 4: Draw a **vertical line** from the marked depth position to a line depicting the **planned rate of water pumping (or acceptable leakage rate)** from the roadway adjacent to the barrier.

Step 5: Draw a **horizontal line** from the rate of leakage (or pumping rate position) all the way across to the right vertical boundary of the graph titled: **Barrier pillar width as a function of water head**.

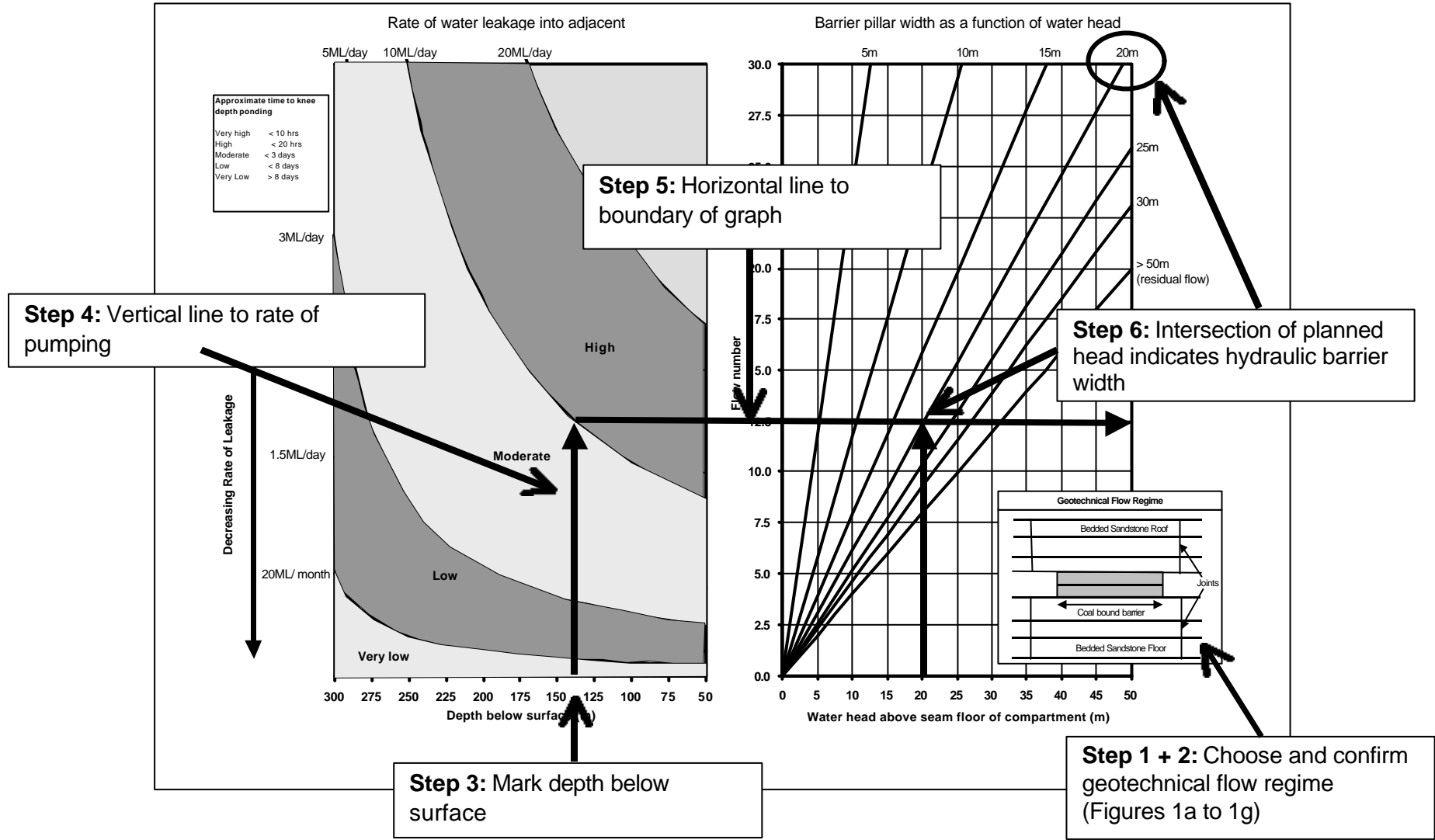
Step 6: Choose an appropriate **planned maximum water head** for the compartment. The **intersection of the line** projected vertically from the chosen **water head to the drawn horizontal line** indicates the minimum required **hydraulic barrier width**.

Remember: If the hydraulic width determined is **less than the mechanical width** (designed by Rock Engineer) – **USE MECHANICAL WIDTH**
If hydraulic width determined is **greater than the mechanical width** (designed by Rock Engineer) – **USE HYDRAULIC WIDTH**
Correct the rate of leakage (SECTION 5.3) for the **length of pillar** being planned.

Figure 51: Determining the minimum hydraulic width of barrier pillars for the design of new compartments (p.t.o)

Hydraulic Design Chart for Barrier Pillars

(Flow Regime = Coal bound + bedded sandstone roof + bedded sandstone floor)



9.7.2 Determining the Maximum Tolerable Water Head – EXISTING BARRIERS

The steps outlined below must be read in conjunction with the design chart depicted in Figure 52.

Step 1: Choose the **geotechnical flow regime** applicable to the roof, coal and floor strata at the position of the proposed barrier pillar from **Figures 49a to 49g**.

Step 2: Go to the **appropriate design chart** depicted in **Appendix iv**. Confirm the choice of design chart by matching the boxed schematic of the geotechnical flow regime with that chosen from **Figures 49a to 49g**.

Step 3: Mark the floor depth of the proposed barrier pillar on the design chart x-axis titled: **Depth below surface (m)**.

Step 4: Draw a **vertical line** from the marked depth position to a line depicting the **rate of leakage** from the water reservoir to the roadway adjacent to the barrier.

Step 5: Draw a **horizontal line** from the rate of leakage (or pumping rate position) across to the line representing the existing barrier pillar width.

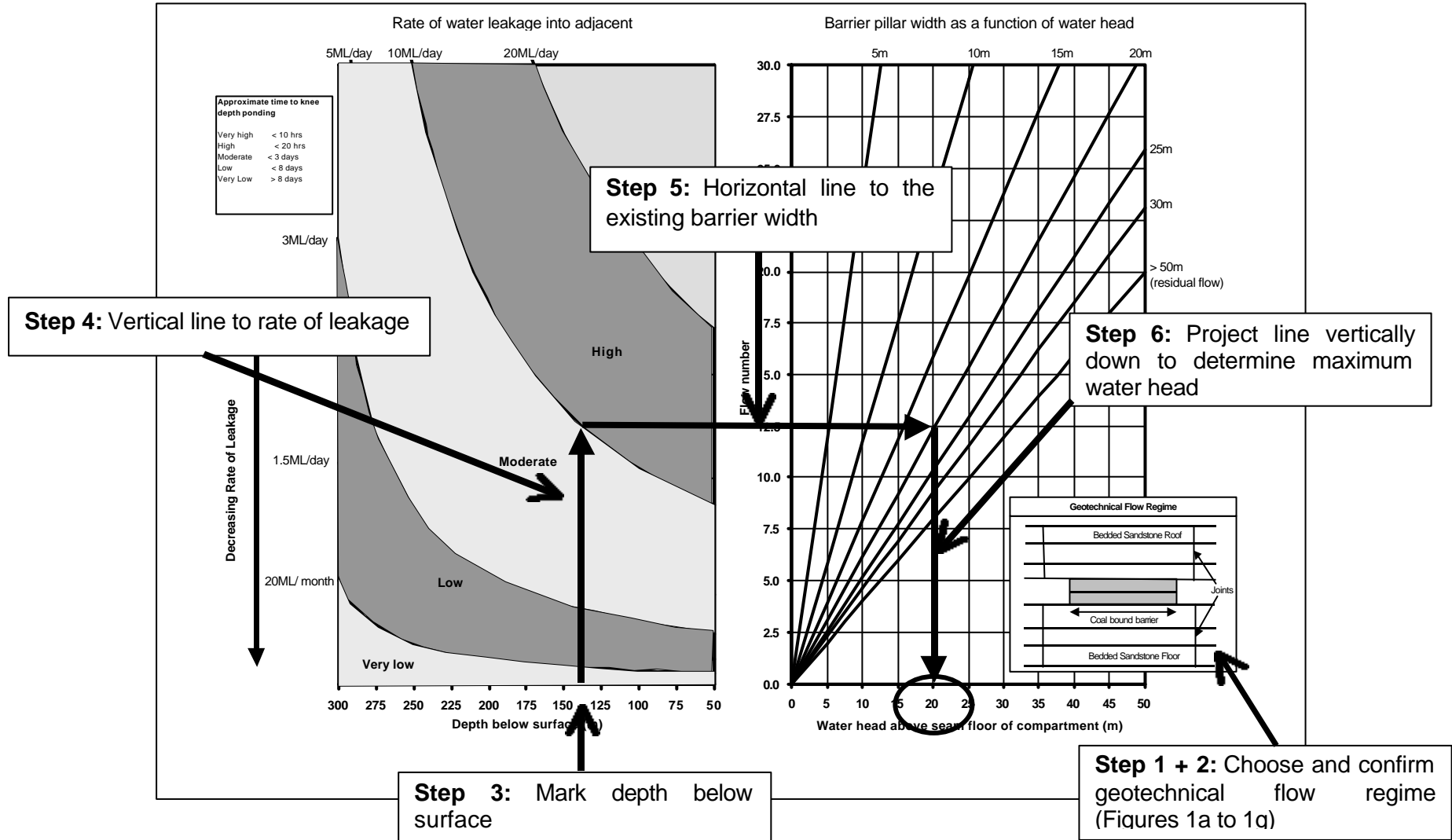
Step 6: Subtending this line vertically down to the x-axis indicates the maximum tolerable reservoir head required for an acceptable rate of water leakage.

Remember: It is assumed that the mechanical design of the barrier pillar has been established.
Correct the rate of leakage (SECTION 7.3) for the existing **length of pillar**.

Figure 52: Determining the maximum tolerable compartment water head for existing barrier pillar bound reservoirs (p.t.o)

Hydraulic Design Chart for Barrier Pillars

(Flow Regime = Coal bound + bedded sandstone roof + bedded sandstone floor)



10 Recommendations for further research

Detailed examinations and analyses of the behaviour of the seals or plugs were outside the scope of the study, however underground investigations revealed that water leakage at the coal/seal interfaces could be highly significant.

It is recommended that further research into the understanding of fluid flow at the interface of the seals/plugs be conducted to enable the full spectrum of hydraulic conditions to be addressed through engineered design. Collieries currently spend huge amounts of capital to plug splits made in continuous barriers with little understanding of the influence of these seals on compartment water retention.

Further research into seal/coal interfaces and their influence on fluid flow should give insight into optimum seal thickness required for a particular barrier pillar configuration, extent of injection grouting required around the seal and the relationship between barrier pillar widths and seal widths. Engineered judgements on all aspects of seal construction will have a direct cost spin-off to the coal industry at large.

11 Conclusions

The international literature survey conducted showed that the current status of the hydraulic design of barrier pillars is inadequate. Most international empirical criteria currently used address the mechanical stability of the barrier pillars and the strength reduction influence of water on these pillars. No design guidelines or mathematical formulations exist to stipulate hydraulic barrier pillar widths based on geotechnical flow regimes, driving water heads or acceptable flow rates into mines.

Locally, the mechanical design of barrier pillars is based on the design principles used for the square in-stope pillars. No hydraulic considerations are made when designing these continuous barriers. It is normally accepted that the mechanical design is sufficient to obtain widths that will effectively manage water retention. The international and local survey revealed that no engineered design exists for barrier pillars fulfilling a hydraulic function.

Operating ranges for the design charts were formulated from the responses to the industry wide questionnaire. Ninety percent of South African collieries that store water underground can be classified into the seven geotechnical flow regimes identified, thus most collieries will have an appropriate barrier pillar hydraulic design chart. The field data gathered gave further insight into the range of operating colliery depths, seam heights, range of barrier widths, effective compartment water heads and condition of strata that form conduits for flow.

The intrinsic permeability of the coal seams and hosting strata are extremely low. The literature supports the assumption made that all significant fluid flow occurs along discontinuities rather than through a porous medium. Observations made during underground visits to collieries in the Witbank, Highveld, Free State and Natal coalfields also support fracture driven rather than porous medium flow. Monitoring of flow rates and water pressures across barrier pillars was done to calibrate discontinuum based numerical models that were used as the primary analysis tools. To obtain time based recorded water pressure degradations, a model residual aperture of 0.15mm was calibrated. Very close correlation of actual flow rates recorded for various collieries with that obtained from the models was obtained.

The most significant output of the numerical models was the formulation of mathematical expressions that govern flow in the seven geotechnical regimes defined. The flow rate, fracture length and hydraulic gradient was thus governed by a unique set of equations for a particular geotechnical flow regime. Approximately 70% of operating collieries were used to define the seven predominate geotechnical flow regimes.

The series of design charts formulated allow use for the design of optimum barrier pillar widths to match a predetermined water head and pumping capacity (or rate of leakage) for new planned water compartments. Conversely, the design charts enable the maximum compartment water head to be determined in mines with existing barrier pillars. Additionally, the design charts provide the user with the ability to determine a suitable roadway pumping rate to maintain a predetermined level of water leakage from the compartment.

It is critically important that the user identify the geotechnical flow regime around the water compartment before embarking on using the design charts, since each flow regime has its applicable chart. The mechanical design of the barrier pillars must be established before using the design charts to determine the optimum hydraulic barrier pillar width. Under no circumstances should the hydraulic width be used if it is less than the width required for mechanical stability.

An important aspect of water leakage in and around water compartments is the influence of civil constructed seals and plugs. Insight into the hydraulic influence of the seal/coal interface is recommended for further research.

12 References

- Acid Drainage Technology Initiative. 2000.** A handbook of Technologies for Avoidance and remediation of Acid Mine Drainage. "Green Lands" magazine – Winter 2000.
- Bieniawski Z.T. (1987).** Strata control in mineral engineering, John Wiley & Sons, New York.
- Borecki M., & A. Belinski (1964).** Results of investigations on rock pressure by the longwall system of coal mining in the upper silesian coal field, Proceedings of the 4th International Conference on Strata Control & Rock Mechanics, Columbia Univ., NY.
- Budavari, S., 1983.** Rock Mechanics in mining practice, The South African Institute of Mining and Metallurgy, Monograph series M5, Johannesburg.
- Carman P.C. (1937).** Fluid flow through granular beds, *Transactions of the Institution of Chemical Engineers*, 15, 150-166.
- Chinese coal mine floods,** Mining Journal (London) V. 303, No. 7787, Nov. 16 1984 p. 347
- Cook, N.G.W., Hodgson, K., Wagner H., 1969.** The effectiveness of boundary pillars as water barriers. Research report no. 40/69, Project no. 1/105/661/105/66, Mining Research Laboratory, Johannesburg.
- Davies, A.W., Baird, W.K.** Water dangers. Min. Eng. (London) v. 136 No. 188 Dec 1976-Jan 1977 pp. 175-184
- Esterhuizen, G.S., 1998.** The effect of structural discontinuities on coal pillar strength, SIMRAC project no COL005a, Faculty of Engineering, University of Pretoria.
- Esterhuizen, G.S., 1991.** The stability of barrier pillars in coal mines, Faculty of Engineering, University of Pretoria.
- Fauconnier, C.J., Kersten, R.W.O., 1982.** Increased Underground Extraction of Coal, The South African Institute of Mining and Metallurgy, Monograph series No. 4, Johannesburg.
- Garritty P. (19?).** Water percolation into fully caved longwall faces, Proc.....,
- Goodman R.E., 1980.** Introduction to Rock Mechanics, University of California at Berkley.
- Griffith, E.** Mine drainage Practice in the Anthracite region of Pennsylvania. Trans. Soc. Min. Eng. AIME v. 168 1946 pp. 127-144
- Hodgson, F.D.I.,** Geological, geohydrological and ecological factors affecting increased underground extraction of coal, University of the Orange Free State.
- King H.J. and B.N. Whittaker (1971),** A review of current knowledge on roadway behaviour, especially in problems on which further information is required, Proceedings of the IME Symposium on Roadway Strata Control, Inst. Min. Metall., pp. 73-87.
- Koehler, J.R., Tadolini, S.C., 19..** Practical design methods for barrier pillars, USBM, Denver Research Centre, Denver, Colorado.

Koehler J.R., Jones S.D., Demarco M.J. (1989), An application approach to barrier pillar design for improved resource recovery. *Proceedings Of the 30th US Rock Mechanics Symposium*, Morgantown, WA, 403-410.

Koehler J.R. & S.C. Tadolini. 1995. Practical Design Methods for Barrier Pillars. *US Bureau of Mines Information Circular IC 9427*, US Dept of the Interior,

McKinnon, S.D. 1988. Water barrier pillar design. Research report no. 12/88, Project No. GR1D, Rock Mechanics Laboratory, Johannesburg.

Moebis, N.N., Sames, G.P., 1989. Leakage across a bituminous coal mine barrier. Report of Investigations 9280 / 1989, U.S. Dept of Interior, Bureau of Mines. Pittsburgh, Pennsylvania.

McKee C.R., A.C. Bumb, R.A. Koenig. 1988, Stress-dependent permeability and porosity of coal and other geologic formations, SPE Evaluation Formation, March, 81-91.

Miller J.T., D.R. Thompson 1974, Seepage and mine barrier width, *Proceedings 5th Symposium on Coal Mine Drainage Research*, National Coal Association, Washington DC, 103-127.

Miller, J.T., Thompson, D.R., Seepage and Mine Barrier width. Proceedings, 5th Symposium on coal mine drainage research. Natl. Coal Assoc., Washington D.C., 1974, pp.103-127.

Peng S.S. (1992), Surface Subsidence Engineering, Society of Mining Metallurgy and Exploration Inc., Littleton, Colorado.

Peng S.S. (1992), Coal mine ground control, John Wiley & Sons, New York.

Peters, T. W. Mine drainage problems in North Derbyshire. Min. Eng. (London) v. 137 No. 200, Mar 1978, pp. 4633-473

Rose R.E., S.E. Foh (1984), Liquid permeability of coal as a function of net stress, SPE/DOE/GRI unconventional Gas Recovery Symposium, Pittsburgh, My 13 –15.

Rosenbaum, D. (1994) Water Blowouts at Underground Mines - Outcrop Barrier Pillars Reclamation Advisory Memorandum #114, Kentucky Dept of Mining and Reclamation, 1994.

Salamon, M.D.G [Ed S. Budavari], 1983. The Role of Pillars in Mining. Rock Mech. in Mining practice, chapter 8, P. 173-200.

Salamon, M.D.G., Oravec, K.I., 1976. Rock Mechanics in Coal Mining, Coal Mining Research Controlling Council, Chamber of Mines of South Africa.

Salamon, M.D.G., Munro A.H., 1967. A study of the strength of coal pillars. Journal of the South African Institute of Mining and Metallurgy, Johannesburg.

SME Engineering Handbook (1992), Society of Mining Metallurgy and Exploration Inc., Littleton, Colorado.

Somerton W.H., I.M. Soylemezoglu, R.C. Dudley (1974), Effect of stress on permeability of coal, USBM Report, Contract H0122017.

Stripp, G.P., 1989. Methane emission characteristics of South African coal seam strata, PhD thesis, University of the Witwatersrand.

van der Merwe, J.N. 1998. Practical Coal Mining Strata Control – Second edition. Itasca Africa, Johannesburg.

Weiss, E.S., Perry J.W. and Stephan, C.R. 1993. Strength and leakage for coalmine seals. 25th International Conference of Safety in Mines Research Institutes. Pretoria.

Whittaker, B. N, & Singh, R. N. (1978). Design Aspects of Barrier Pillars Against Water-logged Workings in Coal Mining Operations, Proceedings of the First World Congress of Water in Mining and Underground Work, Granada, Spain, 1978, 675-692.

The worst ever mining disaster in India, Journal of Mines, Metals and Fuels (Calcutta) V. 23 No. 12 Dec 1975 p.5552.

Wilson A.H., 1972. Research into the determination of pillar size, Vol. 131.

Wu, K.K.; Fredland, J.W.; Krese, J.M.; Lawless, M. Factors in the evaluation of coal barriers to prevent inundation and the effectiveness of federal regulation., Soc. Min. Eng. AIME pre-print 80-88, 1980, 11 p.

Appendix I: Summarized response to the national industry questionnaire

Safe design of water barrier pillars - Summarized questionnaire response

Colliery	Compartment	Total extraction		Pillar sizes (m)		Bord width (m)	Mining height (m)	Seam depth (m)	Water head (m)	Current volume (m3)	Barrier width (m)
		y/n	% ext	L	W						
Forzando	east 1	n	75	6.8	6.8	6.8	2.2	54-76	2	216ML	40
	T-ijunction	n	70	8.2	8.2	6.8	2.2	76-78	1.5	20ML	100
Bank		n	59.2	11.5	11.5	6.5	5.5	94	13	935500	12
		n	59.2	11.5	11.5	6.5	5.5	67	28	681700	15
		n	71.3	7.5	7.5	6.5	3.5	41	4	735000	not given
Bosjesspruit	west	y	67.2	22	22	6.4	3	168	10	3348264	50
	east	y	43.8	28	28	6.7	2.9	179	3	2979324	50
	E720S	y	38.2	28	28	6.6	3	180	3	1633735	25
Khutala	2S1W1	n	55	14.4	19	6.43	3.86	106.6	100.93	415000	19.12
Golfview	Golfview 1	n	70	6	6	6	2.1	45	2	30000	6
	Douglas 2	n	70	6	6	6	2.01	47	2	10000	6
Rietspruit		n	not given	not given	not given	6.5	2.7	40.3 and 74.6	1.8	1820ML	not given
Greenside	2 seam	n	50	16.5	16.5	6.5	3.8	80	0	2885860	not given
	1 seam	n	54	14.5	14.5	6.5	3.8	85	0	6038773	not given
	2 seam	n	73	7	7	6.5	3.5	75	0	2616189	not given
Twisdraai W	west	n	not given	27	27	7	3.5	180	180	146000	30
	south	n	not given	27	27	7.2	3.5	170	170	146000	30
Tshikondeni		y	not given	32	32	not given	2.7	450	200-400	not given	not given
New Denmark	501	y	89	25	25	6.5	2	200	40	5400000	19
	601	y	90	25	25	6.5	1.95	200	18	3320000	19
	701	v	82	25	25	6.5	1.9	200	26	2075000	19
Durnaco	1	n	65	25	15	5	2	180	33	788.5ML	100

APPENDIX II Detailed analysis

New Denmark Colliery

The colliery employs primarily longwall mining and thus has a higher ingress of water than any other single colliery. The water is stored in huge compartments at great depth. Waterhead is excessive in all of these compartments and leakage, through the seals and the coal pillars, poses a major problem. Figure A1 shows the leakage across a seal built into the barrier. The waterhead behind the seal is approximately 21m.

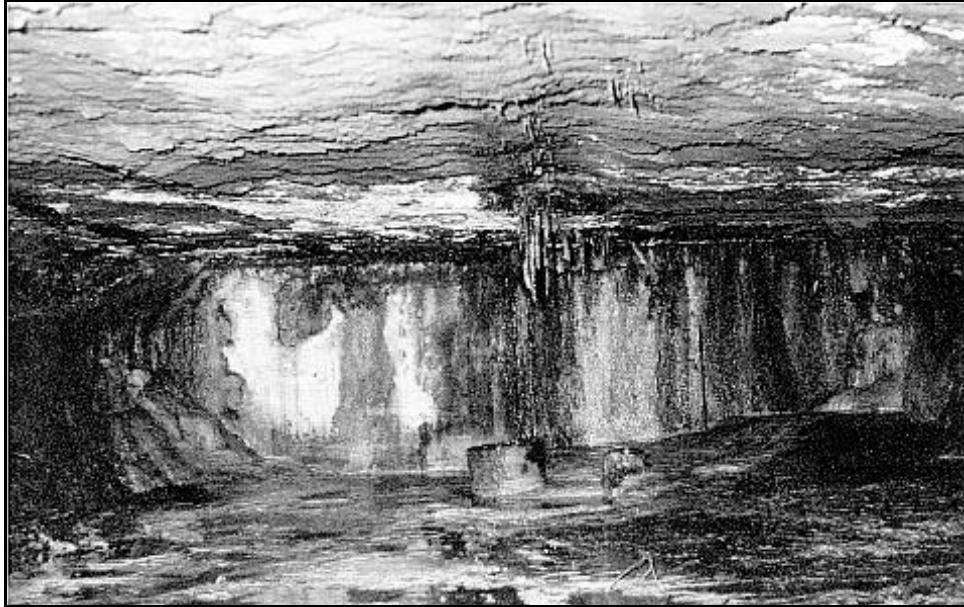


Figure A1: - Leakage across a seal, built into a barrier.

Figure A2 shows the scaling and leakage along a continuous barrier pillar with a waterhead of approximately 35m. It was noted that the seepage was along the bedding planes of certain bands in the coal. The source of the water on the floor was twofold; at a low contour point along the barrier and through the weaker floor strata.

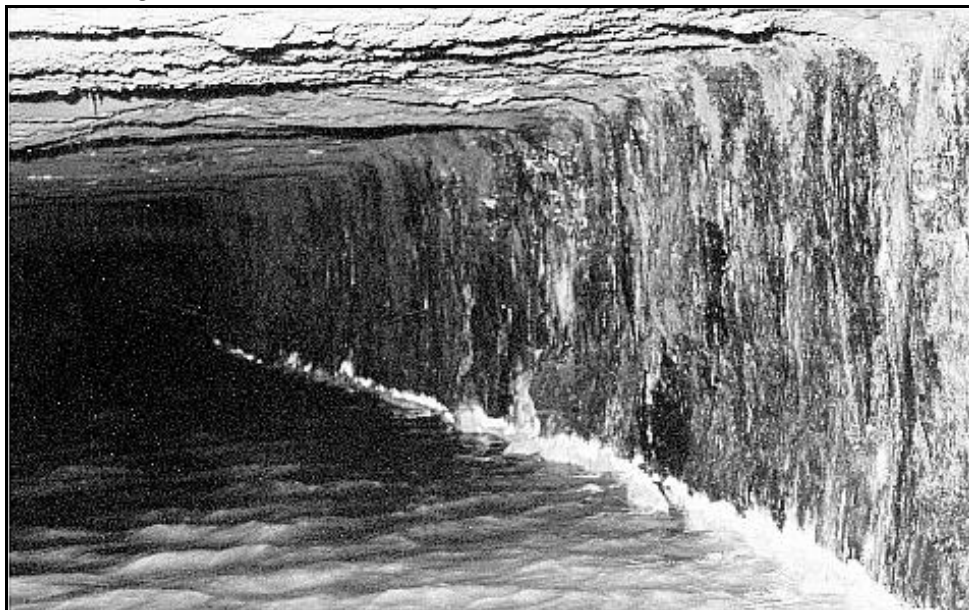


Figure A2: - Leakage along a continuous barrier

The seals built into the barrier posed a bigger problem than the actual barrier itself. The leakage was fracture driven.

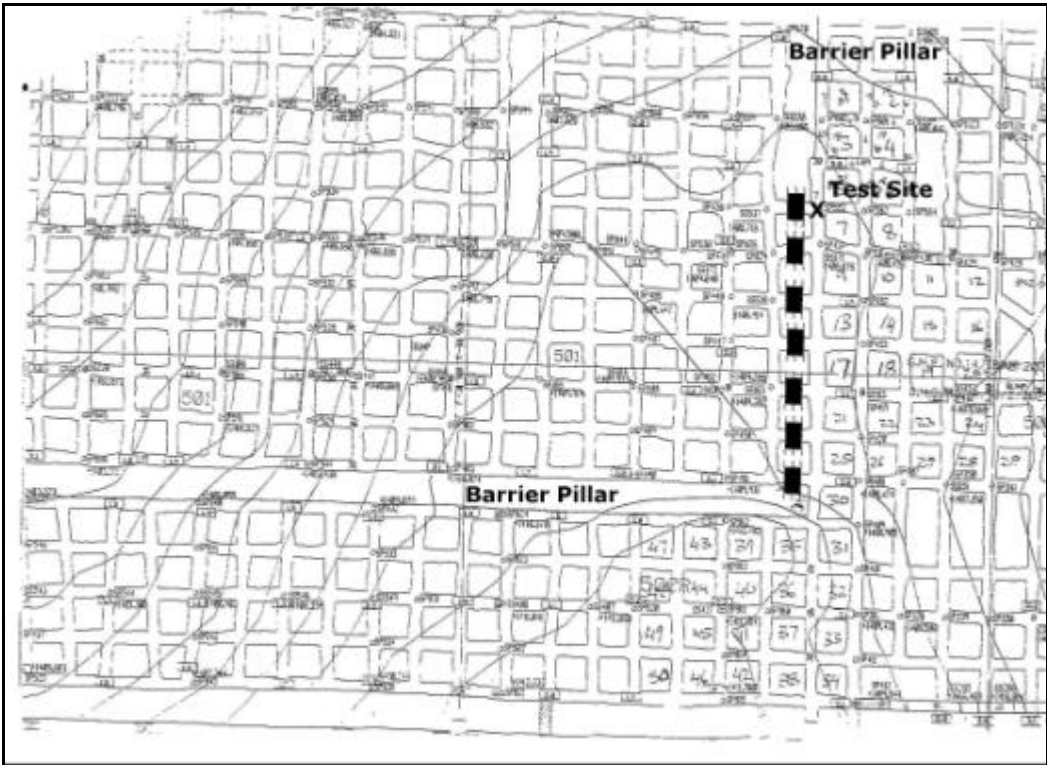


Figure A3: – New Denmark compartment and test site location

Geotechnical Survey

The barriers, including long barrier pillars, small square pillars, and seals, were examined for the 501 and 601 compartments.

New Denmark is mining the No. 4 Seam, which ranges in thickness from 1.8 to 2.5 m., at an average depth of 190 m below surface.

The roof is generally a competent and massive sandstone with occasional bedding partings, and locally the presence of coal fossils provide additional horizontal discontinuities of limited extent. Jointing is very sparse in the roof: tension cracks in bords occur more frequently.

In the coal seam horizontal bedding partings are present, and up to seven were noted at any one point in the mine. These are generally concentrated towards the top of the seam. Cleats, or joints, were present in the coal, dipping at approximately 60 to 70 degrees to the south-east.

The seam floor is apparently a siltstone, although this was nowhere visible. It is apparently reasonably well bedded.

In general, continuous barrier pillars are 18m wide, square pillars are 18m by 18m square, and roadways are 6 m wide.

501 Compartment

Lengths of extensive continuous barrier pillar around the Eastern and Southern sides of the water compartment. In this area the water head is approximately 28m, giving a water pressure of 0.28 MPa (280kPa).

In general the roof was dry, but water leaked in places through the coal, in some areas (particularly on the South side) continuously over lengths of 10 to 20m. Leakage appeared to be mainly through horizontal bedding and joints, leaving iron-staining running down the pillar surface from these discontinuities, which were generally weathered showing a yellowish clay infill. On the East side of the compartment there appeared to possibly be some movement in more heavily stress fractured parts of the coal. Where there was minimal stress damage, the flow of water appeared generally less. Water was only observed dripping from the hangingwall where joints, faults or tension cracks occasionally occurred.

At the south-east corner of the compartment seven seals were present in the barrier, separated by square, 18m by 18m pillars. Up to 0.5 m scaling was apparent from the sidewall coal of these pillars in the vicinity of the seals. Water was leaking principally around the seals in the coal. In most cases shotcrete had been applied to the coal and the water was running behind the shotcrete until a hole was found. A lesser quantity of water was leaking over the top of each seal. In general it appeared that the rate of water leakage was low (litres per day, not litres per minute).

The sandstone roof strata was well exposed close to the seals as several metres of it had been blasted down during earlier mining operations. There were few bedding planes visible. One at approximately 2m above the coal seam showed clear water seepage.

601 Compartment

The north-east corner of the barrier around the 601 compartment was examined. Certain key differences were apparent in this area. Water head was less, approximately 18m, giving rise to 180 kPa water pressure.

Again the main barrier was 18 m wide but here generally showed almost no leakage through it. A seal at the corner of the compartment showed similar leakage around the sides, and top where again almost 0.5 m of coal had scaled away. Water was dripping from a hangingwall tension crack some 5 m from the seal.

Around the corner, on the East side of the compartment a roadway through the pillar had been sealed off (with the seal covered over with shotcrete) and a 6 m wide refuge chamber had been cut centrally within the 18 m wide barrier pillar. The effective pillar width between water compartment and refuge chamber was thus only 6 m. The coal faces in the chamber were all shotcrete covered. Approximately 0.5 m spalling had occurred prior to shotcrete application. It was apparent that the 6 m pillars either side of the refuge chamber were deteriorating. Slabs of shotcrete were peeling from the top, overhanging, section of coal. Damage increased along the sides of the pillars, being negligible at the back of the chamber where the full 18 m pillar continues, to being worst at the ends of the 6 m wide sections. Water leakage through the pillar followed a similar pattern, and was apparent from wetness in the shotcrete. In general, dampness in the shotcrete was confined to the top 80 cm of the coal seam. Water was also present in droplets across the roof, not only in the refuge chamber, but in the roadway adjacent to the barrier.

A thin bed of sandstone, 3 to 5 m thick, was present in the immediate roof. This had a well-defined upper bedding parting containing yellow weathered clay material (kaolinite) and minor coal. A section of this bed had collapsed in the intersection area of the refuge bay. From the wetness of the exposed parts of the bed in the roof it appeared that the bedding parting and possibly the bed itself, were acting as conduits for the slow leakage of water from the compartment.

Conclusions

Except for one or two cracks around the edges of seals, no areas were observed where high rates of flow of water out of the groundwater compartments were apparent. Despite this there was extensive water on the floor, and areas around the 501 compartment were partially flooded.

Slow water seepage through the barrier pillar appeared to be concentrated through horizontal bedding partings, primarily in the coal seam, but also in the roof sandstone, and presumably also in the floor. Some seepage seemed to occur in the weaker, or more fractured sections of the coal. In particular this was the case around seals and smaller pillars where coal damage was more intense.

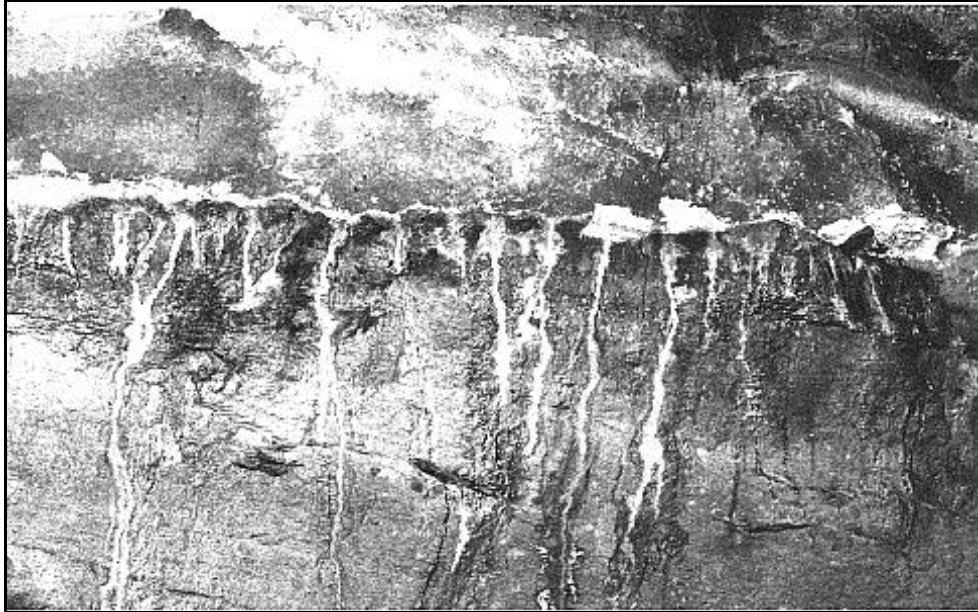


Figure A4: -Calcite leaching along the coal/roof contact



Figure A5: -Extent of sidewall spalling along barrier pillar

Pillar loads

Figure A6 and A7 shows the instope and barrier pillar vertical loads prior to total extraction and after total extraction, respectively. The vertical loads were obtained by simulating the New Denmark compartment geometry using the elastic boundary element program LAMODEL. Prior to longwall extraction, average barrier pillar loads range from 4MPa to 8MPa. Total compartment extraction increases the average barrier pillar loads to 6MPa to 10MPa. The 10m wide roadways chosen for the UDEC models was based on producing the pillar loads obtained from the elastic LAMODEL simulations.

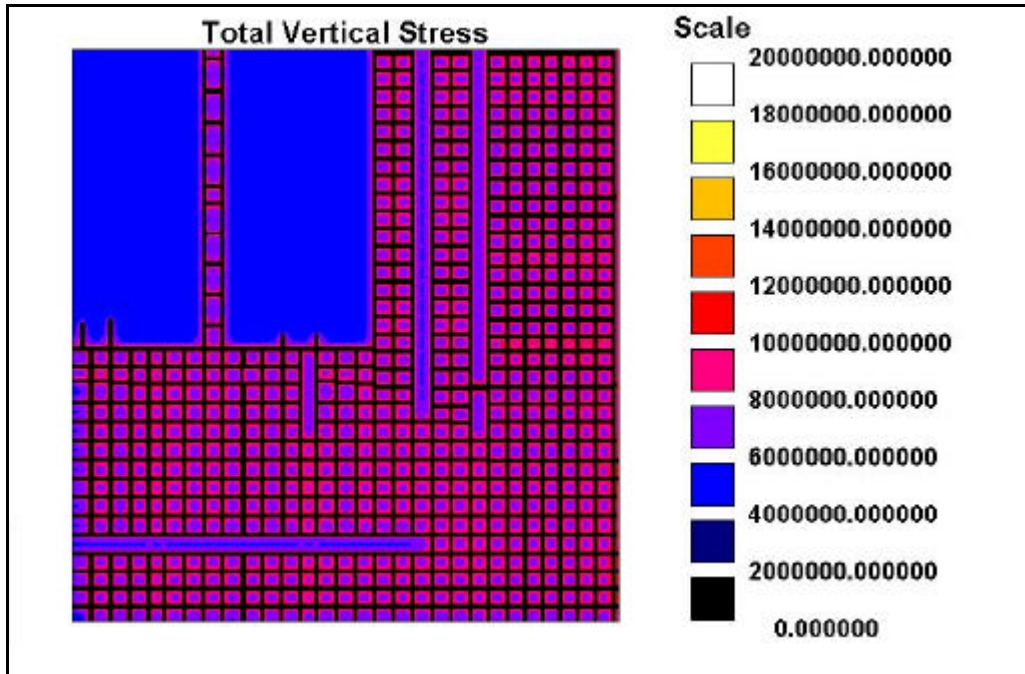


Figure A6: - Pillar loads prior to the longwall panels being extracted

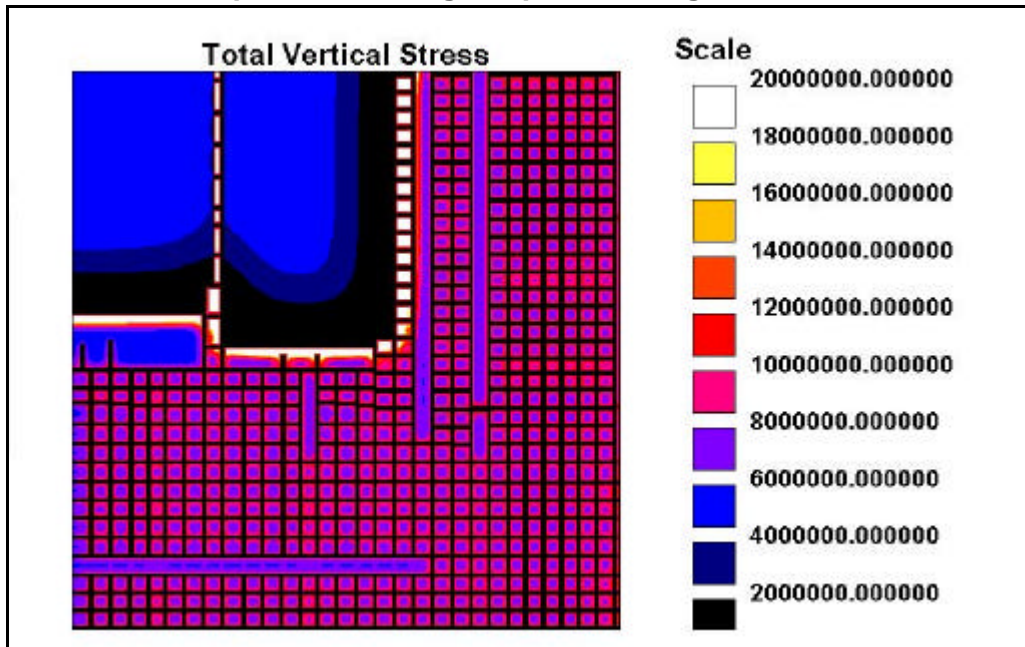


Figure A7: - Pillar loads after both Longwall panels have been extracted

In situ permeability tests

Test methods were designed to provide input permeability data for numerical model back analysis. The actual recorded pressure degradation from the water compartment to monitoring sites was then used to derive the residual discontinuity aperture, which was the primary fluid modelling parameter used to depict in situ permeabilities. Figure A8 illustrates the setting (plan view) of the borehole sites in relation to the bounding compartment barrier pillar. In Figure A8, R represents roof boreholes, F floor boreholes and S coal seam holes.

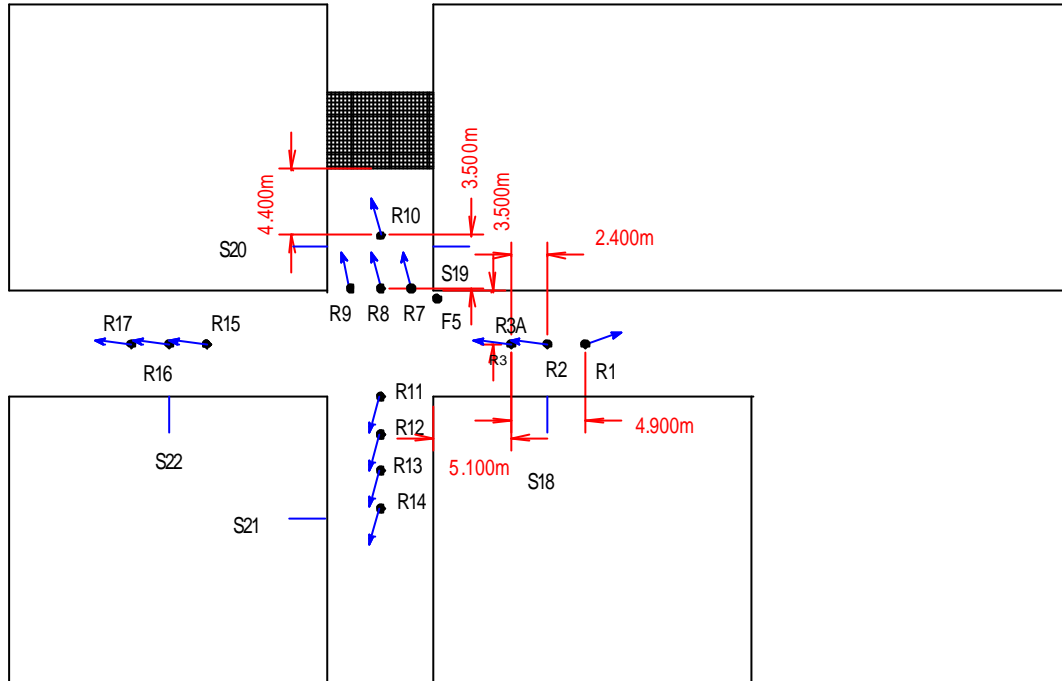


Figure A8: – New Denmark position of instrumentation

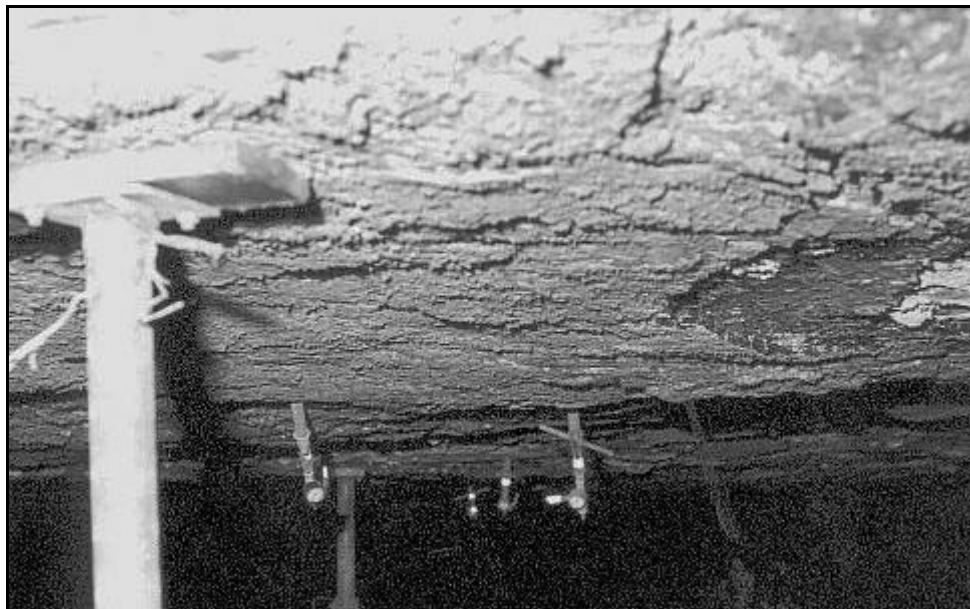


Figure A9: – Installed roof instrumentation

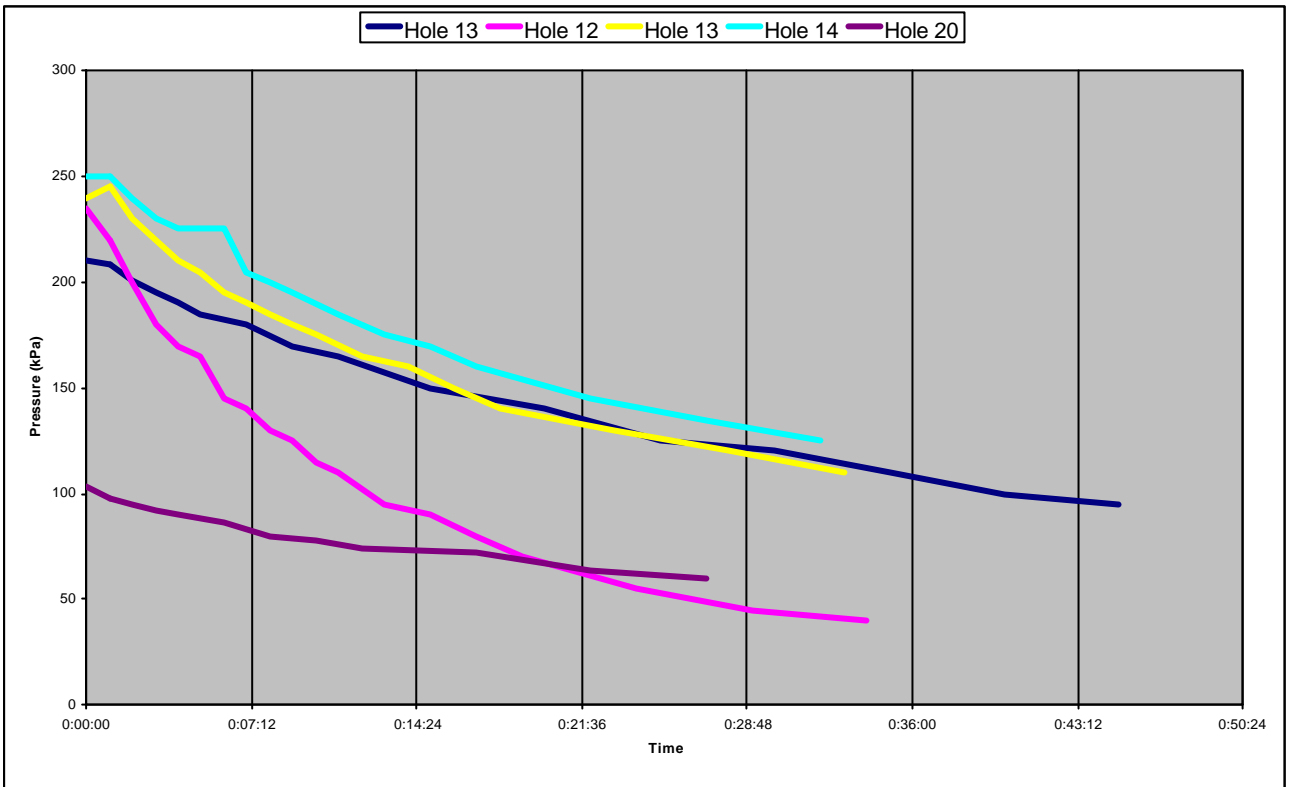


Figure A10: - Recorded pressure degradation at New Denmark

Twistdraai Colliery

Twistdraai colliery has twice been flooded probably due to leakage of water beneath the seals through weak incompetent strata. Due to the known high rates of water leakage from barrier bound compartments, a suitable site was chosen for in situ monitoring of water flow from the roof, coal and floor strata. Figure A11 shows the test site in relation to the 50m wide compartment barrier pillar.

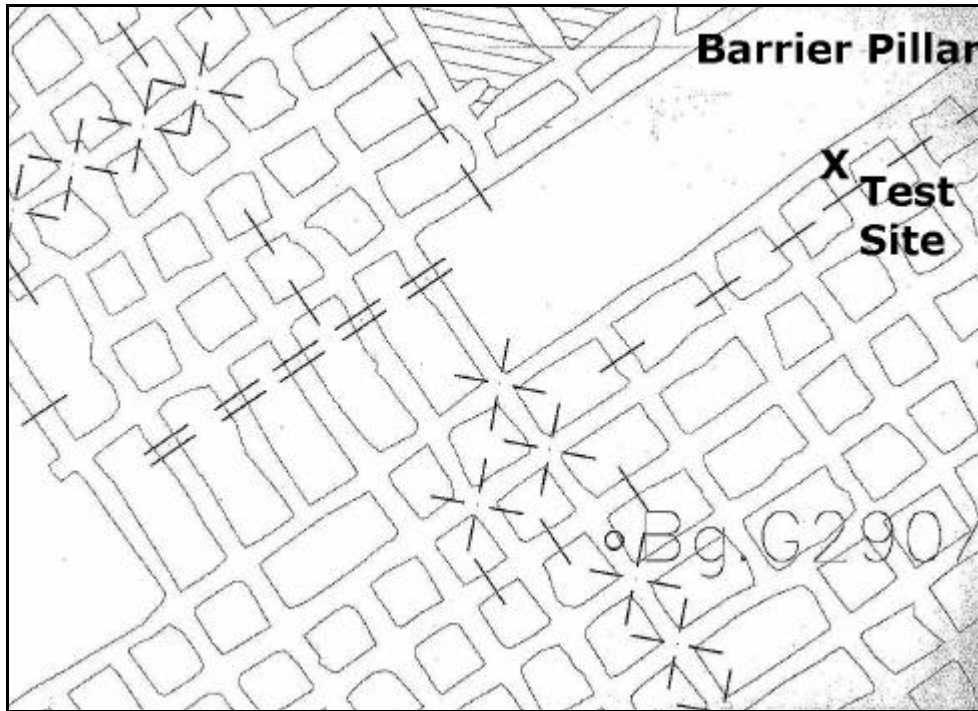


Figure A11: Twistdraai layout and test site location



Figure A12: - Roadway side of the 50m wide barrier pillar demarcated for instrumentation

Geotechnical Survey

Observations focussed on the path of water ingress from the water compartment into existing accessways. Comments are made on the seam that constitutes the barrier pillar and the nature and persistence of discontinuities that traverse the roof strata. The goafed area incorporating

the water compartment is situated on the 4 Seam Lower (C4L) at approximately 90m below surface.

Seam thickness varies between 3m and 3.5m. Three to four distinct coal bands constitute the full seam thickness. The classification for distinction of individual bands is unclear though from observations coal quality and hence chemical petrology could vary between individual bands. Water leakage along the length of the barrier pillar occurs at the interface between the top uppermost coal bands as seen in Figure A13. The contact between the coal seam and the overlying siltstone although abrupt appeared fairly welded. No water flow was observed at this contact.



Figure A13: -Water leakage at top coal/roof contact

Calcite staining of the barrier pillar sidewall was observed. This staining was sporadic rather than consistently associated with water flow. It could be conceptualised that the calcite staining is associated with leaching from coal bound minerals (e.g. Aragonite) rather than residing in the water contained in the compartment. Iron staining of the barrier sidewalls is present wherever water flows from partings within or outside the seam. The source of the iron is probably from the water. Mineral washout from existing discontinuities could influence the volume of aperture available for flow. No joint sets traverse or are bound by the coal.

Concrete seals were recently constructed at splits in the barrier pillar to create the current compartment. The width of the barrier is approximately 50m. The barrier pillar at the time of the visit was subjected to a 6.6m head of water. Seals are generally 1m thick. Polymer resin grouting consolidates the interface between the seals and seam. Sixteen injection holes are fan drilled around the seal and injected with the lightweight resin. It was reported that the resin could volumetrically expand by up to 75 times the original placed volume.

The immediate 5m of roof consist of well-laminated siltstones and gritstone. Distinct open partings define the laminations for the immediate 0.5m of siltstones. The siltstones are rich in biotite micas, enhancing the sheet-like layering of incumbent beds. Cohesion on bed interfaces is low, evidenced by the soapy texture of the bed surfaces. Where bed surfaces are smooth, it is expected that friction and dilation angles are extremely low. It is fairly easy to initiate sliding on beds by hand.

Bed laminae grade from 2mm thick to 5cm thick with increasing distance from the coal seam. Contacts between the different rock types are abrupt. A crude upward coarsening sequence can be extrapolated from the coal seam to the massive sandstones located 5m above.

Ripple marks, as shown in Figure A14, were noted on some exposures of siltstones. The ripple marks had average wavelengths and amplitudes of 150mm and 30mm respectively. These features could have a major bearing on water flow due to their influence on bedding apertures. Any slip induced on siltstone laminae will act to open partings with ripple marks (undulations). The extent of opening will be dependant on the dilation angle, which is a function of ripple mark wavelength, and amplitude.

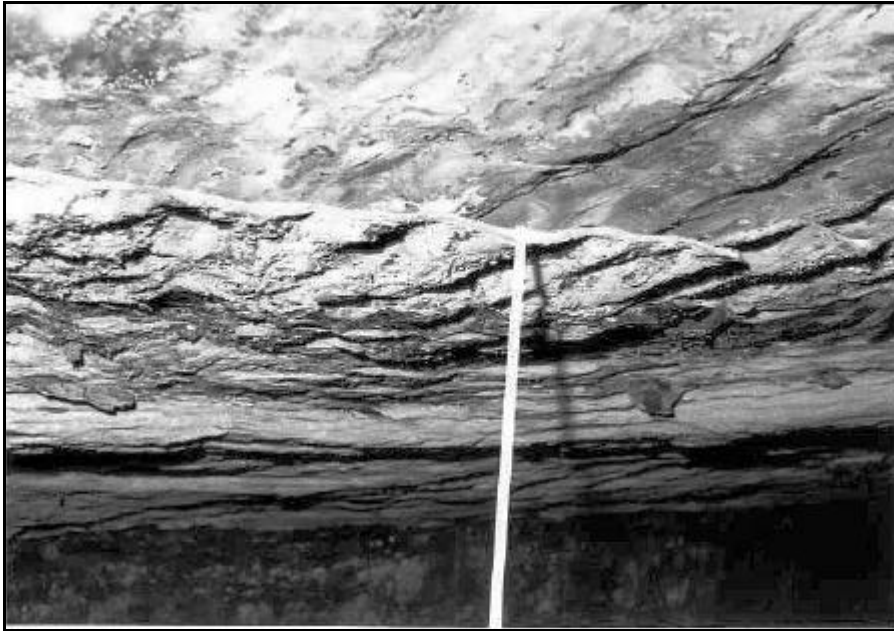


Figure A14: – Ripple marks

Lenses of siltstone/sandstone as shown in Figure A15 were observed in the roadway next to the barrier pillar. These lenses resembled deltaic deposit inter-fingering. The formation of the lenses has resulted in the eroding of siltstone beds immediately above the coal seam.



Figure A15: -Lenses of siltstone and sandstones forming weak discontinuous inter-fingering

These minor erosion channels have been filled with coarse-grained sandstones. The change in rock type and strengths may influence localised loading conditions around the barrier pillar.

The discontinuities observed to influence water flow are the interfaces between the coal bands and the laminations of the siltstones. Flow along the above mentioned structures were limited to the first stress fracture intersected in the barrier pillar. Stress fractures appeared to extend to approximately 0.5m into the pillar. Water flow from the roof seemed to be limited to the first 0.5m of strata. This distance represents the densely bedded siltstones. It is possible that roof relaxation is most prominent within the first 0.5m of siltstone hence the discernible flow.

The 2.5m thick dolerite dyke observed had a burnt zone extending approximately 1.5m on either side of the dyke contacts. Although this dyke with its chill zone traverses the water compartment perpendicularly, no leakage was observed.

Pillar loads

The barrier pillar is subject to elastic vertical loads of up to 4MPa after goafing of the totally extracted compartment.

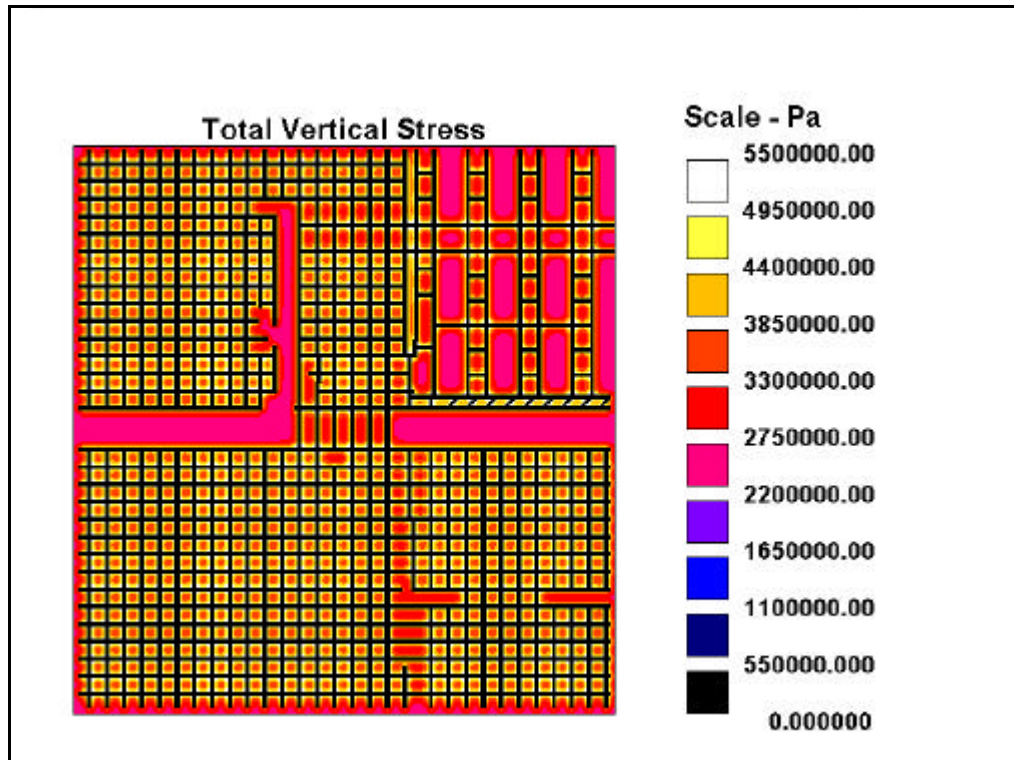


Figure A16: - pillar loads after development

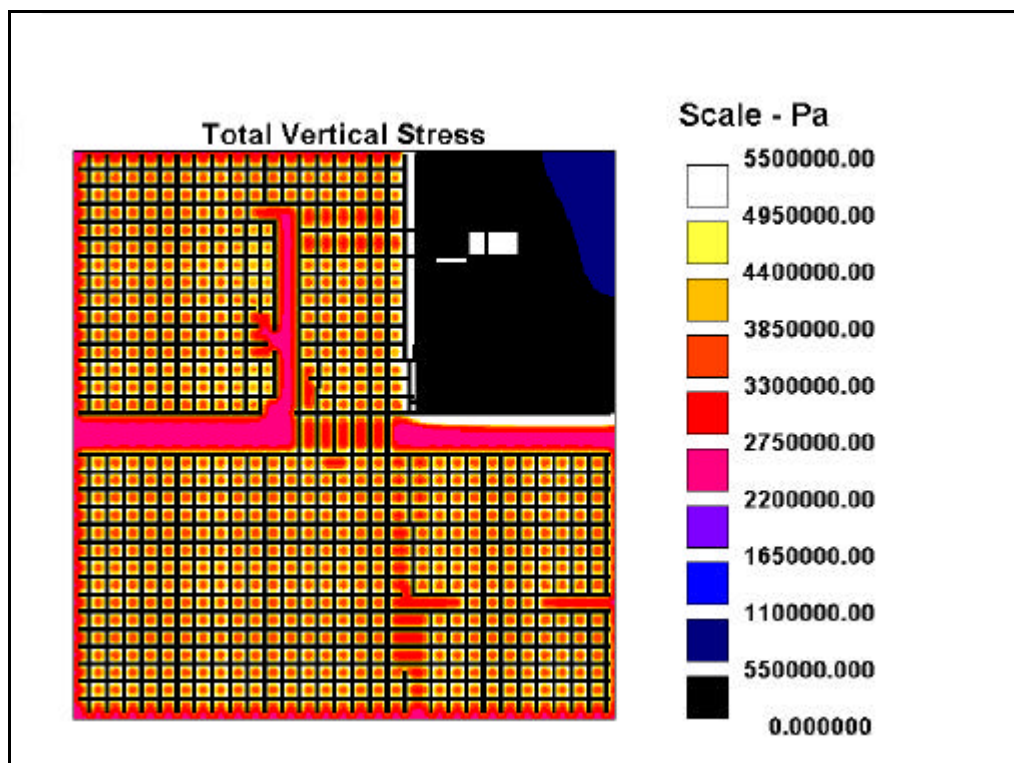


Figure A17: - Pillar loads after extraction

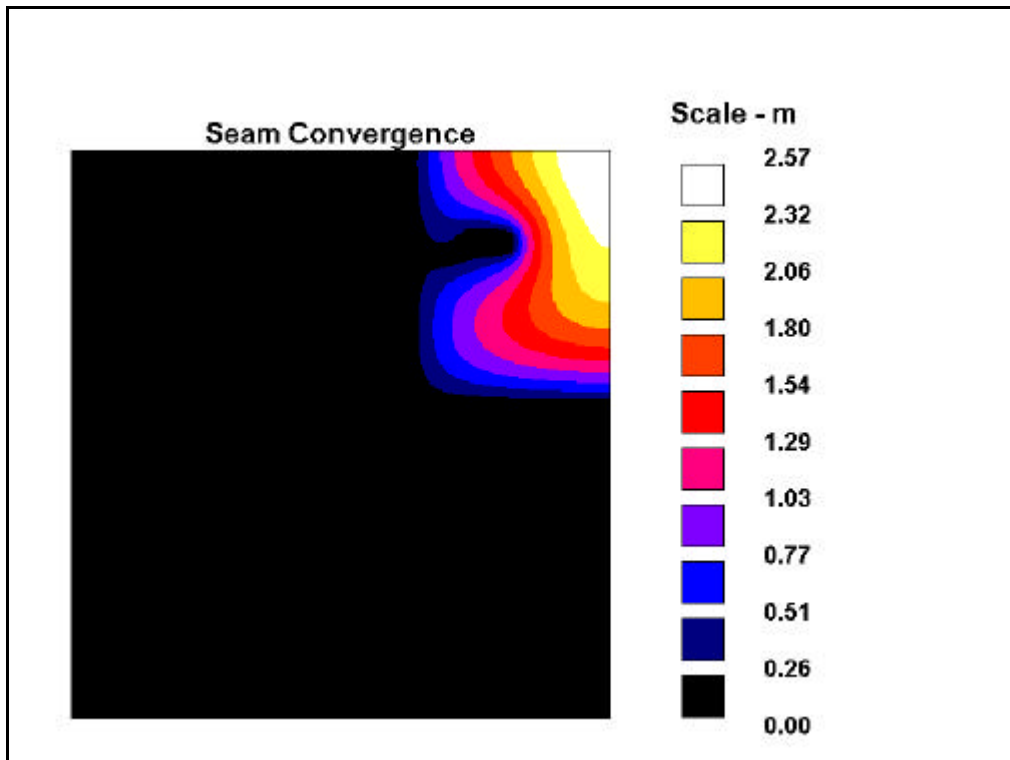


Figure A18: – Convergence after pillar extraction

In situ monitoring

The layout, length and pattern of boreholes drilled for the Twistdraai site was similar to that of New Denmark. These are schematically represented in Figures A19 and A20.

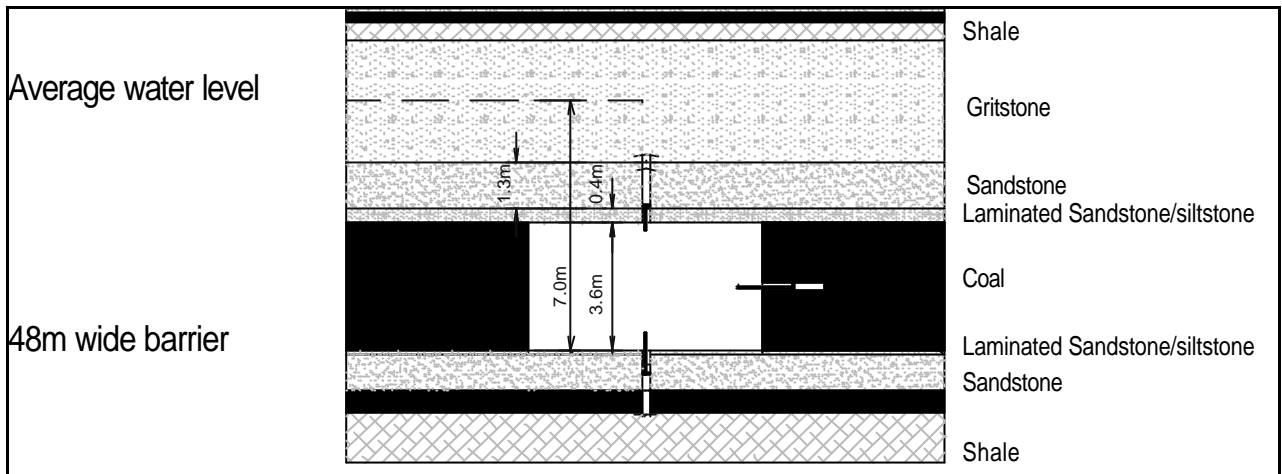


Figure A19: – Schematic monitoring boreholes in relation to the barrier pillar

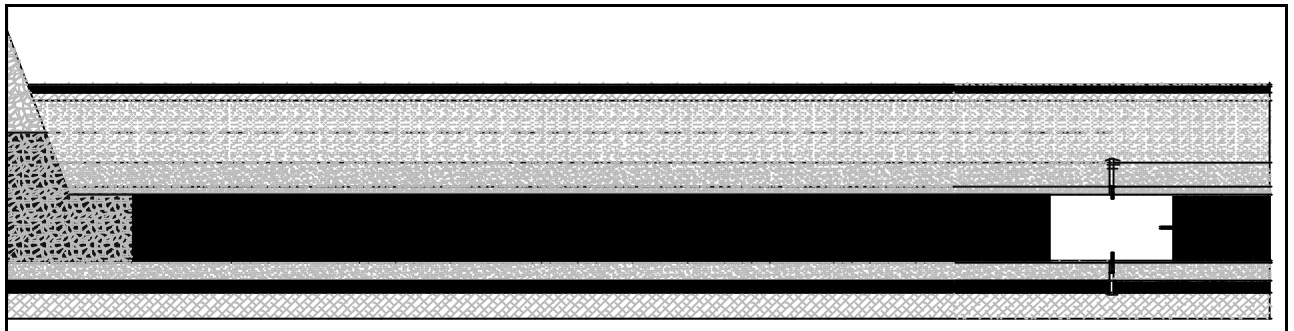


Figure A20: - Monitoring in relation to the water compartment

The pressure degradation over time is shown in Figure A21. The actual results were used to calibrate the residual aperture used in the UDEC models.

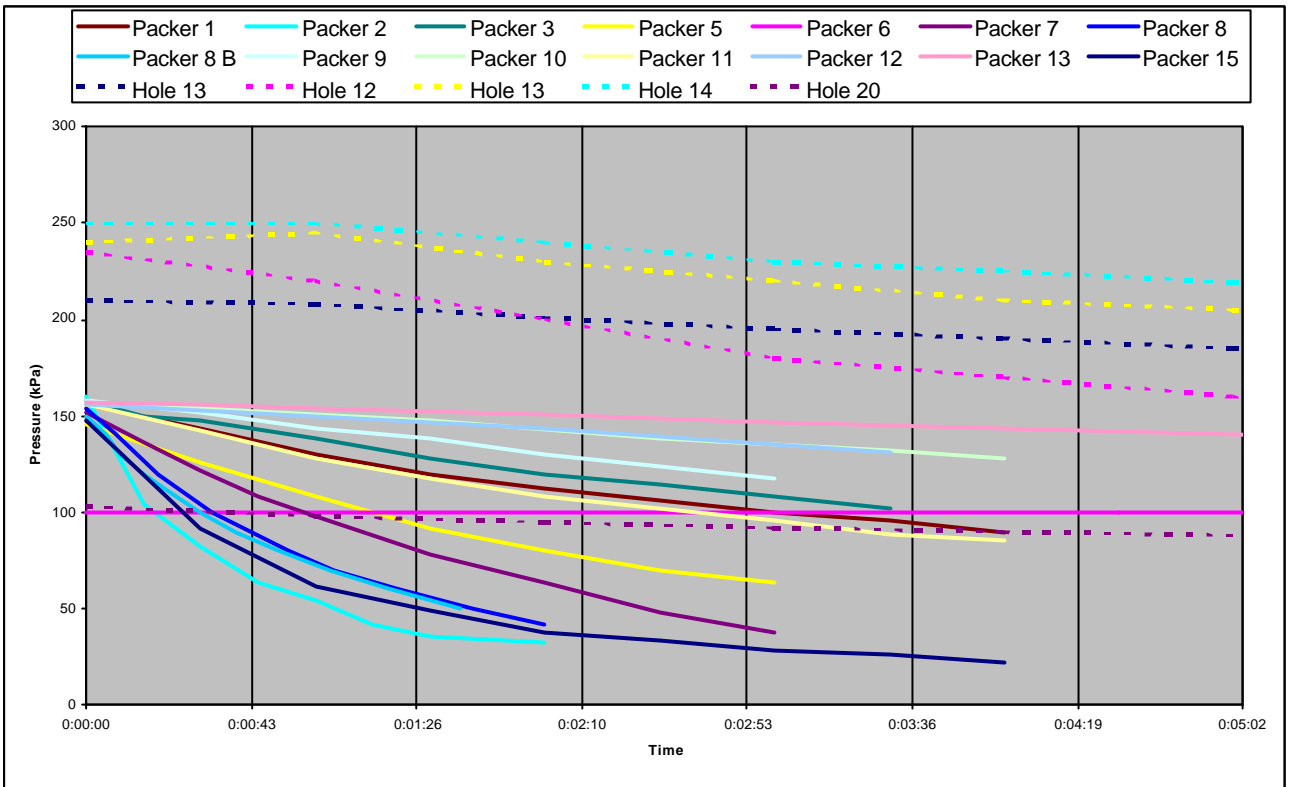


Figure A21: - Pressure degradation at Twistdraai Colliery

Appendix III Uncombined flow charts for roof, coal and floor strata

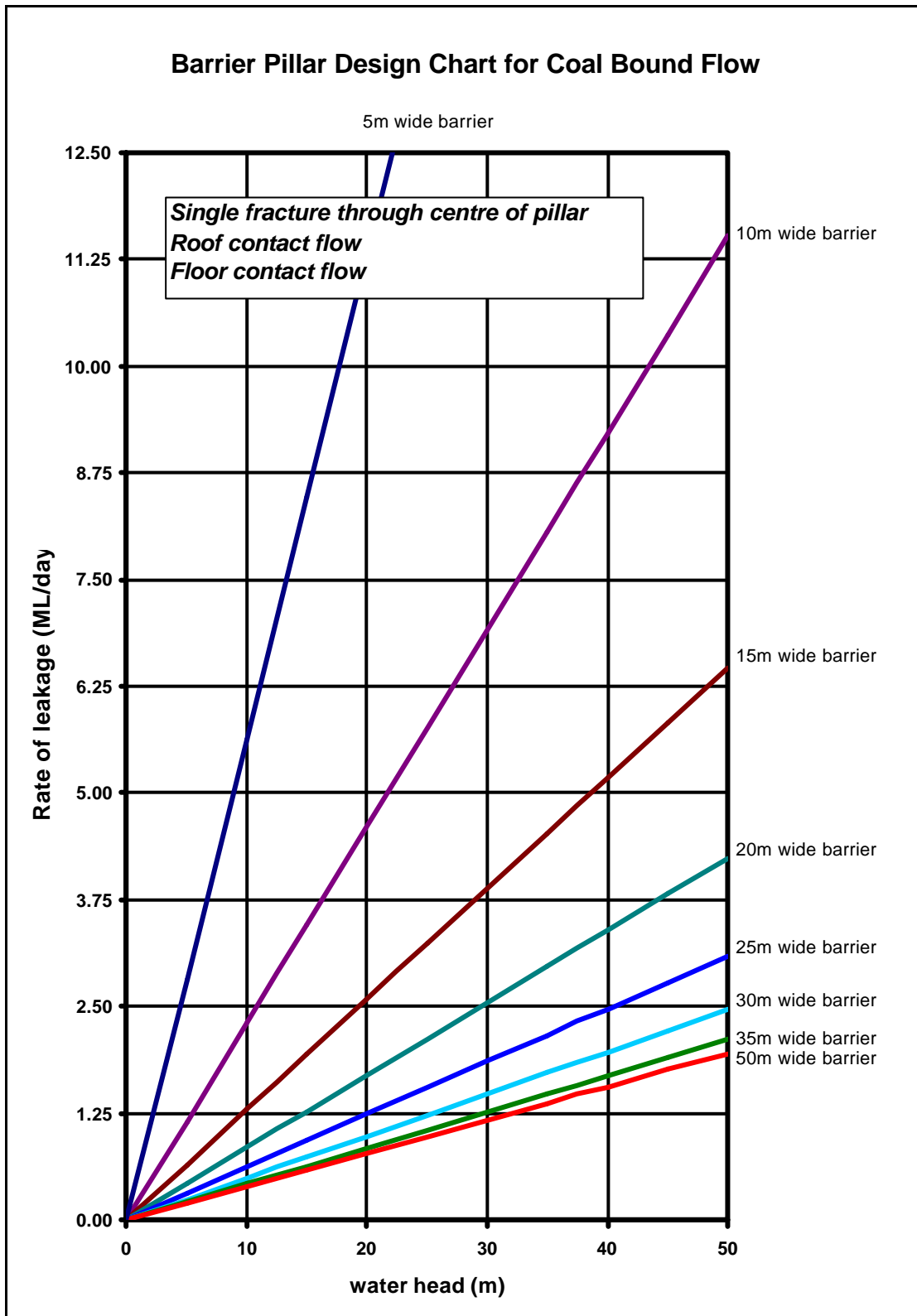


Figure A22: Design chart for coal bound flow only

Barrier Pillar Design Chart for Discrete Joints in Roof

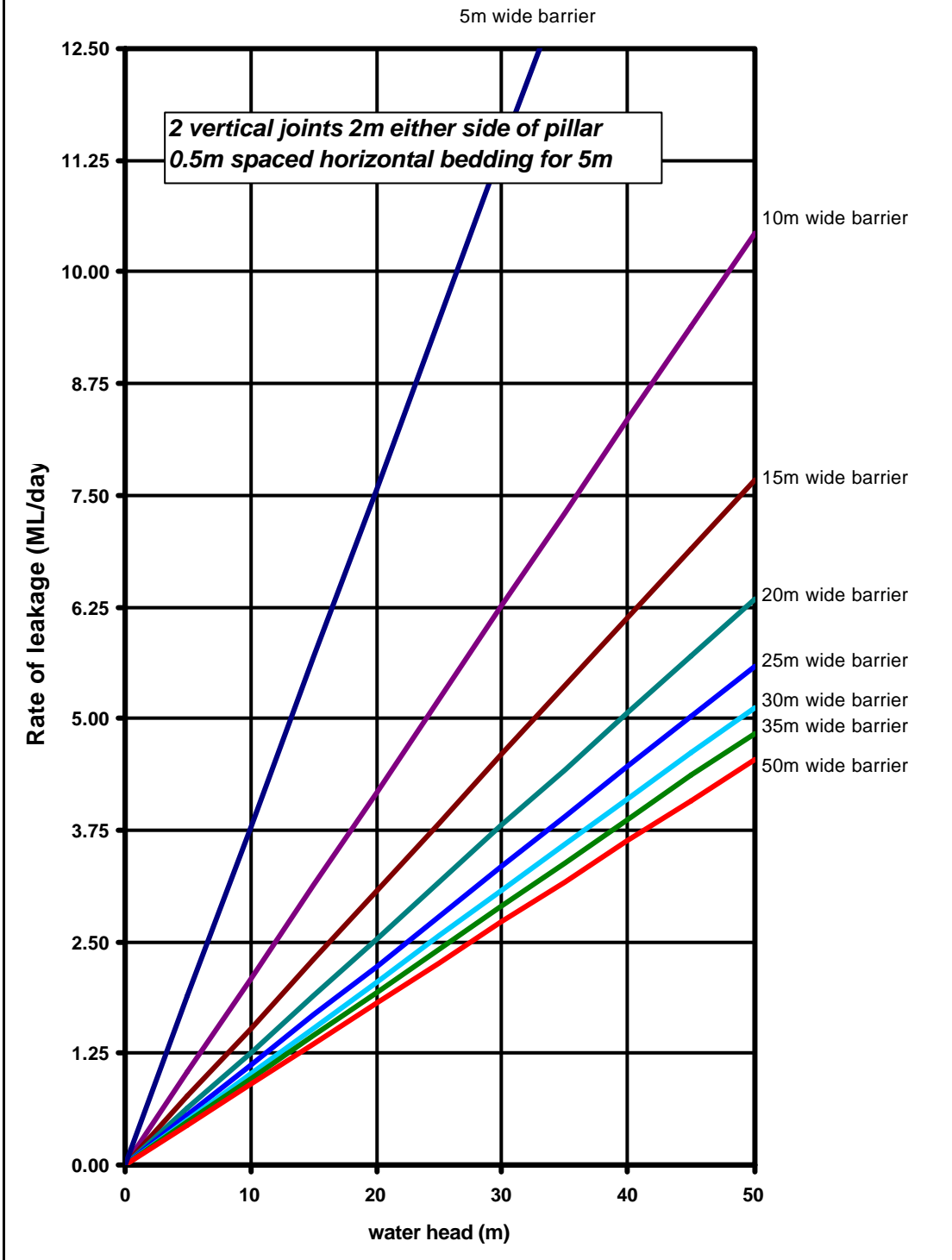


Figure A23: Design chart for competent roof only

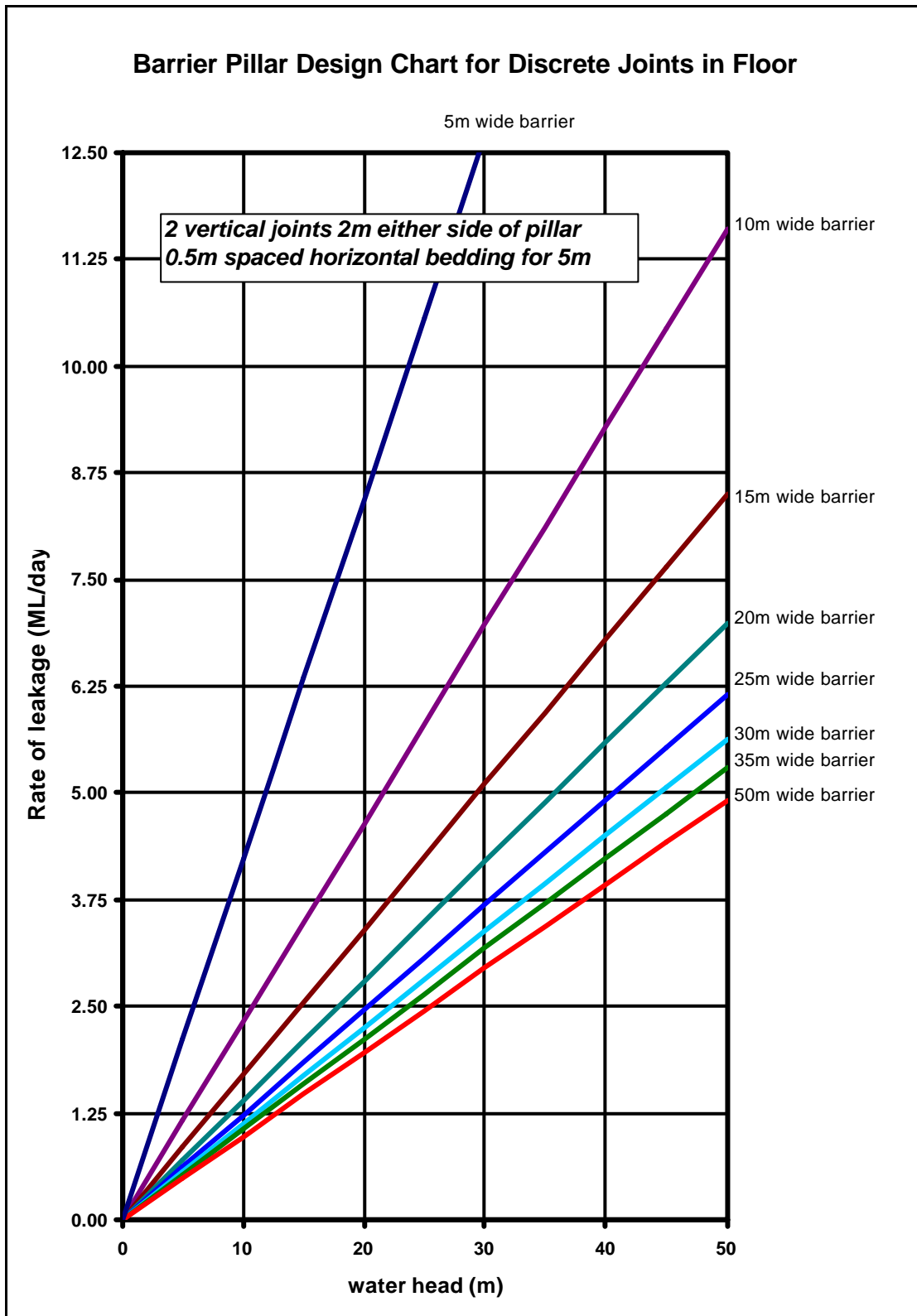


Figure A24: Design chart for competent floor only

Barrier Pillar Design Chart for Soft Roof

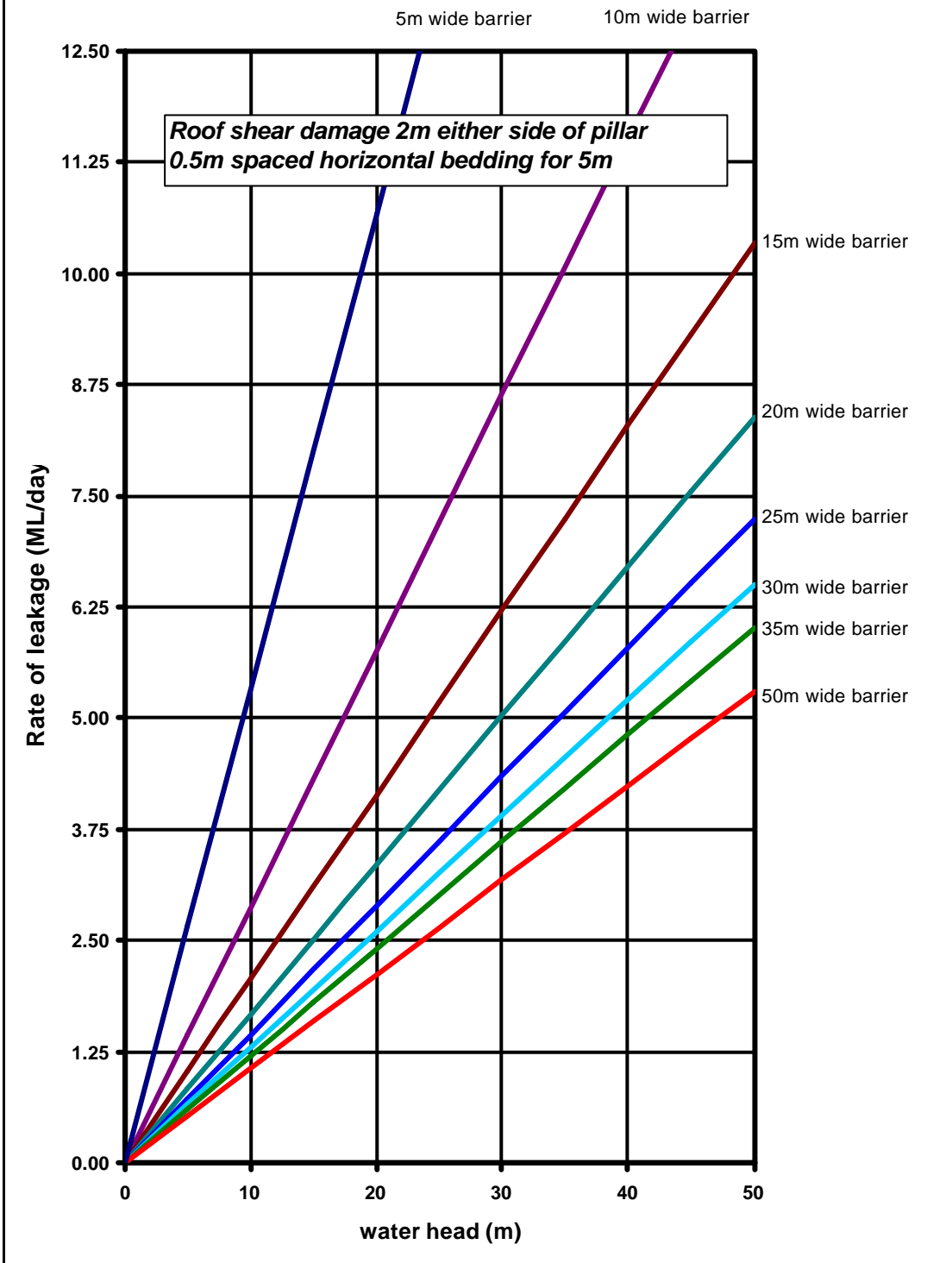


Figure A25: Design chart for incompetent roof only

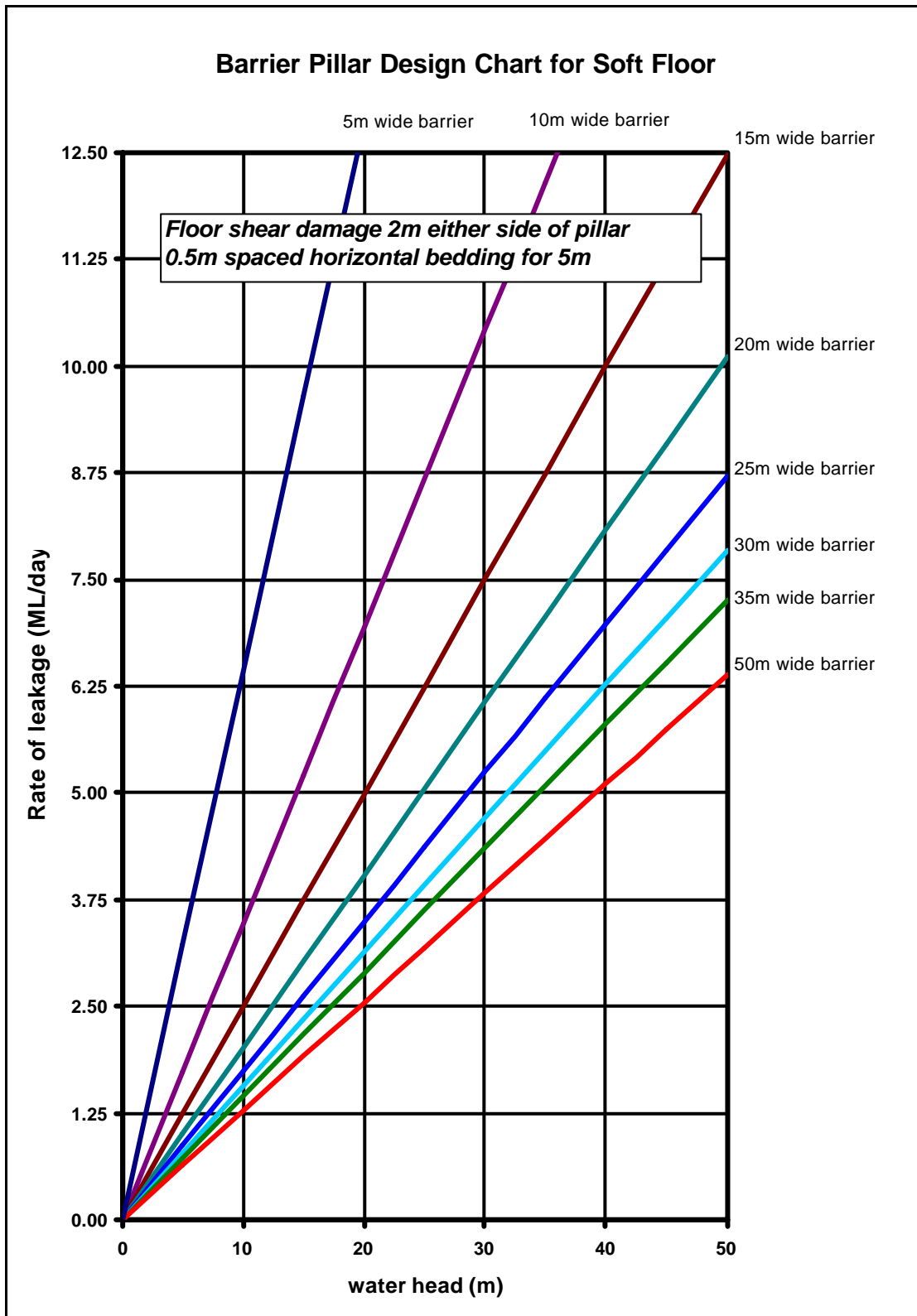
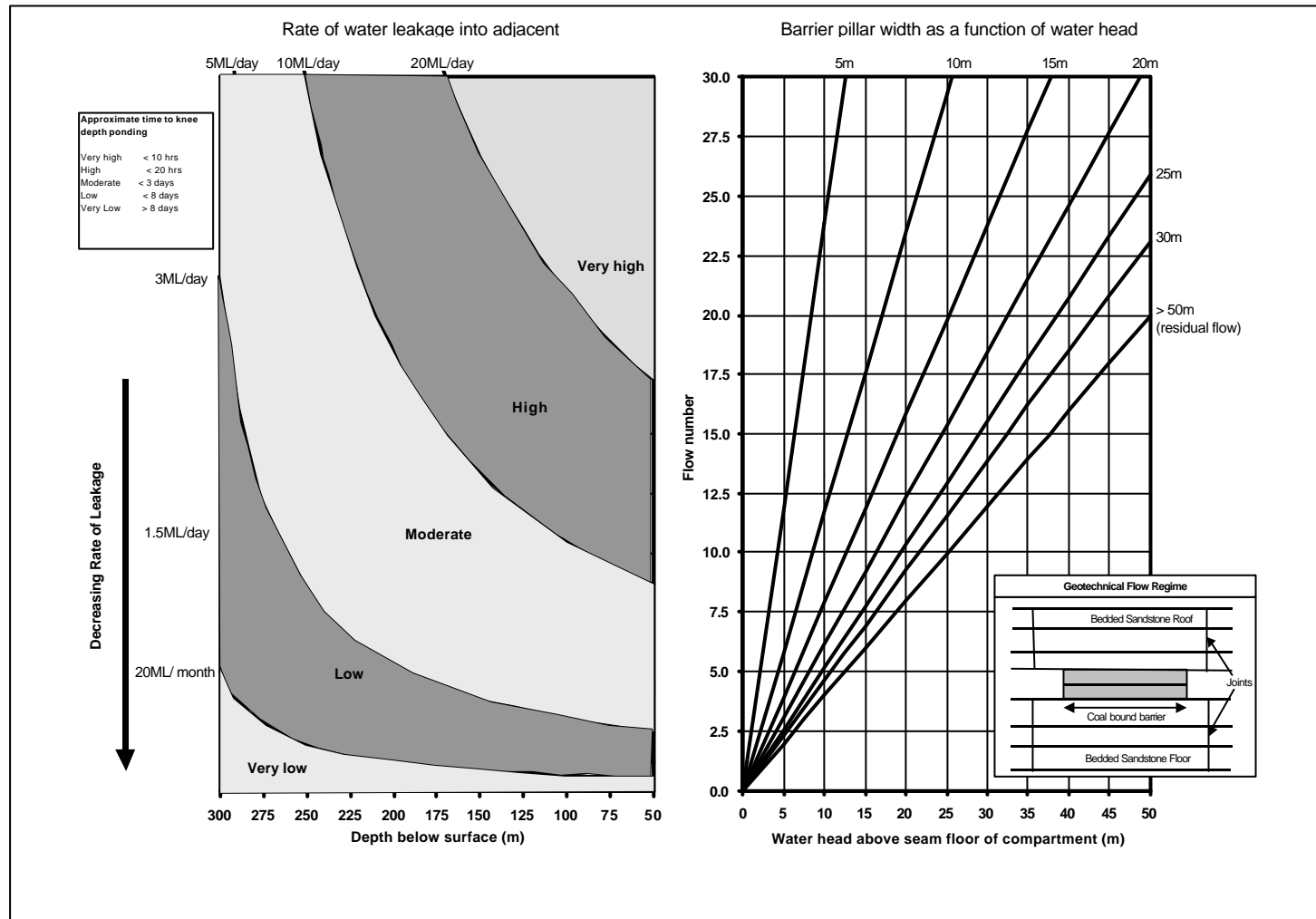


Figure A26: Design chart for incompetent floor only

APPENDIX IV DESIGN CHARTS

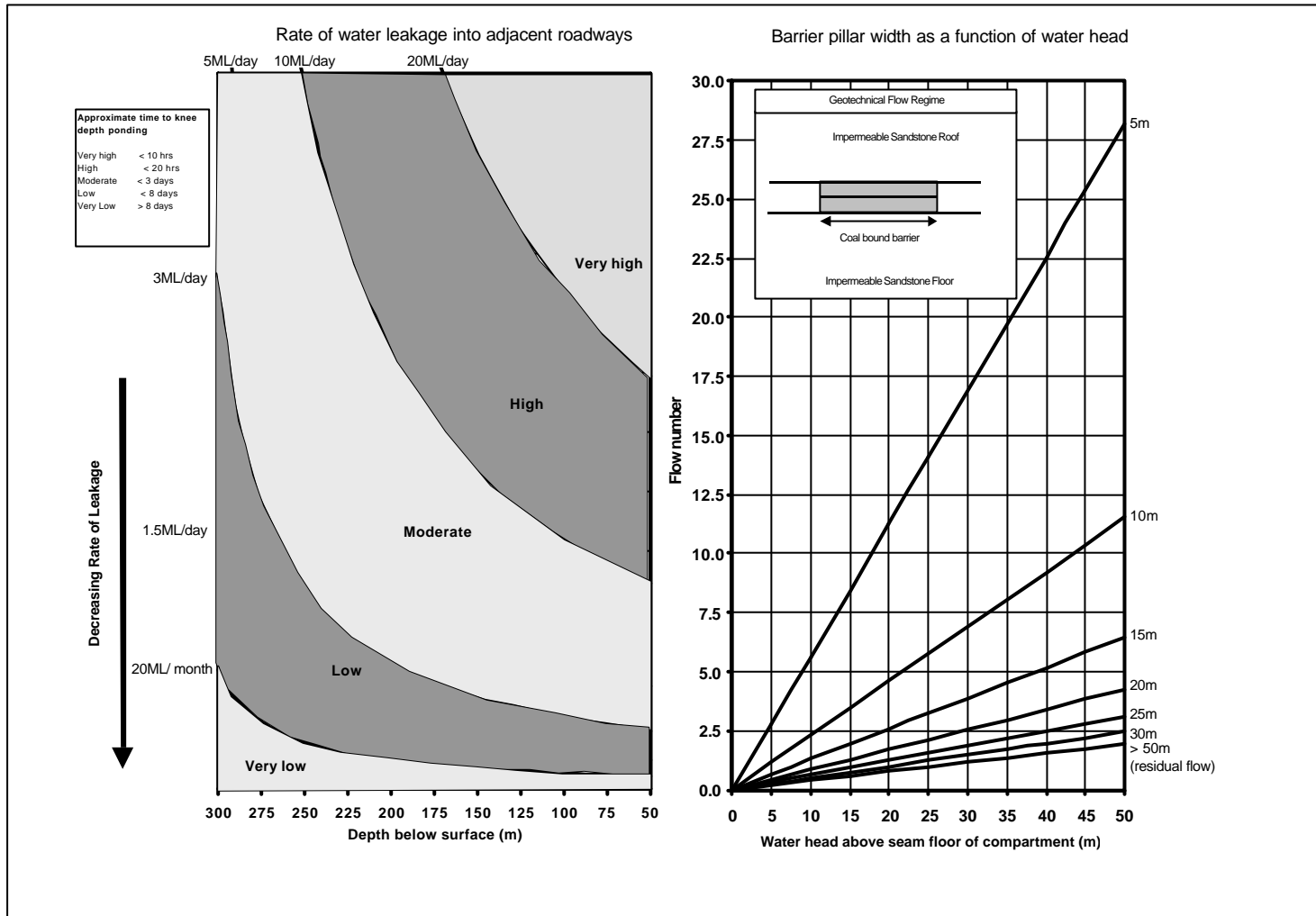
Hydraulic Design Chart for Barrier Pillars

(FIGURE 5a = Coal bound + bedded sandstone roof + bedded sandstone floor)



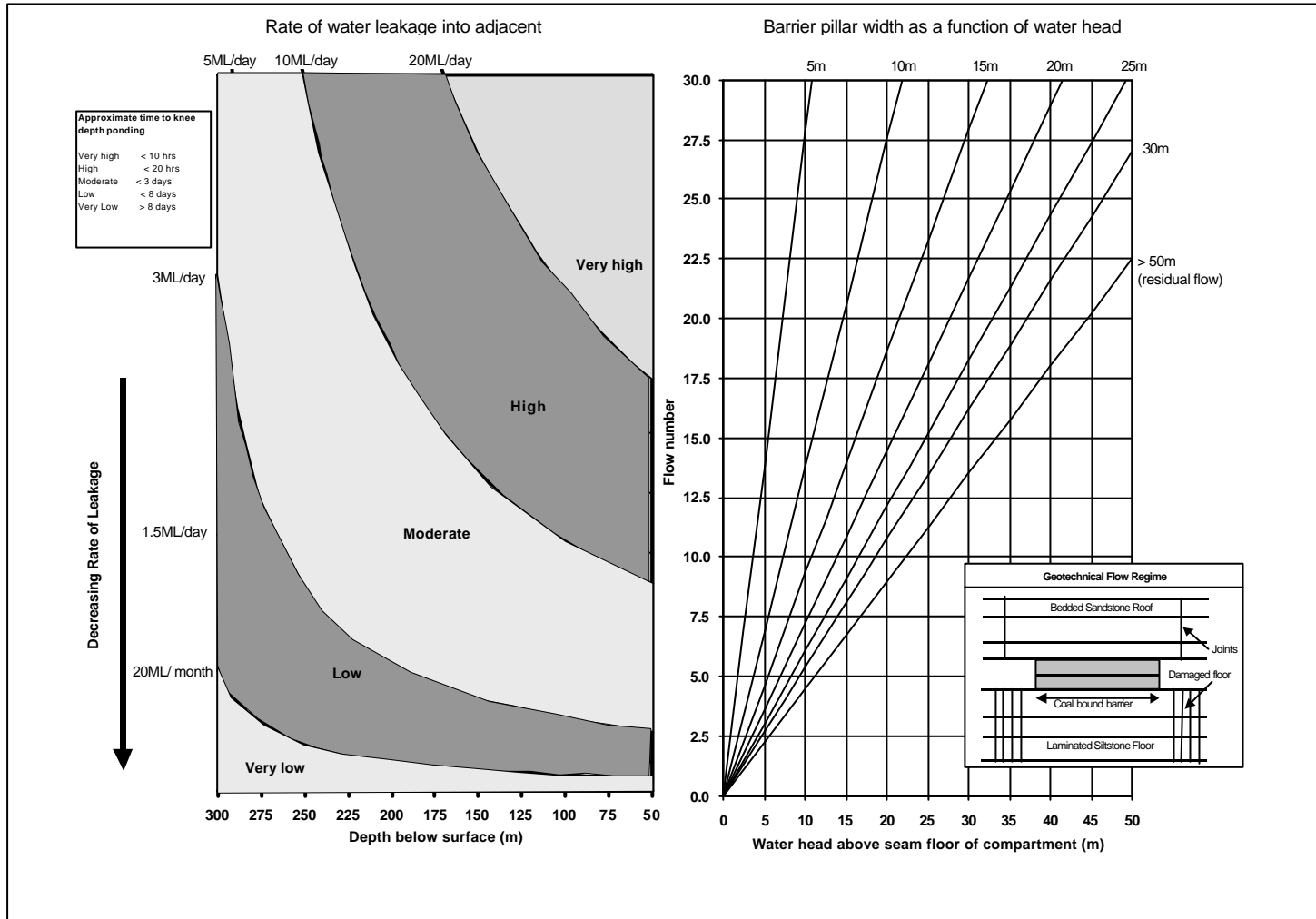
Hydraulic Design Chart for Barrier Pillars

(FIGURE 5b = Coal bound only)



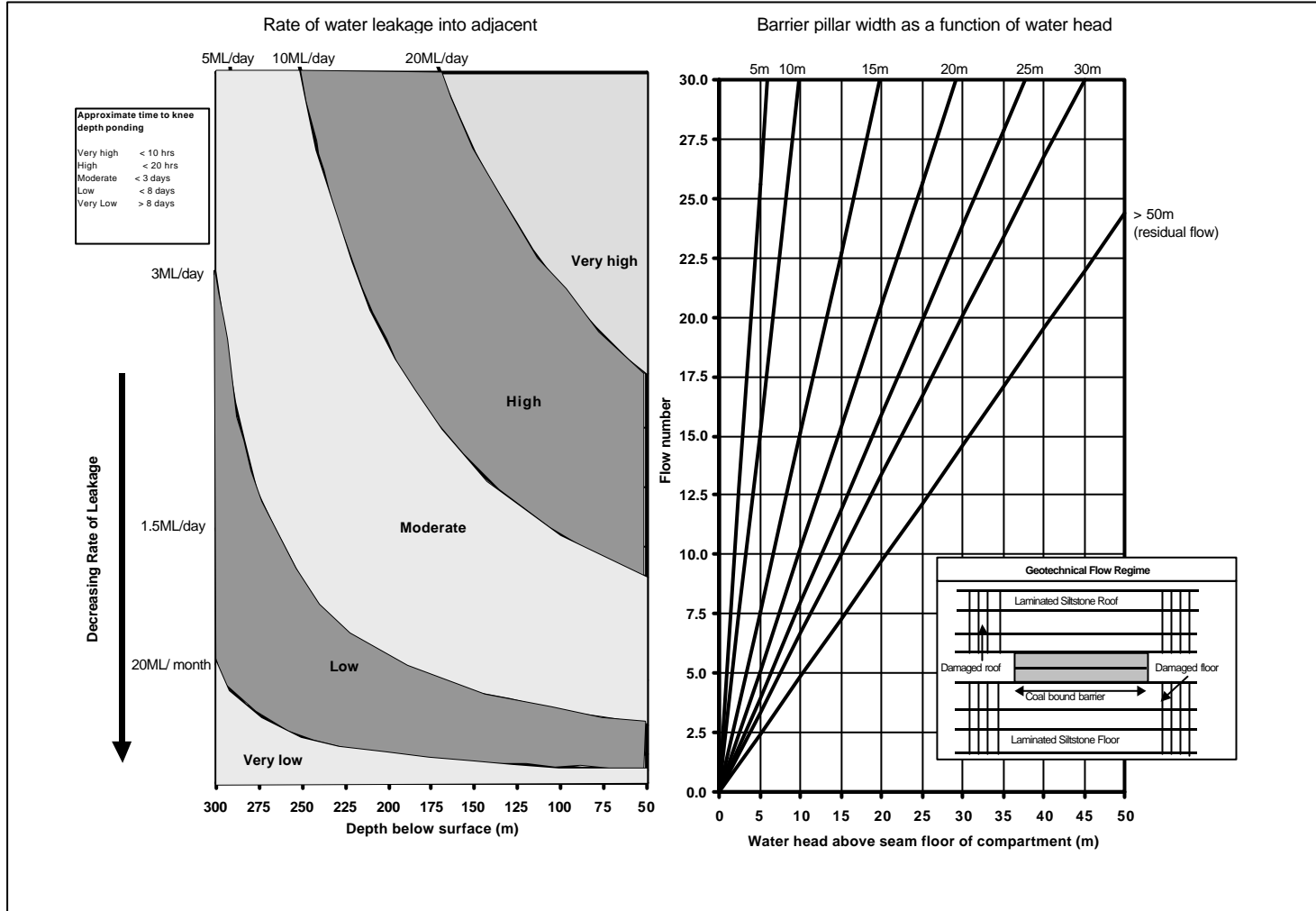
Hydraulic Design Chart for Barrier Pillars

(FIGURE 5c = Coal bound + bedded sandstone roof + laminated siltstone/gritstone floor)



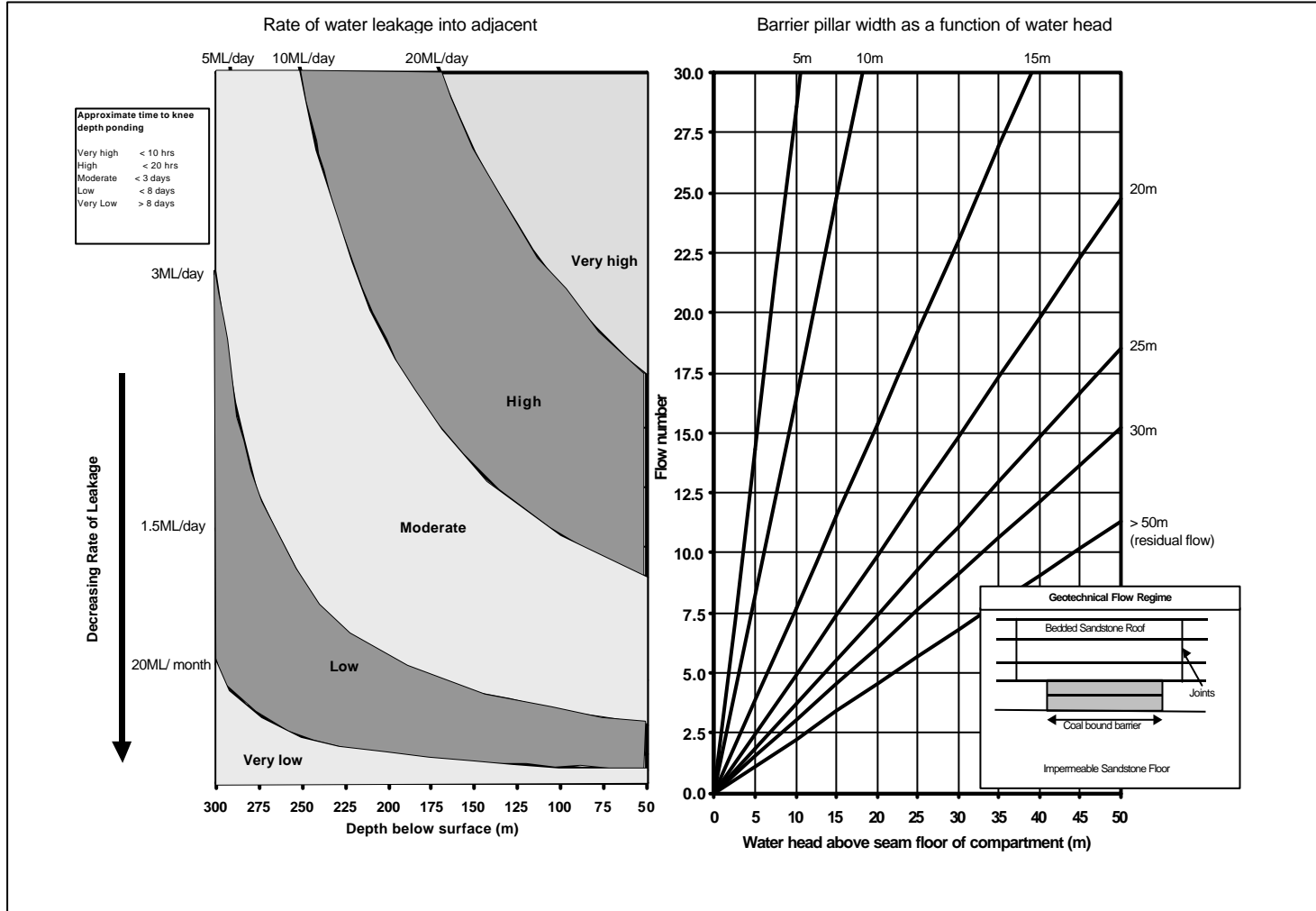
Hydraulic Design Chart for Barrier Pillars

(FIGURE 5d = Coal bound + laminated siltstone/gritstone roof and floor)



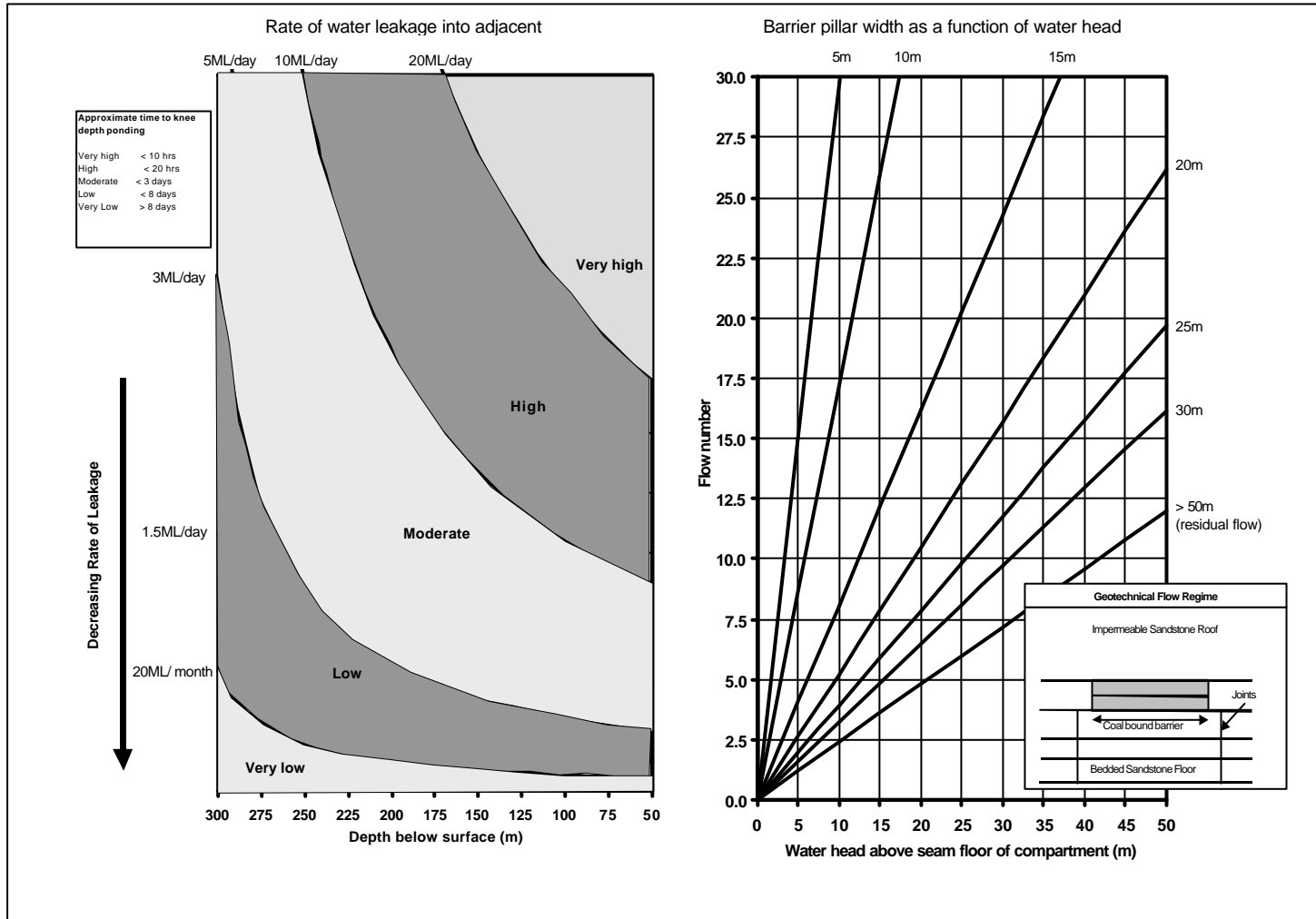
Hydraulic Design Chart for Barrier Pillars

(FIGURE 5e = Coal bound + bedded sandstone roof + massive impermeable floor)



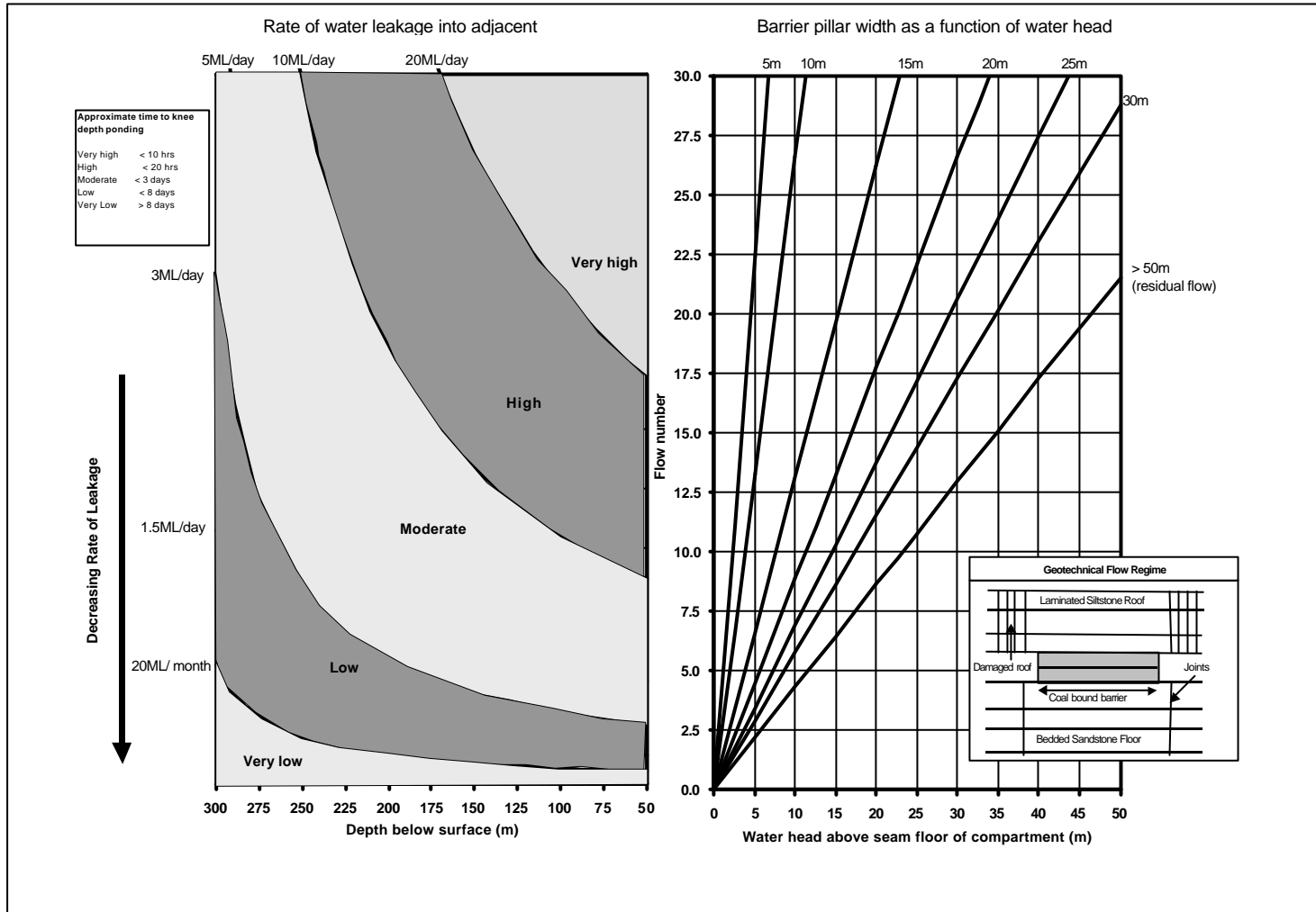
Hydraulic Design Chart for Barrier Pillars

(FIGURE 5f = Coal bound + massive impermeable roof + bedded sandstone floor)



Hydraulic Design Chart for Barrier Pillars

(FIGURE 5g = Coal bound + laminated siltstone/gritstone roof + bedded sandstone floor)

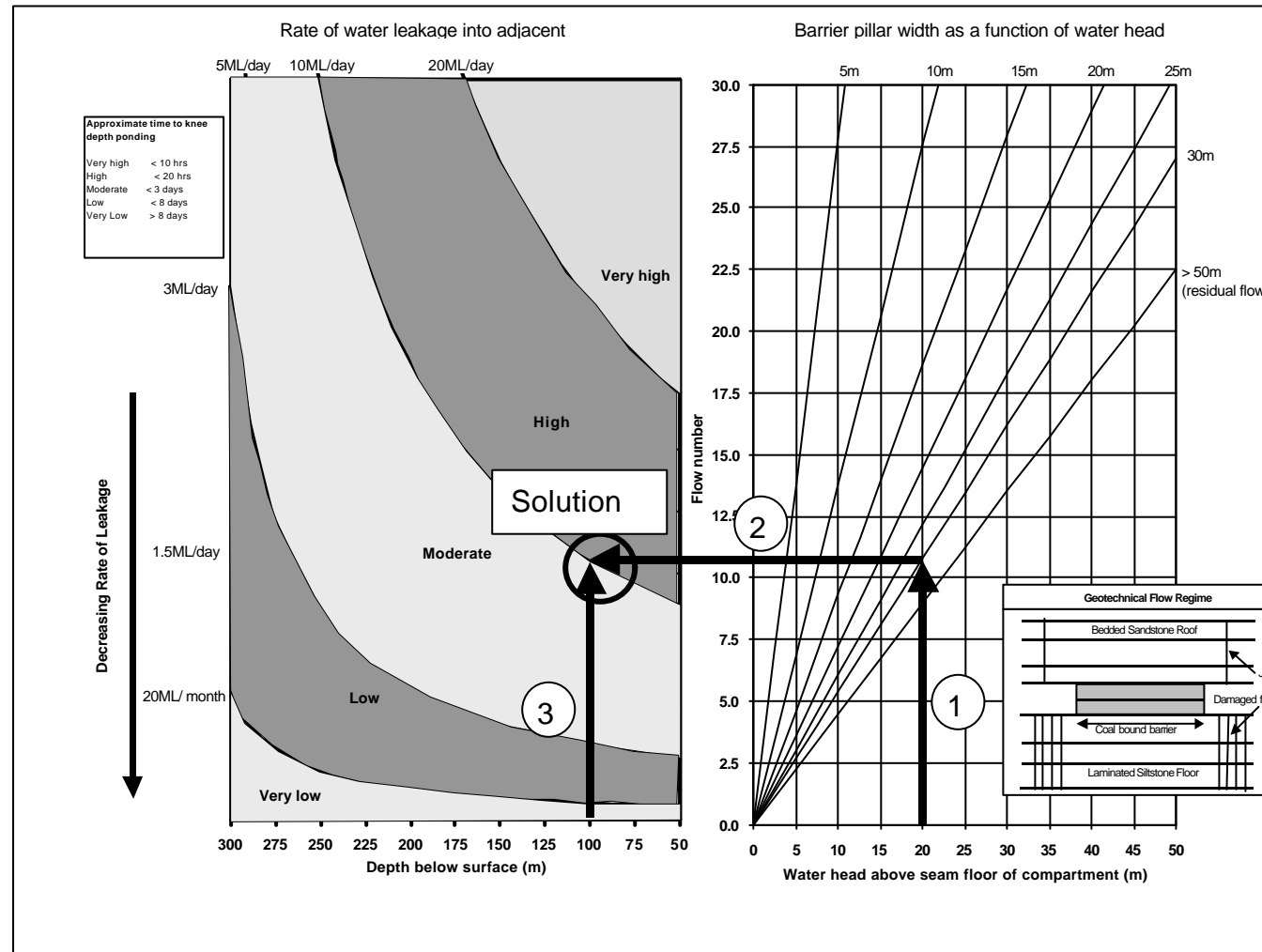


Example 1

APPENDIX V Example applications

Hydraulic Design Chart for Barrier Pillars

(FIGURE 5c = Coal bound + bedded sandstone roof + laminated siltstone/gritstone floor)



A coal mine 100m below surface plans to leave a 30m wide, 1km long barrier pillar along a goafed water compartment. The roof strata consists of **well bedded competent sandstones** and the immediate floor strata is **laminated siltstones**. For a maximum allowed water head of 20m, what rate of roadway dewatering can be expected?

→ Path to solution

① Steps to follow

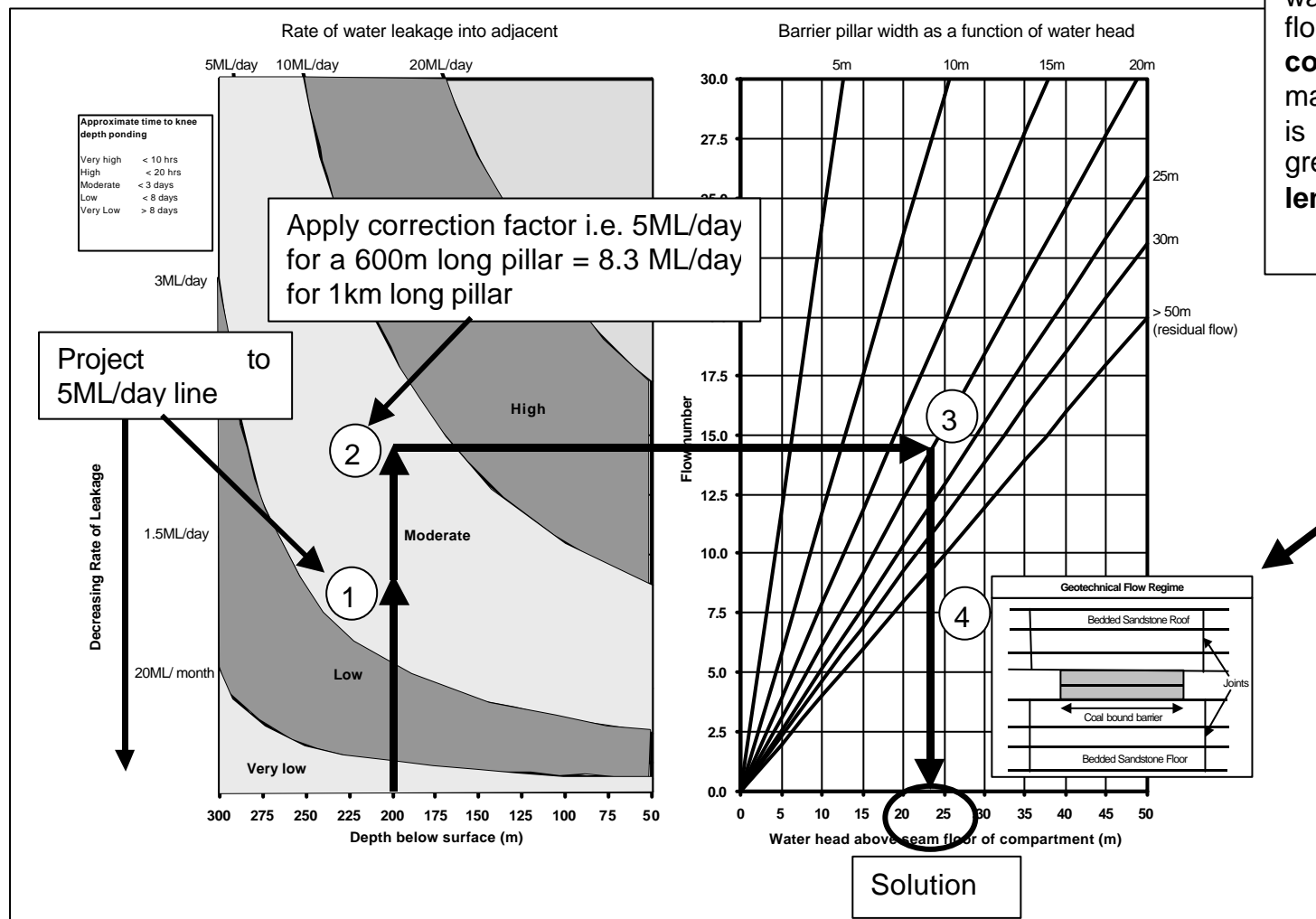
Confirm correct design chart for bedded roof and laminated floor strata (Figure 1c chosen thus design chart Figure 5c to be used)

Solution: The rate of leakage into the roadway adjacent to the pillar will be 10 ML/day. To prevent knee depth ponding in the roadway, a pumping cycle of 10-20 hours needs to be in place.

Example 2

Hydraulic Design Chart for Barrier Pillars

(FIGURE 5a = Coal bound + bedded sandstone roof + bedded sandstone floor)



A coal mine **200m** below surface plans to leave a **20m wide**, 600m long barrier pillar along a goafed water compartment. The roof and floor strata consists of **well bedded competent sandstones**. What maximum compartment water head is required to prevent water leakage greater than **5ML/day** along the length of the barrier.

- ➔ Path to solution
- ① Steps to follow

Confirm correct design chart for bedded sandstone roof and floor strata (Figure 1a chosen thus design chart Figure 5a to be used)

Solution: A maximum compartment water head of **23m** will prevent leakage greater than **5ML/day** for a 600m long barrier pillar.

APPENDIX VI GPR scan

GPR Tests Colliery A

The aim of the tests was to determine whether GPR is a viable tool for examining fractures in coal pillars to depths of 2 m or more. The test site, illustrated in Figure A27, is a site used for investigation into the properties of barrier pillars surrounding water storage areas underground. The GPR tests took place on either side of the main test area.

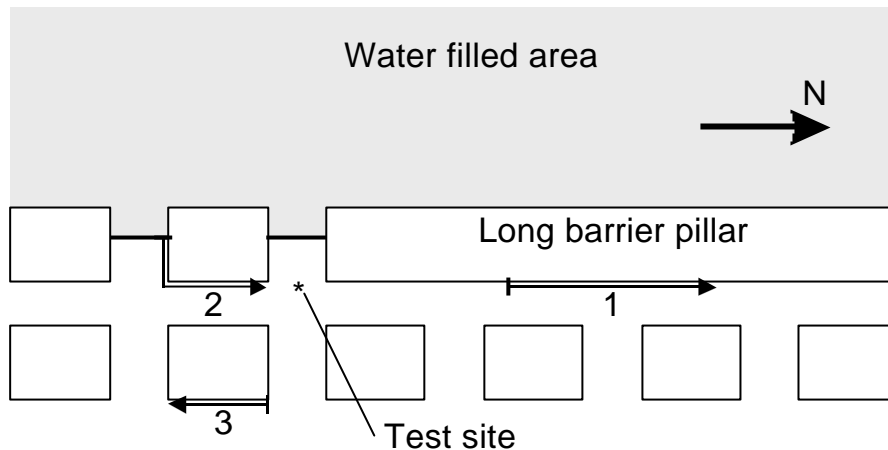


Figure A27. Survey site map

Test description

Three lines were scanned with the GPR. The first was on the long barrier pillar. The line was 50 m long, 25 m on either side of the centre of the second roadway from the Itasca test site. The second line was on the adjacent pillar, while the third line was at the back of a pillar in the next line of pillars from the water compartment.

The tests were run at a frequency of 500 MHz. A high frequency is required to image fractures: lower frequencies simply penetrate the fracture without being reflected. For typical coal electrical properties, a wavelength of 20 cm and a penetration of 5 to 10 wavelengths would be expected, leading to a resolution of 10 cm, and a penetration of 1 m to 2 m.

The three lines are plotted in Figures A28 –A30. Data was acquired at two ranges, 50 ns and 70 ns. From the results, there is definitely no data beyond 50 ns, so only the 50 ns data is presented here. The two way travel speed of radar waves in coal is approximately 5 cm/ns, so a range of 50 ns corresponds roughly to a penetration of 2.5 m.

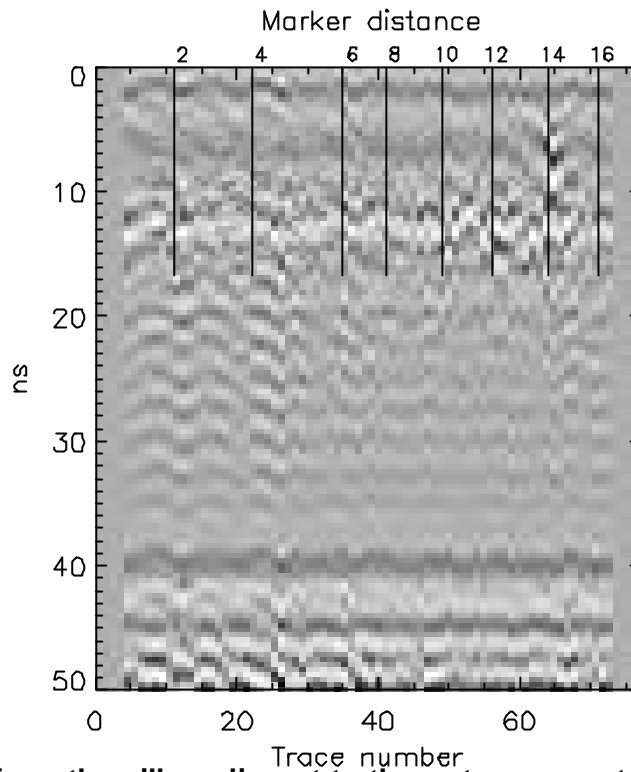


Figure A28. Results from the pillar adjacent to the water compartment. Data from 0 m to 6 m are taken along the East - West Roadway, while data beyond 6 m are taken along the main North - South Roadway.

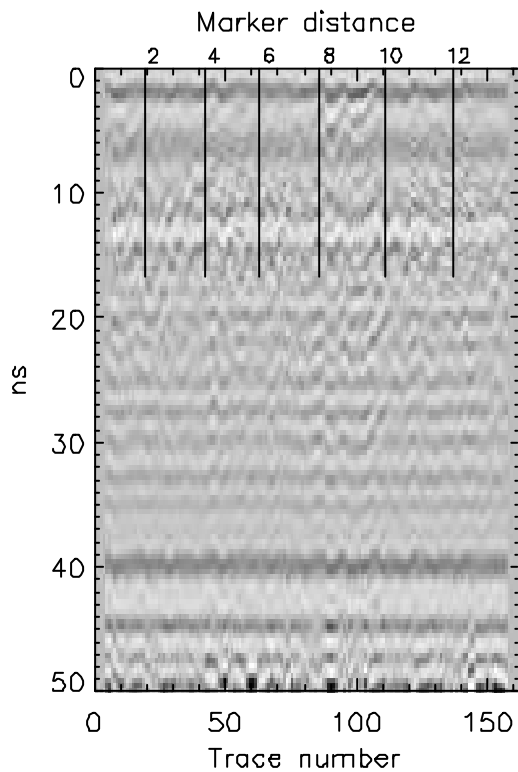


Figure A29. Results from the back of the pillar one roadway from the water compartment.

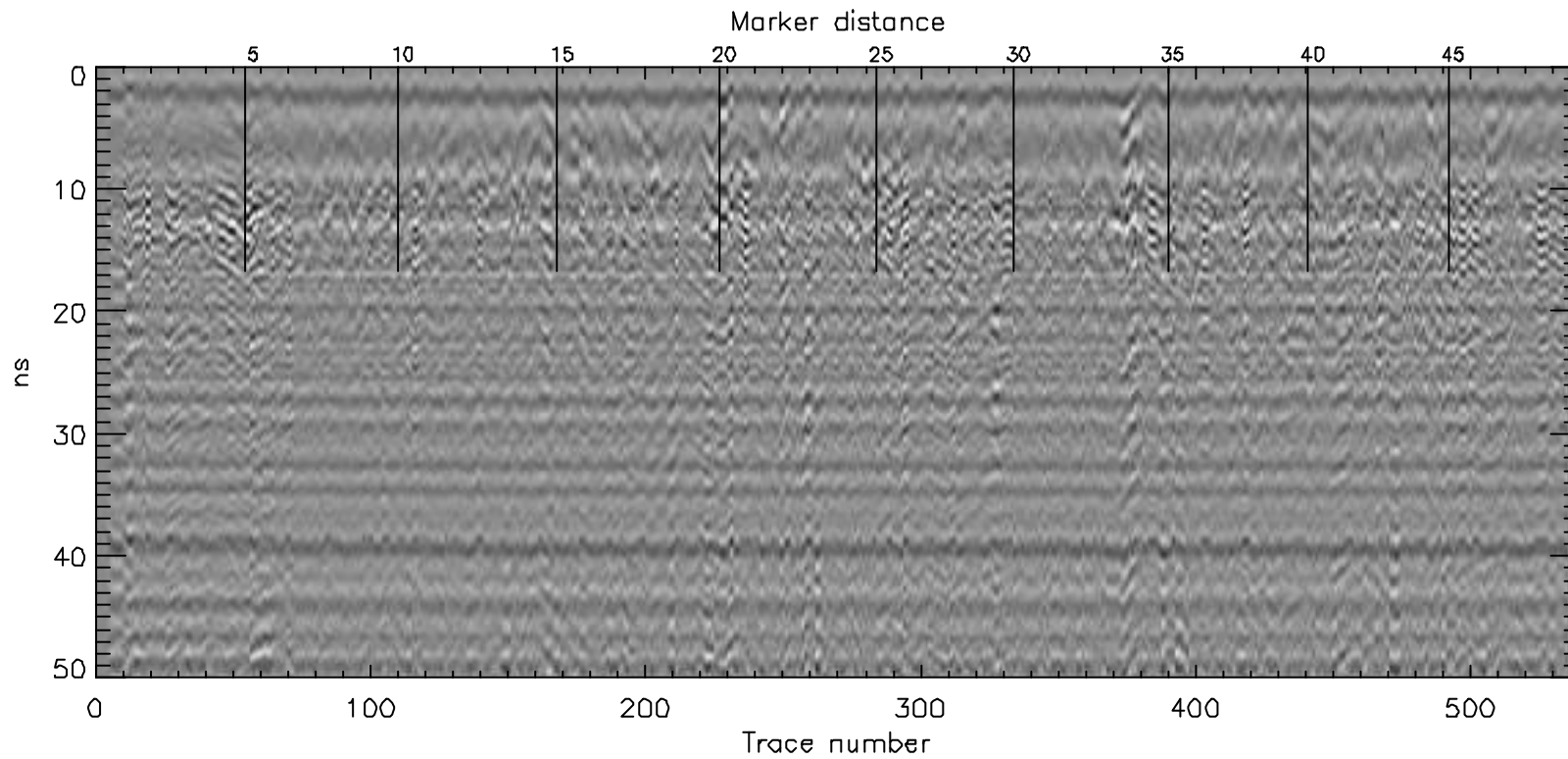


Figure 30. Results from the long profile along the long barrier pillar.

Results

From the radargrams, a number of conclusions can be drawn:

- The depth of penetration of the radar in the coal environment of Colliery A, using the GSSI SIR2M radar and 500 MHz antenna, is definitely less than 1 m, and probably lies between 15 ns and 20 ns (corresponding to a range of 0.75 m to 1m). Horizontal reflectors beyond 20 ns correspond to ringing in the radar antenna, and not to reflectors in the coal.
- All the dominant reflectors present in the early time of the data correspond to air reflectors. The slope of radar reflectors is determined by the velocity of the medium, and the slope of all the reflectors in the data taken at Colliery A corresponds to a two way travel speed of 15 cm/ns, more than triple the expected velocity in coal.
- No fractures have been imaged directly. However, qualitatively there appears to be less absorption in the first 10 ns in the pillar back from the water compartment, corresponding to a lower level of fracturing. In the profile recorded on the pillar adjacent to the plug, there is definitely more energy absorbed in the first 6 m of the profile than in the later part of the profile, indicating more fractures in the East – West direction than in the North – South direction. It is not really possible to compare the results from the long barrier pillar to those from the short pillar, because the quality of the data is not high enough.
- Radar penetration is no better in the drier pillar away from the water compartment than in the pillars close to the water compartment, implying that poor GPR performance is due to coal conductivity rather than to the presence of conductive water in the coal.

Conclusions

GPR has not been successful in this case in coal. Coal is never a good radar environment, but varies from place to place. In the pillars at Colliery A, the overall conductivity of the coal appears to be too high to make meaningful measurements.